

1989

Effects of selected nitrogen-containing aromatic compounds (NCACs) on physiological properties in *Escherichia coli*

W. James Catallo III

College of William and Mary - Virginia Institute of Marine Science

Follow this and additional works at: <https://scholarworks.wm.edu/etd>



Part of the [Biochemistry Commons](#), [Environmental Sciences Commons](#), and the [Microbiology Commons](#)

Recommended Citation

Catallo, W. James III, "Effects of selected nitrogen-containing aromatic compounds (NCACs) on physiological properties in *Escherichia coli*" (1989). *Dissertations, Theses, and Masters Projects*. Paper 1539616602.

<https://dx.doi.org/doi:10.25773/v5-rm6v-6q37>

This Dissertation is brought to you for free and open access by the Theses, Dissertations, & Master Projects at W&M ScholarWorks. It has been accepted for inclusion in Dissertations, Theses, and Masters Projects by an authorized administrator of W&M ScholarWorks. For more information, please contact scholarworks@wm.edu.

INFORMATION TO USERS

The most advanced technology has been used to photograph and reproduce this manuscript from the microfilm master. UMI films the text directly from the original or copy submitted. Thus, some thesis and dissertation copies are in typewriter face, while others may be from any type of computer printer.

The quality of this reproduction is dependent upon the quality of the copy submitted. Broken or indistinct print, colored or poor quality illustrations and photographs, print bleedthrough, substandard margins, and improper alignment can adversely affect reproduction.

In the unlikely event that the author did not send UMI a complete manuscript and there are missing pages, these will be noted. Also, if unauthorized copyright material had to be removed, a note will indicate the deletion.

Oversize materials (e.g., maps, drawings, charts) are reproduced by sectioning the original, beginning at the upper left-hand corner and continuing from left to right in equal sections with small overlaps. Each original is also photographed in one exposure and is included in reduced form at the back of the book. These are also available as one exposure on a standard 35mm slide or as a 17" x 23" black and white photographic print for an additional charge.

Photographs included in the original manuscript have been reproduced xerographically in this copy. Higher quality 6" x 9" black and white photographic prints are available for any photographs or illustrations appearing in this copy for an additional charge. Contact UMI directly to order.

U·M·I

University Microfilms International
A Bell & Howell Information Company
300 North Zeeb Road, Ann Arbor, MI 48106-1346 USA
313/761-4700 800/521-0600



Order Number 9004164

**Effects of selected nitrogen-containing aromatic compounds
(NCACs) on physiological properties in *Escherichia coli***

Catallo, William James, III, Ph.D.

The College of William and Mary, 1989

U·M·I
300 N. Zeeb Rd.
Ann Arbor, MI 48106



**EFFECTS OF SELECTED NITROGEN-CONTAINING AROMATIC
COMPOUNDS (NCACs) ON PHYSIOLOGICAL PROPERTIES IN
*ESCHERICHIA COLI***

A DISSERTATION

Presented to

**The Faculty of the School of Marine Science
The College of William and Mary in Virginia**

In Partial Fulfillment

**Of the Requirements for the Degree of
Doctor of Philosophy**

by

William James Catallo III

1989

APPROVAL SHEET

This dissertation is submitted in partial fulfillment of
the requirements for the degree of

Doctor of Philosophy

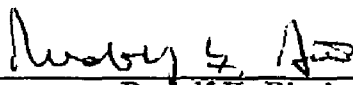


W. James Catallo III

Approved, August 1989



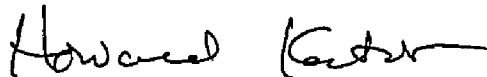
Michael E. Bender, Ph.D.
Committee Chairman/Advisor



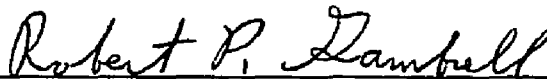
Rudolf H. Bieri, Ph.D.



Gene M. Silberhorn, Ph.D.



Howard I. Kator, Ph.D.



Robert P. Gambrell, Ph.D.
Louisiana State University
Baton Rouge, LA 70803

TABLE OF CONTENTS

	<u>Page</u>
ACKNOWLEDGEMENTS	v
LIST OF TABLES	vii
LIST OF FIGURES	viii
ABSTRACT	xi
OBJECTIVES OF THE RESEARCH	2
INTRODUCTION	6
I. Complex Pollutant Mixtures in the Environment	6
II. Sources and Environmental Chemistry of NCACs	8
III. Toxicity and Mobility of NCACs in Biological Systems	14
IV. NCACs in Plant Alkaloids	17
V. Description of the Test NCACs	18
VI. Chemistry and Biochemistry of Tetrazolium Salts and Formazans	20
VII. Electrochemistry of Tetrazolium Salts	25
VIII. Tetrazolium Salts and Biological Electron Transport	30
IX. INT and Toxicity Evaluation	31
X. INT Reduction Kinetics and Bacterial Outer Membrane Characteristics	33
XI. Toxicity of Tetrazolium Salts	35
MATERIALS AND METHODS	37
I. Reagents and Stock Solutions	37
II. FTNMR Analyses	39
III. Spectrophotometry	40
IV. Electrochemistry	41

TABLE OF CONTENTS (cont.)		<u>Page</u>
MATERIALS AND METHODS (cont.)		
V.	Identification of a 4-azafluorene Degradation Product	45
VI.	Microbiological Techniques	45
VII.	Electron Transport (INT Reduction) Assays	47
VIII.	Viable Cell Enumeration	47
IX.	Spheroplast Generation	50
X.	Oxygen Consumption Assays	51
XI.	Transmission Electron Microscopy (TEM)	52
XII.	NADH-PMS-INT Assay	52
XIII.	Eukaryotic Cell Systems and Cell Free Preparations	53
XIV.	Mutagenicity Evaluation of INT and INTF	54
RESULTS AND DISCUSSION		
I.	Chemical Structure and Solution Behavior of INT and INTF	58
II.	Electrochemistry of INT	67
III.	Mutagenicity Evaluation of INT and INTF	88
IV.	The Revised Direct INT Bioassay	95
V.	Solution Behavior of the NCAC Reagents	102
VI.	Identification of a 4-AF Oxidation Product	108
VII.	NCAC/INT Bioassay Results with Mechanistic Interpretations	108
VIII.	Effects of Solvents on INT Reduction Kinetics	138
IX.	Ultrastructural Evidence of NCAC-Mediated Membrane Effects	141
X.	Results of INT Reduction Assays in Assorted Eukaryotic Systems	149
SUMMARY OF CONCLUSIONS		
LITERATURE CITED		
VITA		

ACKNOWLEDGEMENTS

A list of those who have contributed to this work would fill another volume and would not convey my gratitude or debt to them. In keeping with the best tradition of triage in these matters, I thank the following people while exonerating them from any poor work on my part. I am indebted to my committee, Michael Bender, Rudolf Bieri, Gene Silberhorn, Howard Kator, and Robert Gambrell for guidance, encouragement, research materials, and laboratory space. Before his untimely death, John M. Zeigler was a mentor, committee member, and friend. His kindness, sanity, and humor have been, and are, sorely missed. I owe hearty thanks to my "virtual" committee, Roger Mann (Chairman), William MacIntyre, and Ashok Deshpande. While having no official status on my actual committee, they donated their time, laboratories, materials, and personal support, and were available at all times for discussions. There are no particulars that can summarize the value of their help and friendship. It was a privilege to work in the laboratory of Dr. Robert J. Gale (Chemistry Dept., Louisiana State University, Baton Rouge) during the winter of 1988 and to interact with his students, Roberto Wong and Kenneth Carney. I learned a great deal from Dr. Gale and his coworkers and anything that is correct or worthwhile about the electrochemistry of the present work is due to them. Thanks also are extended to John Greaves, Leman Ellis, Elaine Mathews, Ernest Warriner, Buddy Matthews, Brian Meehan, Christopher Abelt (Chemistry Dept., William and Mary), Jane Wingrove, Martha Rhodes, David

Cleland, Kenneth Moore, Bart Theberge, Susan Carter, Teresa Haynes, Louise Lawson, Phyllis Howard, and Marilyn Zeigler for advice, materials, and support.

My wife, Mary Lyon, endured the tension and periodic insanity of this degree without a quaver, and her strength has been an inspiration. Thanks again to Bill, Angela, and Peter Catallo, Helen S. Catallo, Jean S. Travis, Jul Seco, and Angela Christian for love and encouragement over the years.

LIST OF TABLES

<u>Table</u>	<u>Page</u>
1. Published half-wave reduction potentials ($E_{1/2}^{\text{red}}$) for TPT and INT at different working electrodes	27
2. Effect of sonication time on INT response and viable cell density in <i>E. coli</i>	104
3. Effects of quinoline and 4-azafluorene concentration on overnight viability and direct count cell densities in <i>E. coli</i>	130

LIST OF FIGURES

<u>Figure</u>	<u>Page</u>
1. Examples of published structures and reaction routes for TPT, INT, and their formazans	24
2. Direct INT Reduction Assay Procedure	49
3. Fourier transform nuclear magnetic resonance (FTNMR) Spectra.....	60
4. Direct reduction of INT by NADPH	66
5. Normal pulse polarogram of INT	69
6. Differential pulse polarogram of INT.....	71
7. Normal pulse polarogram of INT on vitreous carbon electrode	74
8. Cyclic voltammogram of INT on vitreous carbon electrode.....	76
9. Cyclic voltammogram of INT on vitreous carbon electrode.....	78
10. Spectrochemical identification of minimum INT reduction potential on Pt mesh electrode	81
11. Electronic absorbance spectra of INT and INTF standards in 50 % ethanol:PBS.....	83
12. First reduction wave characteristics as a function of pH. INT Reduction on vitreous carbon electrode	86
13. SAGE mobility of PSV ₂ -neo plasmid DNA relative to linear and supercoiled ladder DNA standards	91
14. Effect of ethidium bromide, INT, and INTF on SAGE mobility of PSV ₂ -neo plasmids and supercoiled ladder DNA	93

LIST OF FIGURES (cont)

<u>Figure</u>	<u>Page</u>
15. Comparison of INT reduction assays. Maximum INTF response vs. incubation period (8, 16, 36 h)	98
16. <i>Escherichia coli</i> growth curve	101
17. A. Electronic absorbance spectra of 4-AF and 4-AF degradation products after reaction with DMSO	106
18. A and B. Electronic absorbance spectra of 4-AF and photodegradation products. C. Electronic absorbance spectra of quinoline and quinoline irradiated for 12 h	110
19. Mass spectra. A. Quinoline standard. B. 4-azafluorene standard. C. 4-azafluorene degradation product (4-azafluorene-9-one)	112
20. Effect of quinoline concentration on INT Reduction Rate in <i>E. coli</i>	114
21. Effect of 4-azafluorene concentration on INT Reduction Rate in <i>E. coli</i>	117
22. Effect of quinoline concentration on INT reduction kinetics in <i>E. coli</i>	119
23. Effect of 4-azafluorene concentration on INT reduction kinetics in <i>E. coli</i>	121
24. Effect of tributyltin chloride concentration on INT Reduction Rate in <i>E. coli</i>	123
25. INT reduction kinetics in various <i>E. coli</i> cell systems	126
26. INT reduction kinetics in deep rough mutants (<i>rfa</i>) and gram(+) cell systems	128
27. Effect of quinoline concentration on cellular oxygen demand in <i>E. coli</i>	133

LIST OF FIGURES (cont)

<u>Figure</u>	<u>Page</u>
28. Effect of threshold concentration of quinoline on PMS-mediated reduction of INT by NADH	136
29. Effect of solvent system (8% final) and threshold concentration of quinoline on lag period and INT reduction rate	140
30. Transmission electron micrographs of control and quinoline-HCl treated <i>E. coli</i>	144
31. Effect of calcium ionophore A23187 (CI) and phorbol myristate acetate (PMA) on INT reduction in resting macrophages from the Toadfish <i>Opsanus tau</i>	153

ABSTRACT

This research examined the effects of quinoline and 4-azafluorene on respiratory electron transport rate (ET), outer membrane permeability and topology, oxygen consumption, and viable cell density in *Escherichia coli* cell suspensions. ET was estimated spectrophotometrically using INT (2-(*p*-iodophenyl)-3-(*p*-nitrophenyl)-5-(phenyl)-2*H*-tetrazolium chloride), which is reduced *in vivo* to a red colored formazan (INTF). Both test compounds caused anomalous dose-response behavior in INT assays: in a defined window of doses, ET rates near or above the controls were observed. These doses showed altered INT reduction kinetics, decreased cellular oxygen demand, and decreased viable cell densities. Experiments with *E. coli* spheroplast preparations, gram(+) cells, and deep rough mutants suggested that the toxicants increased outer membrane permeability and inhibited normal respiratory function. Results of cell-free ET assays and transmission electron microscopy further indicated altered outer membrane structure and inhibition of respiratory ET *via*, 1) secondary topological effects on the periplasm and inner membrane, 2) redox cycling of electrons in the respiratory chain, or 3) both 1 and 2 together.

Quantitative studies of INT chemical structure and aqueous electrochemistry at Hg, C, and Pt electrodes were conducted to address analytical shortcomings in the literature. Data include nuclear magnetic resonance spectra, results from normal and differential pulse polarography, cyclic voltammetry, ring disk electrode, and spectroelectrochemical experiments. The route of INT reduction involves a slow one electron reduction to a tetrazolanyl radical followed by a fast one electron reduction and addition of one proton to yield formazan. Results on C and Pt electrodes indicated interfering reactions involving adsorbed hydrogen species and the possibility of underpotential production of hydrogen gas.

**EFFECTS OF SELECTED NITROGEN-CONTAINING AROMATIC
COMPOUNDS (NCACs) ON PHYSIOLOGICAL PROPERTIES IN
*ESCHERICHIA COLI***

OBJECTIVES OF THE RESEARCH

NCACs are ubiquitous environmental contaminants arising primarily from pyrolysis of organic matter and discharge of coal- and petrochemicals. In general, NCACs have not been examined from a detailed toxicological perspective (*i.e.*, with respect to mechanisms) even though chemical and quantum mechanical considerations suggest that diverse reactivity (*e.g.*, redox cycling, protein denaturation) and high mobility (*e.g.*, biomimesis, amphiphilicity) are likely in biological systems. The primary goal of the present work was to examine the mechanisms of acute toxicity of two common NCACs, quinoline and 4-azafluorene (4-AF), in optimized, aerobic, *Escherichia coli* cells. The biochemical variables of major interest were electron transport (ET), oxygen consumption, outer membrane stability, and cell viability. It was hypothesized that if the NCAC reactivities mentioned above were appreciable, then the chosen biochemical variables would be altered in a nonlinear fashion with increasing dose, and the magnitude and nature of these alterations could be used to infer specific mechanisms of toxicity.

The effects of NCAC treatment on cellular ET were estimated spectrophotometrically by measuring changes in the rate of reduction of 2-(*p*-iodophenyl)-3-(*p*-nitrophenyl)-5-(phenyl)-2*H*-tetrazolium chloride (INT) to its red-colored formazan (INTF) with dose. Changes in the kinetics of INT reduction with dose were of primary interest. In gram(-) bacteria such as *E. coli*, INT reduction can occur only at the plasma membrane and in the cytosol, and lipoidal outer membrane layers must be traversed before this can

occur. As a result, diffusional lag periods before observable INT reduction would be expected in normal cells. It was hypothesized that significant NCAC-mediated alteration of outer membrane structure or composition would be manifested as a change in INT diffusional lag period and therefore the kinetics of INT reduction. Further, if the NCACs participated in redox cycling in the respiratory chain, it was expected that INT reduction rates would be altered (stimulated or depressed) in certain doses as a result of changes in the concentration of reducing equivalents. In any case, the results of testing these hypotheses would illuminate the assumption of a direct proportionality between INT reduction and the metabolic status of control and treated cells. This assumption forms the basis of numerous applications of INT found in the literature.

To have confidence in mechanistic interpretations derived from experiments in whole cell suspensions, it is necessary to understand the chemistry of all components of the experimental system. A review of the literature on INT and related tetrazolium compounds indicated that errors in chemical structure, reaction routes, and electrochemistry were widespread (*cf.*, Section VI, Introduction). A secondary objective was therefore to obtain quantitative data on the chemical structures of INT and INTF and the electrochemistry of INT in buffered aqueous media. It was also necessary to examine INT reactivity in cell free systems containing biochemical reducing agents, the NCAC reagents, killed *E. coli* cells, and artificial electron carriers. The electrochemical experiments were directed towards determining the minimum potential of INT reduction at various electrodes and examining the mechanism of this reduction. It was hypothesized that INT is reduced *via* a two electron reduction (proceeding through a tertazolinyl radical), followed by

disproportionation with one proton (hydride transfer). Interfering electrode reactions involving adsorbed hydrogen species were also postulated.

Subsidiary experiments were performed to elucidate anomalies encountered in the INT assays, to provide data not found in the literature, and to evaluate the use of INT reduction assays in other experimental systems. The potential mutagenicity of INT and INTF was examined using the Ames assay, and an electrophoretic DNA binding assay was performed so that safe handling/disposal procedures could be formalized. Preliminary experiments in eukaryotic cell systems (peritoneal macrophages, marine phytoplankton) and cell free preparations (liver S-9) were conducted to evaluate the potential uses of INT in these systems. Additionally, thin layer chromatography (TLC) followed by mass spectrometry was employed to identify an oxidation product of 4-AF which was encountered in the toxicity assays.

The introductory sections I. - V. provide a review of the literature on the general environmental chemistry and toxicology of NCAC compounds. These subjects are approached from the larger perspective of complex pollutant mixtures in the environment, sources of pyrogenic contaminants, reactivities of different classes of organic compounds, and mobility of polar and amphiphilic materials in environmental and biological systems. Hopefully the review will provide a background and rationale for the experiments of the current work.

Subsequent sections (VI. - XI.) offer a review of the historical literature on tetrazolium salts with emphasis on INT and closely related compounds. Research on tetrazolium structure, chemistry, electrochemistry, and uses in biochemistry and toxicology are reviewed and the need for quantitative analysis is indicated. Also discussed are tetrazolium reduction kinetics and their

relationship to bacterial outer membrane processes, the evaluation of cellular toxicity using tetrazolium reduction assays, and the few data on mammalian toxicity and mutagenicity of tetrazolium salts. This should provide both a quantitative understanding of tetrazolium salts in the context of the present work and justify the chemical analyses performed.

INTRODUCTION

I. Complex Pollutant Mixtures in the Environment

Ever since the *Torrey Canyon* and West Falmouth oil spill study results were publicized in the late 1960's, there has been widespread interest in the fates and effects of petroleum and petrochemical mixtures in the environment [1-3]. Observations of organismic response to petroleum and chronic hydrocarbon contamination have shown that different oils, and the various fractions and compounds comprising them, have different acute and chronic toxicities and manifest different kinds of effects [4]. In practice, however, it has been frequently overlooked that crude oils, coal tars, combustion-generated particulates, and syncrudes are chemical assemblages of extreme complexity [4-8]. Consequently, toxicity evaluation has centered on only a small number of well-characterized model compounds and simple mixtures [1, 8].

Although complete analytical resolution is not yet possible, studies of pyrogenic and fossil organic mixtures have demonstrated the presence of thousands to tens of thousands of different compounds [1, 4 - 9]. Depending on the mixture, representative chemical classes generally include a spectrum of paraffins, naphthenes, liquid hydrocarbon solvents, naphtheno aromatics, polycyclic aromatic compounds (PAHs), N-, S- and O- heterocycles, organometallic complexes, terpenoid compounds, nitroso species, nitriles, carbolines, quinones, alcohols, N-oxides, various charged and uncharged free radicals, and their alkyl homologues extending in some cases above C₁₃ [7 - 14].

During the 1970's, attempts to

elucidate the spatial and historical distributions of pollutant chemicals in the environment led to the discovery of extended PAH and N-heterocyclic series in soils and sediments proximal to urban industrial areas [10, 11]. The latter group of compounds included species of up to eight fused rings, with alkyl homologues up to C₇ [11]. These identifications were followed by the demonstration of the global distribution of polycyclic compounds from petrochemical discharges and particulate fallout from anthropogenic and natural pyrogenic sources [12, 13]. The presence of these materials, particularly the aromatic heterocycles, was postulated to be biologically significant, with some authors suggesting that natural background levels of mutagenic species in this class could have influenced natural selection and the descent of species over evolutionary time [14]. Subsequent research during this period showed that sedimentary levels of pyrogenic PAHs, heterocycles, and their homologues have increased rapidly since the American Industrial Revolution [15] and at least one epidemiological study has strongly correlated ambient levels of PAHs and heterocyclic materials in an industrial area to local patterns of increased human cancer relative to a proximal rural area [16].

The presence of reactive chemicals in widely used chemical products and human environments has led to the conclusion that toxicity assessment must begin to address the effects of mixtures [17], and that toxicological models and protocols should expand to encompass all potentially significant chemical species. Despite this consensus, there has been marginal progress towards integrating what Blumer (1975) called "the chemical fine structure [of complex mixtures]" with toxicological models and attempts to "[fully anticipate] biological impacts" [2]. Recognizing this need, Malins (1981) also called for more research on "...the environmental fate and biological effects of the polar

components...and the products of chemically and biologically altered hydrocarbons [which] remain almost completely unknown..." [18]. Blumer, Malins, and others have stressed the need for pure and applied research on hitherto unexamined materials with an emphasis on mechanisms and processes, as well as the incorporation of new data into an ecological framework [12 – 18]. They have emphasised that research should be developed that addresses subjects such as larval ecotoxicology, synergism/antagonism in complex mixtures, photochemical effects on pollutant reaction routes, and acute effects on central homeostatic processes (*e.g.*, electrophysiology, respiration), nutrition, and behavior. Although there are significant methodological reasons why progress in this direction has been slow, a number of investigators recently have initiated studies of novel pollutants in fractionated pyrogenic mixtures. For example, Malins and coworkers have shown that nitrogen-containing aromatic compounds (NCACs) are mobile and reactive in biological systems and have the potential to be very significant from both the cellular/organismal and ecological standpoints [19 – 22]. In a series of exemplary papers spanning more than a decade, a complex suite of NCACs, PAHs, aromatic amines, nitro- and cyano-PAHs, and other materials in creosote and sediments in Puget Sound have been characterized and correlated to the presence of an array of physiological abnormalities, neoplasia, and proliferative disorders in exposed benthic fish [19 – 22].

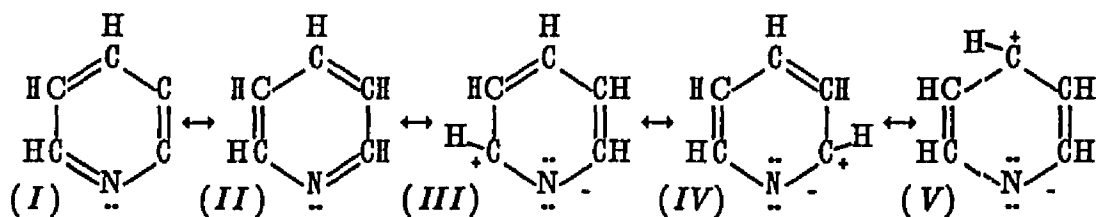
II. Sources and Environmental Chemistry of NCACs

The environmental presence of NCACs is the result of the same processes that proliferate PAHs and other condensed ring aromatics: anthropogenic

combustion of fossil and recent organic matter, petrochemical discharge, forest and marsh fires, and geochemical seeps [7, 12 – 14, 23 – 25]. Similarly, they reflect the composition of the starting materials and the conditions (pyrolysis temperature, trace gas content, degree of photolysis) and time of combustion (μ s to millions of years) [14]. High levels of NCACs have been identified in the mutagenic polar fractions of urban particulate matter [26], cigarette smoke [27], automotive exhausts [28], crude oils [29] and high boiling point distillates [30], syncrudes and synfuel process wastes [31], coal tar pitch volatiles [32], and creosote [25]. In environmental mixtures, the total observed NCAC content is specific to the particular mixture (source material, pyrogenesis), the analytical procedures employed (fractionation, acidification/saponification, chromatographic methods/detectors, etc.) and the physicochemical processes to which the mixture is exposed prior to and during collection/processing. In industrial particulates and weathered oils, NCAC concentrations typically range between one and two orders of magnitude below the total PAH content, but this might well be an artifact of poorly developed methods and unoptimized instrumentation [4, 6, 7, 14]. In the case of combustion-generated particulate matter, it is likely that NCACs desorb at high temperatures and enter the gas phase, or are bound within the matrix of the particle through covalent or metallic interactions [33]. In deposited material, processes such as aqueous solvation, photolysis, and complexation with soluble metals or acid-base interactions with dissolved materials cause rapid removal of NCACs from the source hydrophobic materials. In fresh asphaltic crudes and distillates, NCACs are more concentrated, with levels between 0.2 – 0.8 mg/kg in Arabian crude oils, to several percent in fresh creosote [25]. In crude and coal oils, the highest concentrations of NCACs occur in the $> 350^{\circ}$ C boiling point distillates along

with porphyrins, O- and S- heteroatomic polynuclear material, and transition metal-NCAC complexes, none of which have been studied with great analytical resolution [9]. Nitrogenous materials such as NCACs are undesirable in finished distillates because they poison catalysts and form gums (usually pyrolytically or photochemically *via* reaction with xanthins) in fuel oils, and efforts are taken to remove them [9]. Hence, in refined petroleum products such as light oils, kerosene, and fuel oils, there are low levels of NCACs relative to the C_1-C_4 benzenes and naphthalenes. However, in the so called Bunker oils, NCACs are expected in significant quantities because these oils are blends of light and residual fractions [14].

An important feature of the heterocyclic moieties of NCACs is the predominance of zwitterionic resonance structures in the ground state [34], illustrated for pyridine in structures *III* through *V* below.



This characteristic, and the presence of a nonbonding electron pair localized on the heteroatom in all electronic configurations allows for high water solubility and low octanol:water partition coefficients relative to aromatic hydrocarbon species of the same ring number [35, 36], acid-base reactions at physiological and environmental temperatures and pH [34], chelation of metal cations in aqueous media [37], and facile participation in biological redox reactions [37 - 39]. The N-heterocyclic ring is electron deficient relative to benzene and this

explains the resistance of NCACs to electrophilic substitutions. The presence of pyridine ($\mu = 2.26 D$) and benzene ($\mu = 0.0 D$) moieties on NCACs makes these compounds, especially the bi- and tricyclic species, somewhat amphiphilic, and this points to important biophysical and toxicological differences between NCACs and PAHs of the same ring number (below). The lone pair of electrons and the ability of the rings to accommodate both positive and negative spin-unpaired states (as well as "dative" bonding at the nitrogen) allows for a range of chemical, enzymatic, and photochemical reactions leading to reactive species [40]. For the majority of the several unsubstituted NCAC's studied under realistic conditions, photochemical degradation in aqueous environments proceeded with disappearance quantum yields (Φ) on the order of, or greater than the PAHs of the same ring number [35, 36]. There is some evidence that aqueous photochemical reactions of quinoline may give rise to mutagenic diol N-epoxides [46], and that the presence of N-heterocycles in organic mixtures exposed to sunlight gives rise to stable free radicals, polymeric ring systems, and charge transfer complexes of biological significance [41 - 43].

As a result of the properties outlined above, the environmental partitioning of NCACs is closer to what might be expected for polar and electron-deficient PAHs (*e.g.*, 1-naphthalene nitrile). At least one study has identified NCACs and polar PAHs (nitriles, quinones) in groundwater near a wood treatment plant [44]. The heterocycles, their oxidized and alkylated homologues, phenolics, and NCAC nitriles and carbonitriles comprised approximately 75 % of the compounds identified and this resulted from transport through clays-silt sediments of high organic matter content. The number of NCACs identified in groundwater was greater than the the number of PAHs and this further indicated selective transport processes favoring NCAC

transport from sediments to groundwater. This interpretation is supported by sorption and aqueous photochemistry studies conducted under approximated environmental conditions [36] and aqueous chelation studies using selected low molecular weight (LMW) NCACs and divalent metal cations [37]. Qualitatively, it could be assumed that percolation of acidic rainwater (pH 4.7 – 6.0) or H⁺ exchange at sediment surfaces would facilitate aqueous solvation and transport. The pKa values of the few NCACs studied are in the range of 4.0 – 5.7. When protonated, NCACs become more water soluble than in the reduced state and this would be reflected in their *n*-octanol:water partition coefficients (log P) as well as their behavior in an environmental sediment–water system.

In a study of sediments contaminated with creosote, Krone *et al.* have observed disproportionately low levels of LMW NCACs when referenced to their concentrations in the source creosote [25]. For example, of the approximately 100 NCACs identified by GC–MS in source creosote, there was a concentration differential based on molecular weight and the total benzene character of the individual compounds. Hence, the source creosote contained 26,100 µg/g quinoline/isoquinoline (FW = 129), 800 µg/g azafluorene (*sic*) (FW = 168), and < 24 µg/g diphenyl pyridine (FW = 231). In the sediments, however, quinoline/isoquinoline was < 0.5 µg/g (< 0.0019 % of source), azafluorene concentration was 0.67 µg/g (0.082 % of source), and diphenylpyridine 2.2 µg/g (9.2% of source). There was a strong relationship between the number of benzene rings per NCAC and its presence in the sediments: as benzene ring number increased above two (*i.e.*, benzoquinolines), the presence in the sediments increased for virtually all isomers. Hence, of the 10 different C₁–quinoline/isoquinoline isomers identified in the source creosote in high levels (*c.* 6500 ppm cumulative), none were detected in the sediments.

Conversely, of the 3 C₁-benzacridine isomers in source creosote, all were detected in sediments. This trend also applied to the carbazoles, benzocarbazoles, and all NCACs with alkyl substituents of two carbons or greater. The Krone *et al.* study was devoted explicitly to NCACs and employed high resolution gas chromatography (HRGC) and HRGC-mass spectrometry (HRGC-MS) with N-specific detection, so these observations do not reflect experimental error or detector sensitivity problems as encountered in analyses devoted mainly to PAHs.

Laseter *et al.* [45] also have reported selective weathering processes involving LMW hydrocarbons and NCACs. GC-MS studies of creosote-contaminated sediments that creosote in the lower horizons of core samples showed little compositional difference from unweathered source materials [45]. Analysis of surface layers, however, indicated that LMW compounds had been selectively removed by aqueous solvation, physical weathering, volatilization, and photolysis.

A clear inference from these studies is that LMW NCACs in sediment-water systems partition with the water particularly under conditions of low pH (acid rain, fulvic materials), and are selectively mobilized from the source materials containing hydrocarbons and high molecular weight NCACs. It would follow, although it has not been conclusively demonstrated, that water soluble fractions (WSF) of mixtures such as heavy crudes, creosotes, coal tars, and pyrogenic products of these substances would contain significant quantities of LMW NCACs in addition to LMW aromatic hydrocarbons and polar products, and that aqueous solvation and probably organometallic associations are major partitioning processes in periods immediately following spills. Hence, in a fresh spill (or in runoff containing industrial/automotive particulates or

heavy petro- or coal- tars) the WSF would be expected to contain the highest levels of NCACs with the concentrations of these materials decreasing with time of weathering.

III. Toxicity and Mobility of NCACs in Biological Systems

In single compound assays, a number of NCAC's, including quinoline, all possible C₁ alkyl quinolines, various benzacridine isomers, dibenzo(*a,h*)acridine, and several of their alkyl homologues have exhibited mutagenic and tumorigenic activity in the Ames/*Salmonella* assay and various mammalian test systems, respectively. NCACs and PAHs from creosote contaminated sediments have been correlated to extract mutagenicity [46], and neoplasia and proliferative disorders in exposed benthic fish [21]. Analyses of coal and shale petroleum substitute polar fractions showed that the "most mutagenic" materials were NCACs and their partially hydrogenated and alkylated homologues [47]. Conversely, aqueous extracts of coal conversion oils yielded one- to five-ring mutagenic amines, NCACs, and their alkyl homologues, with "most of the mutagenic activity" attributed to the amines [48]. Clearly, an assortment of chemicals from the nitrogen-containing polar fractions of these mixtures are toxic and mutagenic, but the identities of the "hottest" fractions are less well established.

In addition to the induction of neoplasia, polar and WSF from heavy crudes, particulates, and creosotes have demonstrated a spectrum of acute physiological effects on exposed organisms [49, 50] that are not observed upon exposure of the same organisms to weathered oil or nonpolar fractions [4]. Most notable among these effects are "necroses", impairment of membrane structure,

altered electrophysiological function (electron transport, respiration), and behavioral abnormalities indicating neural impacts [50]. In WSF, these effects are frequently "threshold" in nature, *i.e.*, physiological responses exhibit anomalous "spikes" in activity *vs.* increasing dose or exposure times [49, 50]. Threshold responses are typical of compounds that 1) are multivalent (react at numerous sites), 2) effect critical structures or mechanisms so that extended feedback control systems are disrupted, and 3) are "biomimetic". It can be seen that certain LMW NCACs would satisfy all of these criteria. Given the amphiphilic nature of NCACs mentioned above, and the related differences in chemical reactivity and log octanol:water partition values (log P) between NCACs and PAHs, it is reasonable to expect significant differences in routes of biological activity. This would apply particularly to chemical processes associated with lipid bilayers in membranes, uptake/depuration, and maintenance of intracellular redox balance. It is known that both log P and bioconcentration factors (BC) of NCACs tend to be much lower than PAHs of the same ring number, and it follows that hydrophobic interactions with membrane bilayers will be different in terms of magnitude and mechanism [51, 52]. High BC factors are proportional to the extent of sequestering of the compound in hydrophobic regions of cells (assuming metabolism is minimal), while low values suggest minimal chemical interaction and/or uptake followed by rapid depuration. In multicompartiment octanol:water systems, the arrival of chemicals of different log P in the n^{th} compartment displays a parabolic response surface given by:

$$\log 1/C = -0.54 (\log P)^2 + 2.47 (\log P) - 1.05;$$

where C is concentration [52]. At all exposure time steps for a single concentration C, the peak multicompartment transport rate is at log P values in the range $\{-1.5$ to $+ 1.5\}$. This reflects the observation that both highly hydrophobic and hydrophilic contaminants have difficulty reaching the n^{th} department, the latter because of difficulty in passing a lipophilic barriers, the former because of quasi- or irreversible associations with hydrophobic centers. As might be guessed from their amphiphilic nature, log P values for NCACs are closer to the peak mobility range than their PAH analogues. For the compounds of present concern, BC is proportional to the log P [51, 52] and a comparison of experimental BC values from experiments with *Daphnia pulex* for representative 2 - 4 ring PAHs and NCACs shows the following order of magnitude differences (log P: BC): naphthalene (3.36: 131) *vs.* isoquinoline (0.87: 2.4); anthracene (4.45: 917) *vs.* acridine (3.84: 29.6), and benz(a)anthracene (6.12: 10^4) *vs.* benz(a)acridine (5.51: 352) [51 - 53]. The implication of all this is that WSF threshold effects such as acute electrophysiological disturbances must be accounted for by reactions of materials that have high mobility in heterogeneous systems, and are labile in different cellular sites. The chemistry of LMW NCACs indicates that they possess these characteristics. In quinoline-exposed rainbow trout (*Salmo gairdneri*) for example, over 50% of total radiolabelled quinoline was absorbed from the water and excreted in unmetabolized form in exposure periods of less than 12 h [54]. Conjugated metabolites were accumulated primarily in the fluids of the following organs:

gall bladder/bile > eye > gut > kidney⁺ > liver⁺ > gill⁺ (+ trace) [54].

Conversely, PAHs interact *via* Van der Waals (hydrophobic) forces and sequester in lipid bilayers. Depuration times are consequently longer and this is reflected in the high BC values in *Daphnia* and other test organisms. Sequestration in bilayers is followed by equilibrium transport into the aqueous cytosolic phase followed by metabolism to polar products. Hence, in the Dolley Varden (*Salvelinus malma*) PAHs accumulated in skin, gills, and liver [54]. Reactivity differences are also important: NCACs have the capacity to undergo reversible (futile) redox reactions *via* free radicals, while PAHs resist such reactions until they are enzymatically oxidized to quinones. In general, the much discussed presence of quinones *in vivo* is controversial, but if they occur the oxidation reaction almost certainly must be cytosolic and prefaced by transport of the PAH into the aqueous phase (a slow process). It would seem from these reactivity considerations that despite the lack of analytical evidence linking toxicities of many WSF to NCAC content, there is ample *prima facie* evidence for the involvement of these compounds in acute effects normally attributed to the hydrocarbons almost exclusively [4].

IV. NCACs in Plant Alkaloids

The lack of environmental data notwithstanding, NCAC compounds have long been prominent in the literature of medicinal botany [55, 56]. Pyridine, quinoline, and isoquinoline ring systems are widespread in higher plants as metabolic poisons that are part of what is sometimes called "chemical defense". The NCAC-derived chemicals are found throughout the heterogeneous class of compounds known as the alkaloids, which are among the most diverse and reactive group of toxins known [55]. While NCAC toxins are

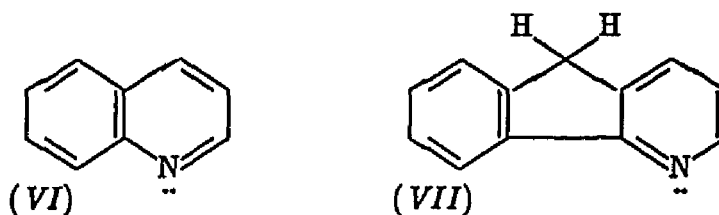
widespread, the relatively inert polycyclic aromatic toxins are comparatively limited in phyletic distribution [56]. Where PAH ring systems occur in plants, they usually are oxidized (as in anthraquinones and naphthodianthrones) and are acutely toxic only after irradiation with sunlight [55, 56]. Interestingly, there is evidence that the "photoactivation" of these quinones is potentiated by the presence of pyrrole and pyridine functionalities (in nitrogen-containing amino acids such as tryptophan and pyridine nucleotides, respectively) that act as required substrates [55 - 58]. The reactions frequently involve the transfer of photoexcited electrons from N-heterocyclic centers to oxygen or some other carrier. Radicals generated in this process undergo redox cycling and/or covalent association with electron-rich centers [58, 59]. Tryptophan and its oxidized metabolites are known cancer promoters, which again suggests that redox active nitrogen-containing compounds may be operating in many toxicological contexts [37, 58].

V. Description of Test NCACs of the Present Work

As the material in the preceding sections has indicated, most of the environmental toxicity data on NCACs has been descriptive, and few NCACs have been examined from the standpoint of biochemical processes [2]. When the hundreds of NCACs, amines, and alkyl homologues identified in petrochemicals are considered in this context, it can be seen that much interesting and relevant work needs to be done. Given the concern with organic pollutants in the environment, it is important that representative NCACs be given the attention that their apparent reactivity and environmental mobility would merit. The pharmacology of NCAC-derived plant toxins suggests that

pollutant NCACs will exhibit mobility and multiple reactivity in cellular environments and that this will be manifested in acute bioassays addressing central homeostatic processes.

The primary goal of this work was to examine the the effects of quinoline (VI) and 4-azafluorene (VII, "4-AF") in the bacterium *Escherichia coli*. Both compounds are prominent (> 500 ppm) components of high boiling point coal tars and creosotes and have been identified in environments contaminated with these materials.



Very little data exist on quinoline beyond those reviewed above, and a 1989 Chemistry Abstracts search on 4-AF showed few chemical data (*e.g.*, there is no value for pKa) and no toxicological data whatsoever. The paucity of relevant data on the single compounds suggested that work with mixtures would be premature. Therefore the bioactivity of the selected NCACs were examined in single compound tests. The biological parameters of primary interest in this work were respiratory electron transport (ET), oxygen consumption, cell viability, and membrane integrity and morphology in wild type (+) *Escherichia coli* cells. *E. coli* is the most well-characterized cell system known, and conditions for its isolation, maintenance, and experimental use have been comprehensively described [59, 60]. In *E. coli* and many other prokaryotes, the systems mediating ET and metabolic oxygen consumption are

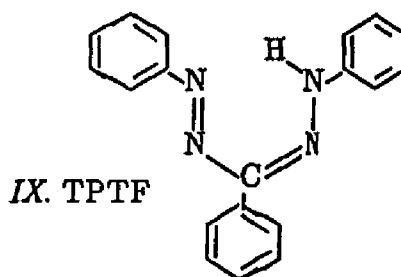
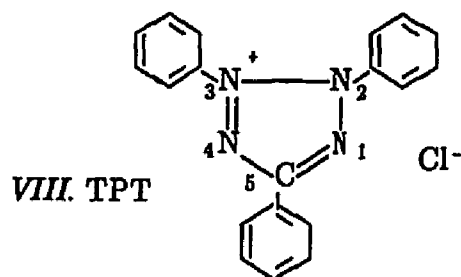
tightly bound to the cytoplasmic membrane [64, 65]. The periplasmic and cytoplasmic membrane systems have a high degree of connectance with the outer membrane and therefore the processes mediated by them were expected to be sensitive indicators of NCAC toxicity [59, 60].

VI. Chemistry and Biochemistry of Tetrazolium Salts and Formazans

Phenyl substituted quarternized tetrazoles (*i.e.*, tetrazolium salts) have long been employed in biological sciences as indicators of respiratory ET in a wide range of organisms and tissues [61 – 65]. In general, however, precise quantitative analysis of the various tetrazolium compounds has been limited, unavailable in the general literature, or unusable. This has given rise to a published assortment of incompatible chemical structures and *in vivo* reaction mechanisms, as well as a persistent series of erroneous extrapolations and conclusions derived from them (below). Although the present study was conducted using INT, most of the basic literature has dealt with the prototypical parent compound, triphenyl tetrazolium chloride (variously abbreviated as TPT, TTC, and TT). The following review, although not comprehensive, covers the pertinent literature on TPT and INT with respect to chemical structure, electrochemistry, and biochemistry. Several of the disagreements and ambiguities in published literature will be indicated, as will the need for resolution of fundamental questions.

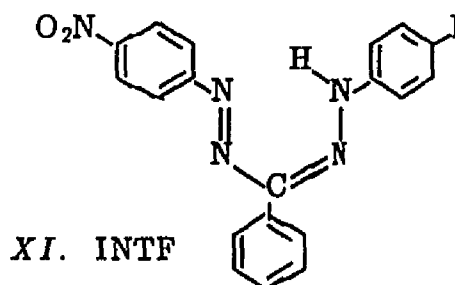
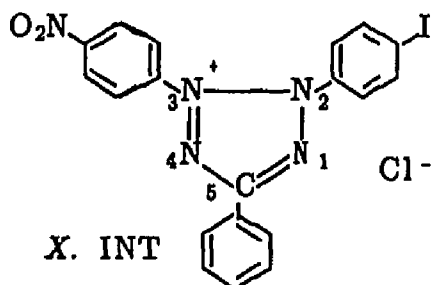
Triphenyltetrazolium chloride (TPT, *VIII*) and its substituted homologues have been used as indicators of biological electron transport since 1941 when it was recognized that they could be reduced *in vivo* to highly colored, insoluble products known as formazans (TPTF, *IX*) [62 – 65]. Since

then, over 1000 tetrazolium salts and their formazans have been synthesized and many of these have been applied to diverse research in chemistry [63], histology [65], botany and cereal science [67], microbial ecology [68 – 71], and aquatic toxicology [72 – 74].



INT (X), an iodonitro derivative of TPT, was first synthesized in 1950 as part of a systematic attempt to develop optimized tetrazolium compounds for biological research [75]. INT was shown to be more easily reduced by cellular electron transport systems to INTF (XI) than TPT, and had the further advantages of being biochemically substantive [75] and relatively insensitive to the effects of light and oxygen [63 – 65, 75].

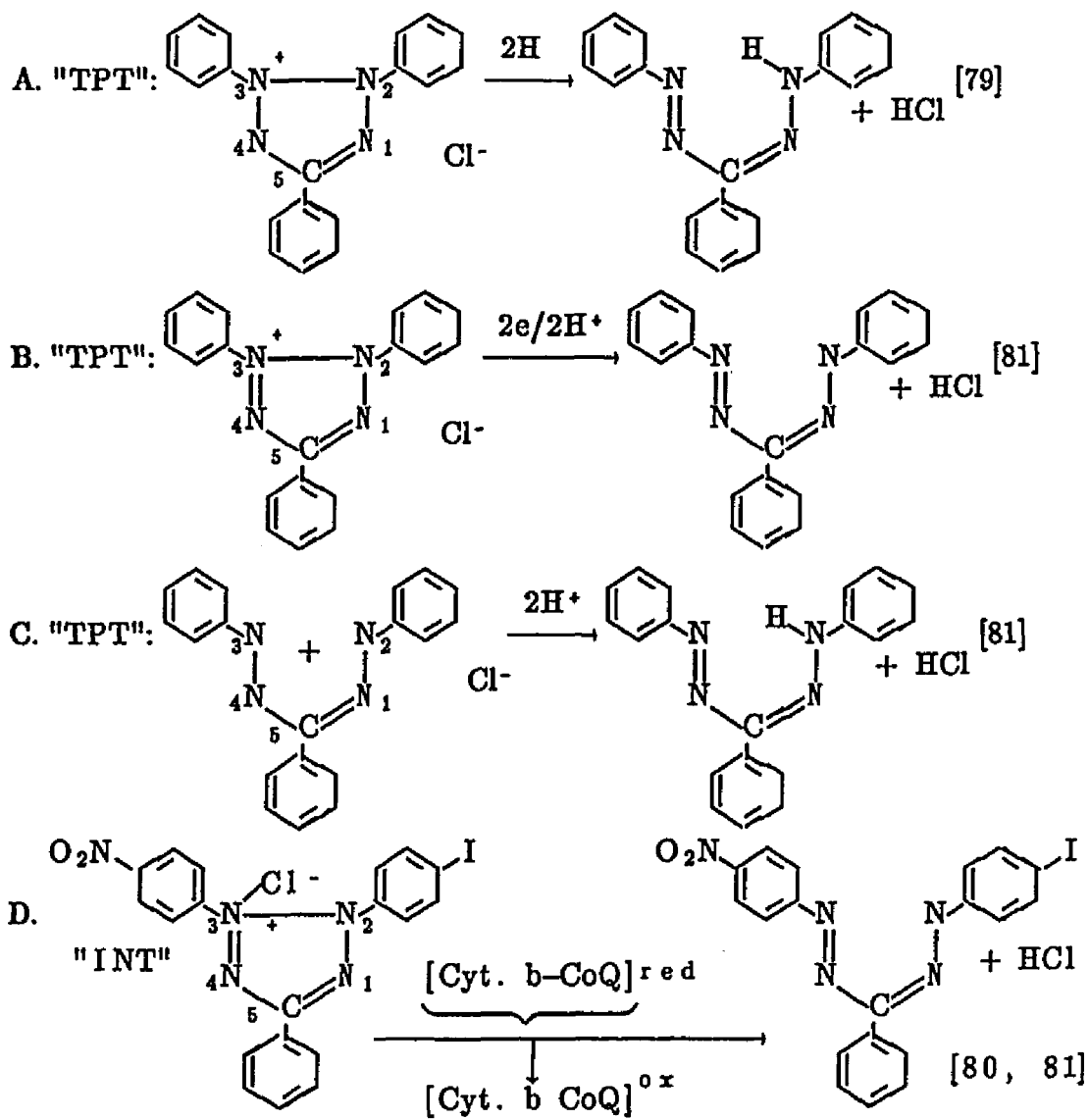
These chemical properties have made INT the electron transport indicator of choice for a number of recent studies, particularly those in which quantitative estimates of electron transport/oxygen reduction are desired [76, 77]. INT reduction is not inhibited



under aerobic conditions, and spectrophotometric determination of INTF color development has been shown to be directly related to the electron transport of chemicals in aqueous solutions and cell suspensions. However, the literature on many salient chemical and biological properties of TPT and INT shows that certain fundamental data on these tetrazolium salts frequently have been inconsistent or inaccurate. These difficulties typically have been manifested as inconsistent representations of chemical structures of TPT, INT and their formazans, TPTF, and INTF, respectively [67, 69, 78 - 81]; wide variance in measured electrochemical quantities such as half wave reduction potential ($E_{1/2}^{\text{red}}$) at the same electrode material [84 - 91]; and, interpretations of structure and $E_{1/2}^{\text{red}}$ with respect to reaction routes, mechanisms, and sites of biological reactivity [79, 81, 91, 92]. There also was a paucity of baseline toxicological data on INT/INTF, so that routine handling and disposal procedures could not be formalized [93].

Selected examples of disparate chemical structures and reduction routes for TPT, INT, and their formazans are given in Figure 1. It should be mentioned at this point that generally consistent representations of TPT, TPTF, and related compounds had been presented in *de novo* synthesis and reactivity papers published in the 1940's [62, 63, 65]. Unfortunately, these studies were conducted in German universities during World War II in research programs devoted to "disinfection" and therefore may not have received wide press or acceptance. Further, these and subsequent papers presented no high resolution quantitative analysis in support of the proposed structures or mechanisms [62, 63, 78], and sometimes featured inconsistent structures [78]. Since the late 1960's, competing structures and putative reaction routes have emerged in reputable journals, also lacking quantitative analytical

FIGURE 1. Examples of Published Structures and Reaction Routes for TPT, INT, and Their Formazans.



support (Figure 1). In some cases, faulty structures from one paper were copied incorrectly to another, resulting in a third variation [80, 81]. From the examples given in Fig. 1, it should be clear where these (and other) inconsistencies would leave a researcher trying to decide on reaction mechanisms and electron balance. It can also be seen why many authors have summarized the chemistry of tetrazolium compounds variously as artificial "hydrogen acceptors" [82], H^+ acceptors [67, 79, 83], hydride ion [65], and "electron pair" acceptors. It is not clear how the proposed reactants and products given in Fig. 1 are to be reconciled (they all supposedly indicate the same reaction) or applied to biological reductions.

VII. Electrochemistry of Tetrazolium Salts

Table 1 contains a summary of published $E_{1/2}^{red}$ values for TPT and INT measured at various working electrodes. The between-study variance in values obtained in similar media and electrode materials can be attributed to a number of factors including low resolution of measurement and a persistent disunity of sign conventions and descriptions of electroanalytical systems [94, 95]. It is noteworthy that studies of aqueous TPT \rightarrow TPTF reduction by organic redox indicators at neutral pH were conducted years before polarography was attempted and reduction potentials for the process were found to be between -0.080 and -0.083 V *vs.* the standard hydrogen electrode (SHE) [63, 67, 96]. Despite the existence of reduction potentials in this range, polarographic $E_{1/2}^{red}$ values on the order of -0.490 V *vs.* SHE are usually cited in biochemical literature [*e.g.* 65, 69, 91]. Many authors have attempted to use this value to infer sites of biological reduction of TPT based on estimates of electrochemical

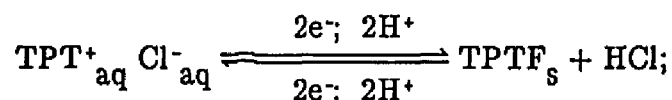
TABLE 1. Published Half-Wave Reduction Potentials ($E_{1/2}^{\text{red}}$) for TPT and INT at Different Working Electrodes.

<u>Compound</u>	<u>Medium/pH</u>	<u>Working Electrode</u>	$E_{1/2}^{\text{red}}$ (V vs. SHE)*	<u>Reference</u>
TPT	H ₂ O/7.0	Hg	-0.44	65
TPT	H ₂ O/7.2	Hg	-0.49	65, 91
TPT	H ₂ O/7.6	Hg	-0.37	89
TPT	H ₂ O/MeOH/7.0	Hg	-1.34	84, 85
TPT	H ₂ O/5.9	Pt	-0.337	84
TPT	H ₂ O/6.7	Pt	-0.332	84
TPT	CH ₃ CN	Pt	-0.21	86
INT	H ₂ O/7.2	Hg	-0.09	65, 91

* Converted to hydrogen scale by the author.

gradients *in vivo* [65]. As discussed later, however, direct comparison of electrochemical reaction mechanisms and $E_{1/2}^{\text{red}}$ values measured at electrodes with enzymatic redox couples in living systems is not necessarily valid.

Based on the chemistry of TPT, TPTF, and related species, hypothetical reaction routes such as the following are frequently cited:

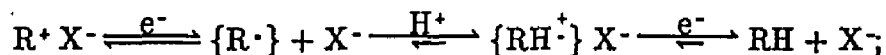


where the left side of the reaction represents a fully dissociated ionic salt and the right side the formazan precipitate. Although this reaction is balanced, there is no evidence to suggest ion pairing with chloride, especially in physiological reactions. Polarographic traces of TPT reduction typically contained three or more waves, with the first corresponding to generation of the formazan, and the others to reduction past formazan to diphenylbenzylhydrazidin and phenylbenzamidrizone [65]. In some studies, the first wave was proposed to be a 4-electron transfer leading directly to the hydrazidine and $E_{1/2}^{\text{red}}$ were obtained from composite waves [88, 91]. It has been noted that adsorption, catalysis, and maxima problems were encountered on Hg working electrodes [84], and it is possible that these conditions obscured important mechanistic observations. For example, many published polarograms show a slow reduction current beginning approximately + 0.3 V from the first maximum [65, 84, 87, 91], which was routinely ignored as an adsorption or contaminant artifact [91]. This is curious because the magnitude and reversibility of this current was shown to be pH dependent: at pH > 6.0, it became resolved into two apparently reversible reduction maxima [84, 91].

Moreover, it was known that the overall reduction of TPT to TPTF in aqueous solution and at Hg electrodes is influenced by pH, with ease of reduction and stability of the formazan increasing exponentially as the pH increases from 7.0 to 11 [85], although Pearse claims just the opposite with no data or citation [91].

It can be seen from Table 1 that the electrochemistry of INT has been studied much less than that of TPT. The substituted aryl groups on the former could be expected to give rise to complex behavior. Apparently there are no published $E_{1/2}^{\text{red}}$ values for reduction of INT to INTF on Pt or C in aqueous media.

Experiments in aprotic media suggest that tetrazolium salts such as TPT (and, by analogy, INT) undergo e.p.e. type reductions to their formazans on Pt electrodes [86]. Accordingly, the initial reduction is a reversible one-electron transfer leading to a tetrazolinyl radical which is then disproportionated by one proton forming a tetrazolinyl radical cation [86]. The radical then accepts another electron to yield the formazan;



where $R^+ X^-$ is the monotetrazolium halide, $\{R\cdot\}$ the tetrazolinyl radical, and RH the corresponding formazan. It should be noted that various aspects of this scheme are insecure, for example, the $\{RH^+\cdot\}$ species has not been demonstrated analytically. Also, electron spin resonance (ESR) studies of the tetrazolinyl radical $\{R\cdot\}$ have been equivocal, with different studies confirming both resonance-stabilized acyclic [97] and quarternized cyclic [93, 98] structures for this system. In protic media, TPT reduction at Hg and Pt electrodes has been

attributed to an e.e.p. sequence, with the disproportionation step occurring after the formation of a TPT anion by a two-electron reduction [84, 85]. In both aprotic and protic media, it has been repeatedly claimed that the primary product at electrodes is either a radical or anion, and that the formazan arises by a secondary chemical reaction that is thermodynamically favored [93]. Protonation was proposed as the rate limiting step in these models, which leaves open the question of the significance of the abovementioned pH effects.

VIII. Tetrazolium Salts and Biological Electron Transport

In addition to the mentioned inaccuracies in the presentation of structural, electrochemical, and mechanistic data on TPT, INT, and their formazans in published literature, there has also been widespread use of unsupported extrapolations from electroanalytical to biological systems. This has taken the form, primarily, of attempts to infer sites and mechanisms of tetrazolium salt reduction *in vivo* from data generated at Hg electrodes [*cf.*, 65 *et passim*]. This procedure involves the following assumptions: 1) *in vivo* redox potentials are known and electron transport mechanisms are well characterized, 2) adsorption/catalysis can be ignored in both biological and electrochemical systems, and 3) the behavior of redox indicators in the presence of enzymes, membranes, and heterogeneous chemical phases is well understood. In general none of these assumptions is justified. As a result of the heterogeneity and physicochemical disparity between biological and electroanalytical systems, sites of biological reduction of TPT, INT, and related compounds cannot be directly inferred from data generated at electrodes. Typically, $E_{1/2}^{\text{red}}$ values for biological electron transport chains (*e.g.* NADH → CoQ → cytochromes → oxygen)

are derived from low resolution experiments in model systems and from theoretical relationships between reactant-product free energy changes and $E_{1/2}^{\text{red}}$ [58, 59]. These estimates do not account for reactivity effects arising from microenvironments, catalysis, and quantum mechanical tunneling of electrons and protons in living systems [58]. Postulating sites of tetrazolium reduction along extended redox systems is further complicated by a lack of understanding of the mechanisms of interaction between electron transport proteins and carriers and the tetrazolium compounds of interest. For example, the most probable reduction route for TPT involves at least three distinct chemical species of widely disparate properties, and these need to be elucidated along with the detailed mechanisms of biological electron transport before reduction sites *in vivo* can be related to $E_{1/2}^{\text{red}}$ obtained *in vitro*. Pearse [91], Altman [65], and others have suggested that *in vitro* $E_{1/2}^{\text{red}}$ can be used to estimate relative "ease of reduction" of different tetrazolium compounds in biological systems, but this is suspect for reasons given above, and of questionable utility in any case. It is not clear how cathodic $E_{1/2}^{\text{red}}$ values (on Hg, no less) for tetrazolium salts *A* and *B* are to be related in biological systems when compound *A* might react at an iron-sulfur center, and compound *B* at a quinone under very distinct and different physicochemical conditions and *via* disparate chemical associations and ET mechanisms.

IX. INT and Toxicity Evaluation

Assuming a proportionality between bulk metabolic activity of a cell suspension and INTF formation [68], the total development of INTF in a given incubation period has been widely used to assess the metabolic status ("health")

and viability of cells and tissues [63, 65, 67, 83, 91, 92, 99]. Tetrazolium reduction assays of wastewater [74, 79], bacteria [73, 81], plankton [80], and protozoans [99], normally have been conducted by incubating cultures or cell free extracts with the indicators for 10 min – several hours in the presence of reduced cofactors (NADH, NADPH) and then extracting the INTF with an organic solvent followed by spectrophotometric quantification. Recently, a direct INT assay has been developed that does not require a formazan extraction step or long incubation periods with the dye [73]. In this procedure, the spectrophotometric time–rate of INTF formation was monitored and the "first–order" slope of the INTF vs. time function was used as an estimator of the metabolic status of control and toxicant–treated cells [73]. In toxicant treatments, decreases in rates of INTF formation relative to untreated controls were taken to be diagnostic indicators of toxicity.

The cited assay, however, suffered from a number of shortcomings, not the least of which were: aerobic *Pseudomonas alcaligenes* were grown beyond stationary phase (S–phase) and spent culture media was used as substrate for INT reduction, 2) only rate data from an undefined "first order" part of the curve were used, and variables such as kinetic response type (linear, sigmoidal, and parabolic) and lag period before observable INT reduction were not examined or mentioned [73]. It is well established that the growth of aerobic microorganisms beyond S–phase is accompanied by exponentially decreasing levels of dissolved oxygen, decreases in pH, and accumulation of respiratory endproducts and wastes in the culture medium [59, 60]. Progressive changes in these parameters normally has profound effects on the metabolic status of the culture (the onset of anaerobic respiration, senescence, and resting stages are observed), and the accumulation of wastes and H⁺ ions are sources of

physiological stress [60]. The use of spent media as a metabolic "substrate" is therefore a contradiction in terms. Further, when differential INT reduction rates are measured in control *vs.* toxicant-treated cells under these conditions, it is not clear that, 1) the response (ET rate) observed will correspond to the response of the same cells under optimal conditions (*i.e.*, there could be differences in reduction of INT by reduced *vs.* oxidized respiratory chains) [*cf.*, 80 for excellent demonstration of NAD(P)H concentration effects on ET] and, 2) population variances (s) of measured ET response are unbiased estimators of σ , or merely the result of stress-induced narrowing of the normal physiological range. That is, there are very real difficulties with the published assay in deciding what is causing the observed toxicity (there are uncontrolled stresses beyond the pollutant exposure) and whether an optimized culture might display a broader range of responses relative to the same pollutant dose (especially in undosed controls).

X. INT Reduction Kinetics and Bacterial Outer Membrane Characteristics

From the material reviewed above, it would seem that the design of any direct INT reduction rate assay should include the use of optimized cell systems and the data should explicitly encompass all kinetic response types. A major reason for this is that variations in kinetic responses in gram(-) bacterial systems would give information on outer membrane effects caused by toxicants. The outer membrane (also called "cell coat", "cell envelope", or "cell wall") is a thick lipid-protein assemblage surrounding the peptidoglycan sacculus, periplasm, and inner (plasma) membrane systems which acts primarily as a molecular sieve and is specific to gram(-) species. In contrast, gram(+)

bacteria are deficient in these lipid coats, and have thick layers of peptidoglycan [60]. In INT assays involving gram(-) bacteria such as *Escherichia spp.* and *Salmonella spp.*, lipoidal outer membrane layers must be traversed by the bulky INT molecule before reduction to INTF can occur (60). For passive and active transport of solutes in isothermal suspensions of *E. coli*, molecular weight (MW), hydrophobicity, and charge are the major determinants of penetration rate [60]. For example, pentose monosaccharides diffuse with rates two orders of magnitude greater than disaccharides of the same pentose [60]. This trend continues up to an "absolute" MW cutoff occurring around 600 daltons. With respect to hydrophobicity, for each 10-fold increase in octanol:water partition coefficient (uncharged species) there is a four- to five-fold decrease in penetration rate for cells with intact outer membranes. If the outer membrane is removed however, the same hydrophobic solute penetrates more readily. Compared with uncharged species of the same MW and hydrophobicity, negatively charged solutes have depressed penetration rates while positive charged species typically show significant increases [60]. It should be kept in mind, however, that these general rules of thumb tend to break down as the absolute MW cutoff is approached.

INT (FW = 505.7 for ion pair; without chloride counter ion, MW = 470.3, ignoring hydration) is close to the MW cutoff for *E. coli* outer membranes, exists as multi-ion (*i.e.*, in addition to the tetrazolium ring charge the 3-p-aryl-nitro group exists primarily as a zwitterion, *cf.*, structure X) and has a hydrophobic phenyl group, so significant diffusional lag times across *E. coli* outer membranes can be expected. Further, INT is hydroscopic and it is possible that packed water molecules exert cage effects that mask some or most of the cationic character as "seen" by the bacterium. Such an effect would tend

to further decrease the penetration rate of the molecule.

In INT assays, toxicant-mediated disruption or alteration of outer membrane structure/function (relative to untreated cells) can be expected to give rise to changes in transport rates of INT across the outer membrane to periplasmic and inner membrane reduction sites. Any such alteration of the diffusion rate to catalytic sites would be manifested as a change in lag period before detectable INTF production. The measurement of lag period before response should therefore provide valuable mechanistic information in cases where toxicants (or purposeful manipulation, *e.g.*, spheroplast generation) alter outer membranes, without increasing the time or labor needed to run an assay. The possible application of INT reduction rate data for inferring membrane effects has not been attempted or suggested in the literature, and the proposed link between membrane status and INT reduction kinetics constitutes a major hypothesis of this study. A primary reason why this kind of application has not been suggested is that utilization of tetrazolium compounds in aquatic toxicology has traditionally focused on the development of rapid assays measuring a single event: mortality (in the form of EC_{50} -type numbers). There has been very little work related explicitly to processes and mechanisms of toxicity. The rather static approach to tetrazolium reduction toxicity assays has worked hand in hand with a consistent oversimplification of conceptual models of tetrazolium compounds and their relationship to processes of biological electron transport.

XI. Toxicity of Tetrazolium Salts

The toxicity of tetrazolium salts has not been examined extensively [93].

Tetrazolium compounds are not only potential DNA complexing agents, but they may form persistent free radicals *in vivo* [93, 97], and yield metabolic products of toxicological significance. Work with cell systems ranging from bacteria, fungi, and protoctists, to higher plants, marine organisms, and mammals has demonstrated that, in general, tetrazolium salts penetrate plasma membranes and associate electrostatically with cellular components such as proteins and mitochondria [65]. Toxicity research on a limited number of tetrazolium salts has indicated "extreme toxicity" [93] in mammalian systems and sublethal doses evidenced neurological disorder. TPT was not found to be mutagenic in *Escherichia coli* or *Salmonella typhimurium* assays with or without metabolic activation, but an alkylated thiazyl derivative of TPT was a direct acting mutagen in both systems [93].

The purpose of this portion of the research was to examine some basic inconsistencies and uncertainties in the literature on INT and provide needed quantitative data. The experimental approach was aimed toward answering specific questions on INT chemistry that arose from bioassays and from insufficiently resolved problems in previous published work. An extensive review of the literature on tetrazolium compounds made it apparent that there has been widespread inconsistency and confusion on fundamental issues relating to these materials, and that basic quantitative data were lacking. Given these difficulties, it was not possible to formulate hypotheses and interpretations explaining the NCAC bioassay results. Further, without a consistent quantitative model of INT structure and electrochemistry, it was not possible to have great confidence in the claims of many recent papers. While interesting in itself, preliminary mutagenicity data were clearly necessary to formalize safe handling and disposal protocols for INT, INTF, and INT/INTF mixtures in the laboratory.

MATERIALS AND METHODS

All glassware was thoroughly washed and rinsed with distilled/deionized water, 4 N HCl, and absolute ethanol. As a precaution against photomodification of NCAC and bioassay reagents, all stock solutions were protected from light by wrapping appropriate flasks and tubes in aluminum foil. Starting solvents, solutions, media, and glassware were sterilized by autoclaving or 0.22 μm membrane filtration.

I. Reagents and Stock Solutions

Synthetic quinoline (Kodak Chemicals, Rochester, NY) and 4-azafluorene (4-AF; Aldrich Chemicals, Milwaukee, WI) were obtained in the highest purities available (99 % and 97 %, respectively) and were stored under nitrogen in a dessicator at 0°C. High purity tributyltin chloride (TBT) stock in pH 7.6 Hank's balanced salt solution (HBSS) buffer was provided by Dr. Charles Rice and was analysed for impurities by gas chromatography (GC). GC analysis gave TBT stock concentration at 5.4 parts per thousand with no detected contaminants or degradation products (*i.e.*, butenes). Stock solutions of working reagents were prepared daily using spectroscopic grade dimethyl sulfoxide (DMSO) for dilution. 4-AF crystals were taken up in small amounts (< 1 ml) of hot 100% ethanol and then diluted with DMSO. These master stocks were diluted to working dose levels prior to bioassays using 1:2 (v/v) DMSO:PBS (PBS = pH 7.2 phosphate buffered saline) [100]. The dilution of NCAC stock solutions with DMSO/PBS was exothermic and care was taken to

avoid thermal effects when treating test organisms in the bioassays (below). While DMSO was the primary nonaqueous solvent, additional experiments were performed using the following solvents in 1:2 (v/v) dilutions with PBS: spectroscopic grade acetone, 100% ethanol (punctilious), acetonitrile, hexane, and methanol.

Water soluble quinoline-HCl was prepared in a separatory funnel by dropwise addition of 4 N HCl to a biphasic quinoline-H₂O system. When solvation of quinoline appeared complete, solution homogeneity was tested by placing aliquots in borosilicate flasks in the beam of a Hughs 3221H red laser. Scattering of light from micelles was not observed indicating an aqueous quinoline-HCl solution. An identical H₂O-HCl blank was prepared without quinoline for use as a control.

INT (2-(*p*-iodophenyl)-3-(*p*-nitrophenyl)-5-(phenyl)-2*H*-tetrazolium chloride; Sigma Chemicals, St. Louis, MO; and Kodak Chemicals, Rochester NY) and INTF (2-(*p*-iodophenyl)-3-(*p*-nitrophenyl)-5-(phenyl)-formazan; Sigma) were obtained by priority mail and were immediately purged with nitrogen and placed in a dessicator at 0°C. After using both the Sigma and Kodak products for more than a year, it was decided that the Sigma INT was preferable for the purposes of this research, even though the HPLC behavior and Fourier transform nuclear magnetic resonance (FTNMR, below) spectra of the two products were in agreement. This preference was based on qualitative observations of appearance, batch consistency, and solution behavior of INT from each source. INT for electrochemical analysis was recrystallized twice in hot, 100 % ethanol and the crystals were dried in the dark. INT stock solutions were prepared by weighing 65 mg INT into 1 ml of absolute ethanol followed by

dilution with 9 ml H₂O. The mixture was heated in a hot water bath until the INT was dissolved, and the resulting solution was passed through a 0.22 μm polycarbonate filter (Nucleopore Corp., Pleasanton, CA, 94566). Care was taken to avoid exposure of INT solutions to light. This precaution was observed because it is explicitly indicated in many publications. Nevertheless, preliminary experiments with INT in pyrex flasks exposed to filtered sunlight showed no photomodification after 30 min. – 1.5 h. exposures, as inferred from FTNMR spectra and retention times on an HPLC C-18 column.

Concentrated stocks of phenazine methosulfate (PMS; Sigma) and reduced nicotinamide adenine dinucleotide (NADH; Sigma) were mixed in sterile pH 7.4 phosphate buffered saline and diluted to final concentrations of 0.070 μM and 10 μM , respectively. Both solutions were 0.22 μm filtered and stored on ice in foil wrapped glass tubes until analysis (below).

II. FTNMR Analyses

INT and INTF standards (Sigma, Kodak) were dissolved in hexadeuterated dimethyl sulfoxide (d_6 -DMSO), 0.22 μm filtered, and transferred to sample tubes for Fourier transform nuclear magnetic resonance spectroscopy (FTNMR). ¹³C and ¹H spectra were run for all standards on a high field General Electric QE 300 NMR Spectrometer and NMR-consistent chemical structures for each compound were generated using substituent chemical shift data (δ_{ppm}), and peak integral – elemental composition methods [34, 101].

Approximately 45 ml of an S-phase *E. coli* culture (see VI, below) in liquid broth was treated with 1.3 mM INT, incubated for 10 minutes at 29° C, and centrifuged for 10 minutes at 1200 *g*. The supernatant was decanted and

the pellet extracted with small volumes of acetone and water in a separatory funnel. The red organic extract containing INTF was recovered, dried under reduced pressure, and the resultant material was dissolved in d_6 -DMSO for NMR analysis. Initial ^1H spectra were analysed at frequencies corresponding to δ_{ppm} 0 – 10.5. After determining that only the reference TMS and H_2O peaks were present between δ_{ppm} 0 – 7.0, only the aromatic spectra (δ_{ppm} 7.0 – 9.0) were recorded.

III. Spectrophotometry

With the exception of the spectrochemical analysis of INT (below), all spectrophotometry was accomplished using a Shimadzu UV 160 double beam recording spectrophotometer with a temperature-controlled Microflow cuvette carriage (Shimadzu Instruments Inc., Columbia MD). The Microflow unit was connected to a water bath incubator *via* peristaltic pump and this allowed for maintenance of constant solution temperature during bioassays.

UV-visible electronic absorbance spectra for NCAC's and bioassay reagents were generated using Hellma QS 1000 quartz cuvettes (10 mm). INT bioassays (below) were conducted at $\lambda = 490$ nm in Fisher Brand optical glass (> 360 nm) cuvettes. All analyses were conducted at $31 - 37.5^\circ \text{C}$. This range of assay temperatures resulted from changes in room temperature and the inability of the Microflow unit to compensate fully for low temperatures in a poorly-heated lab with an exhaust hood running. The within-assay temperatures were periodically monitored by inserting a thermometer into the reference cuvette solution, and were found to vary by less than 2°C .

IV. Electrochemistry

Extensive analyses were undertaken to arrive at an understanding of the aqueous electrochemistry of INT, and to address conceptual difficulties in the published literature. A primary objective was to estimate the potential at which the reduction of INT to INTF begins at various electrodes and to postulate reduction mechanism(s). Other experiments were designed to explore the use of various electroanalytical systems in the examination and quantification of pollutant redox effects in buffered aqueous media and, possibly, in simulated biological media.

All electrochemical work was performed in the laboratory of Dr. Robert J. Gale (Department of Chemistry, Louisiana State University, Baton Rouge, LA) with the supervision of Dr. Gale, and the assistance of Dr. Roberto L. Wong and Dr. Kenneth R. Carney. Analyses were conducted at room temperature with three electrode cells consisting of Ag/AgCl or saturated calomel-KCl (SCE) reference electrodes; platinum mesh, platinum plate, dropping mercury (DME), vitreous carbon, vitreous carbon rotating disc (RDE) and glassy carbon/Pt rotating ring disc (RRDE) working electrodes; and platinum wire counter electrodes [102]. Solutions of INT (1.0 – 10 mM) were prepared as above in sterile pH 7.2 phosphate buffered saline (PBS), with additions of absolute ethanol as needed to prevent filming of the water insoluble INT reduction products. Samples were deoxygenated with dry argon or nitrogen prior to analysis, and electrodes were cleaned with concentrated HNO₃, H₂SO₄, acetone, and absolute ethanol between runs. Hardware included a EG&G/PAR Potentiostat/Galvanostat (Model 273), PAR Polarographic

Analyser (Model 384), PAR Differential Amplifier (Model 116), Pine Instruments RDE3 Potentiostat, Hewlett Packard 7044a X-Y recorder, and Tektronix DS 468 Oscilloscope.

Two spectroelectrochemical systems were assembled for the purpose of establishing the potential at which the onset of INT reduction occurs and for evaluating the use of spectroelectrochemistry for future assays.

1. Reflectance spectroelectrochemistry: An SCE reference, and Pt wire counter electrode were fitted into a cubic teflon reaction chamber (5 cm sides) with a post electrode containing a polished 1 cm² Pt plate at its apex. The electrode was positioned so that a thin cell existed between the plate and a quartz window in the wall of the reaction chamber which was filled with INT-saturated PBS. The reaction chamber was positioned so that the window and the platinum plate electrode were in the beam of a Hughs 3221 H-PC red laser, which was reflected at right angles to a photodetector. The laser beam was modulated using a 42.6 Hz chopper which was monitored by an infrared diode. The reaction chamber electrodes were connected to a D.C. voltage source (EG&G/PAR Potentiostat/Galvanostat Model 273), the working plate electrode, photodetector, and the infrared diode were connected to a PAR Model 116 Differential Amplifier which was connected to the oscilloscope and the X-Y recorder. Since it was not possible to enclose this large system in a Faraday cage, extraneous sources of EMR (fluorescent lights, outlets, other analytical equipment), noise from the power source, and all internal junctions had to be identified and filtered. The function of the amplifier was to discriminate between background signals (intensities = mA to A) and the relatively small sample signal ($\approx \mu\text{A}$) from the reflected laser light reaching the

photodetector. It was hypothesized that the electrodic reduction of INT to INTF_{ads} (aqueous $\lambda_{\max} = 480$ nm) would result in adsorption of intermediates and products and, consequently, decreased absolute reflectance off the working electrode. This would be manifested as decreased amplitude of the 42.6 Hz signal which would be isolated by the amplifier and related to the working potential range. The entire system was enclosed in a black wooden shed to prevent extraneous light from impinging on the photodetector. Voltage was swept from +1.000 to -1.000 V *vs.* SCE.

2. Spectrophotometric analyses of the reduction of 10^{-2} M INT solutions in 50 % PBS/ethanol (v/v) were accomplished using a three electrode cell fitted into 10 mm diameter spectrophotometric cuvettes. The sample beam was directed into the Pt-mesh and transmittance was set instrumentally to 100%. The reference cuvette contained the INT solution and a Pt-mesh electrode with no applied potential. Specifications: SCE reference, 1 cm² Pt-mesh working electrode, and Pt-wire counter electrode; transmittance monitored at 490 nm *vs.* applied voltage using a Beckman Double Beam UV/Visible spectrophotometer, negative sweep @ 1 mV/sec from +0.35 V to -1.0 V *vs.* SCE.

Additional experiments at various electrodes were performed using normal and differential pulse polarography (NPP and DPP, respectively), and cyclic voltammetry (CV). First wave characteristics prompted questions as to whether currents measured in NPP and DPP on vitreous carbon were faradaic. Using the RDE, mass transport controlled reduction was tested by observing

first wave reduction characteristics and solving the Levich equation (done entirely by computer):

$$i = 0.62nFD^{2/3}\nu^{-1/6}c^{\infty}\omega^{1/2},$$

where i is limiting current density, n number of electrons transferred, F is the Faraday constant, D is diffusivity (cm^2/s), ν is kinematic solution viscosity (viscosity/density; cm^2/s), c^{∞} is bulk solution concentration (M), and ω is rotation rate of RDE (s^{-1}). Except when a reaction limits the current, this equation describes the rotation rate dependence of cathodic (and anodic) limiting currents at high overpotentials (in this case, a relatively fast sweep). At a constant rotation rate limiting currents can be related to electrons transferred in a particular wave. Solutions of 0.2×10^{-7} M INT in 1:1 PBS/ethanol (v/v) were analysed ($\omega = 2\pi \text{ rev./s} = 6283 \text{ s}^{-1}$, sweep = 100 mV/s) in a sealed chamber which was degassed between runs. The diffusion coefficient of INT was estimated to be $3.8 \times 10^{-6} \text{ cm}^2/\text{sec}$ using the Hayduk-Laudie chemical constituent method [103]. For comparative purposes, this method was applied to TPT and the estimated D was found to be in error by 14% relative to the experimental D value obtained by Tiselius [84].

Dependence of the first reduction wave on pH was tested using NPP on vitreous carbon with 10^{-2} M solutions of INT in pH 3, 9, and 12 PBS/EtOH (1:1) scan rate 10 mV/s. RDE experiments using DPP in the presence of 10^{-2} M INT were conducted to detect underpotential production of hydrogen (H_2). Conditions: scan 1; C disk 0.0 V vs. SCE (static), Pt ring; swept positive at 100 mV/s from -0.3 V to $+0.5$ V vs. SCE. Scan 2; disk -0.180 V vs. SCE; ring swept positive as above (∂t between scans ≤ 10 s). All solutions were degassed

for 30 min between runs with dry argon, and the working electrode was cleaned and polished.

V. Identification of a 4-azafluorene Oxidation Product

Stock solutions of 4-AF were unstable and chromogenic reactions between 4-AF degradation product(s) and DMSO were observed repeatedly (see Results and Discussion, Section V). Solutions of the 4-AF products in DMSO were spotted on thin layer alumina chromatography plates (TLC) and eluted with an acetonitrile:acetone (75:25 v/v) mobile phase. Developed plates were examined under UV lamps ($\lambda = 254$ nm and 350 nm) and resolved bands were excised and extracted with fresh acetonitrile followed by 0.22 μ m filtration and volume reduction under dry nitrogen. Samples of each extract were then applied to the probe of a DuPont 21-492B MS double-focusing sector mass spectrometer with electron ionization. Spectra were recorded for each of the TLC bands and for 4-AF and quinoline standards.

VI. Microbiological Techniques

Isolates of *Escherichia coli* were obtained from 0.45 μ m filtered Rappahannock River VA surface water using a standard recovery procedure [104, 105]. Eight presumptive ($P \leq 0.01$) *E. coli* isolates meeting the requirements of this procedure were streaked onto brain-heart infusion (BHI) slants and designated as E₁, E₂,... E₈. Colonies from each were transferred to BHI broth and incubated at 44.5 °C with gyrorotary shaking (100 rpm). Growth curves were monitored using optical density at 650 nm and the strain

exhibiting most rapid growth under these conditions was selected for characterization using standardized *in vitro* diagnostic assays for *Enterobacteriaceae* (api20E; API Analytab Products, Plainview NY). The selected strain was conclusively identified as *E. coli* using these procedures ($P \leq 10^{-6}$) and was used in all further work.

Routine preparation of stationary phase (S-phase) *E. coli* test suspensions was performed as follows: cells were picked from BHI slants and transferred to 20 ml of BHI broth and grown overnight at 35.5 – 37.5° C. This culture was amended to 300 ml of fresh BHI broth in 500 ml Erlenmeyer flasks and incubated at 35.5 – 37.5° C with gyratory shaking (100 rpm) for 6.5 – 8.0 h. The S-phase culture medium was transferred to sterile 50 ml polycarbonate tubes at room temperature and centrifuged for 20 min at 1200 *g* in a Sorvall RB-5C centrifuge. The supernatant was decanted and the pellet resuspended to the original volume in sterile PBS containing 0.14% agar. The 0.14% agar increased the viscosity of the suspension medium so that sedimentation during subsequent pipeting steps was minimized. The suspension was vortexed vigorously for 90 s and then sonicated using a Sonifier Cell Disruptor Model W185 (Heat Systems/Ultrasonics Inc. Plainview NY) on the lowest setting (5 one-second bursts). The suspension was again vortexed for 90 s and allowed to stand for 10 min in the incubator. This was used as the starting test suspension for all bacterial bioassay procedures described below.

Isolates of wild type (+) *Streptococcus salivarius* and (+) *Salmonella typhimurium* (118/100 A) were obtained from Ms. Martha Rhodes (Bacteriology Department, Virginia Institute of Marine Sciences, Gloucester Point, VA, 23062), and deep rough (*rfa*) mutants of *S. typhimurium* (TA 98, TA 100) were donated by Dr. Bruce N. Ames (Department of Biochemistry, University of

California, Berkeley, CA). The latter were tested for genetic markers and processed according to protocols [106].

S. salivarius was incubated aerobically for 10 h in BHI broth at 35.5° C with gyrorotary shaking (100 rpm). The (+) and (*rfa*) *Salmonella typhimurium* cultures were grown with the same specifications for 12 h in nutrient broth (Oxoid No. 2, Oxoid USA, Columbia MD). Following incubation, all cultures were taken through the centrifugation–PBS resuspension procedures described above for *E. coli*.

VII. Electron Transport (INT Reduction) Assays

Rates of electron transport (ET) were estimated in the cell systems mentioned above using the reducible dye INT. Using bacterial stock solutions prepared as described above, the procedure summarized in Figure 2 was used for INT assays (modified from reference 73):

Routine controls for these assays included: 1) a "killed" control which followed the assay procedure above using autoclaved cells, 2) NCAC control which tested for reaction between INT, the toxicant, and supporting media in the absence of cells, and 3) solvent control (0.2 ml solvent with no toxicant). Results of the latter control are reported in the results as dose = 0.

VIII. Viable Cell Enumeration

Viable cell densities of *E. coli* test suspensions and NCAC treatments were estimated using direct counts (epifluorescence microscopy) and overnight culture procedures on BHI agar. Cells were prepared for enumeration

FIGURE 2. Revised Direct INT Reduction Assay Procedure.

1.5 ml of bacterial stock culture (10^9 cell/ml)
added to 12 ml dilution tubes containing
0.7 ml PBS/0.3 ml BHI at 37.5° C.

↓

vortexed 3 sec. and placed in water bath
at 37.5° C for 40 min.

↓

0.2 ml of NCAC dose in 1:2 DMSO/H₂O, or
0.2 ml of solvent system (control)
was added to culture; vortexed 3 s; n = 3 - 6.

↓

60 min incubation, 37.5° C.

↓

0.3 ml BHI and 0.2 ml INT solution added to culture
in the water bath, vortexed 1 s, culture transferred to
spectrophotometer; INTF absorbance *vs.* time
monitored immediately at $\lambda = 490$ nm for 210 s.
Electron transport rate given as change in absorbance
at 490 nm per 30 s time interval.

Reference cuvette: all ingredients except INT
which was replaced by 0.2 ml PBS.

↓

Recorded lag time (s) before burst of INTF formation using a stopwatch
(for untreated cultures, lag time typically 60 - 100 s)
and maximum rate of INTF formation per 30 s interval
(*i.e.*, maximum slope of absorbance *vs.* time).

immediately after the 60 minute incubation period shown above for the INT assay.

Direct counts were performed using a procedure adapted from Haas [*pers. comm.*]. Cell suspensions were diluted to approximately 10^6 cells/ml in PBS. 2 ml was placed in a glass column fastened over 0.22 μm Nucleopore polycarbonate filters on vacuum flasks. The filters had been soaked for 24 h in 0.2 % irgalan black (Ciba-Geigy) to provide an opaque background. Forty μl of 6% glutaraldehyde was added followed by 200 μl of 4',6-diamidino-2-phenyl indole ("DAPI", 0.01 % in distilled H_2O , w/v; Sigma). After 2 minutes, 40 μl of 3, 6-diaminoacridine ("proflavin", Sigma, 0.033 % in distilled H_2O , w/v; Sigma) was added followed by incubation at room temperature for 10 min. The mixture was filtered at low vacuum (≈ 20 mm Hg) and the filter mounted on a glass slide.

Observations of DAPI-proflavin treated cultures were made using a Zeiss standard epifluorescence microscope equipped with an HBO Hg lamp and 63X and 100X PlanNeoFluor objectives. The cytoplasm of *E. coli* was stained with proflavin and fluoresced green whereas the DNA of the cells stained with DAPI fluoresced blue. Use of both stains provided a means of cross referencing any equivocal fluorescence that may have arisen from non-cellular staining in the visual field.

IX. Spheroplast Generation

E. coli test suspensions prepared as described and resuspended in pH 7.4 PBS (without 0.14% agar) were centrifuged at 1500 g (27 $^{\circ}\text{C}$, 40 min). The

pellet was resuspended to the original volume in 10 mM Tris buffer (tris(hydroxymethyl)-aminomethane) containing 10 mM ethylenediaminetetraacetic acid (EDTA), and 1 % decyl sodium sulfate (DSS). The suspension was ultrasonicated at low frequency for 15 s and allowed to equilibrate for 5 min at room temperature. The culture was then centrifuged for 30 min (1500 *g*; 27 °C) and the pellet resuspended in PBS (pH = 7.4). 2 mg/ml of fresh lysozyme (Sigma) was added with gentle swirling followed by incubation at room temperature for 12 min. The cells were centrifuged (1500 *g*; 27 °C) and the pellet was resuspended in 5 ml of 100 mM Tris buffer followed by rapid dilution to 1 mM with PBS. The resulting spheroplasts were vortexed, centrifuged again for 20 min (1500 *g*) and resuspended to the desired final volume with PBS. This suspension was held in an incubator at 37.5 °C and INT analysis was performed in the absence of organic solvents or toxicants.

Spheroplasts were lysed by treatment with 1 % DSS and 0.2 N NaOH solutions followed by equimolar additions of 0.2 N HCl. Lysates were assayed for INT activity before and after 0.22 μ m membrane filtration.

X. Oxygen Consumption Assays

Ninety ml volumes of sterile PBS were bubbled with air for 2 h in a water bath incubator at 37.5 °C, and then analysed for oxygen content using a Strathkelvin Model 781b Oxygen Meter (Strathkelvin Instruments, Beardsden, Glasgow, UK). Ten ml *E. coli* cultures were prepared as per the INT assay protocol and added to 90 ml of O₂-saturated PBS in the water bath. At 60 s intervals, 1 ml aliquots were introduced to the electrode chamber and percent O₂ saturation values were recorded over a 15 min time period. This was repeated

in duplicate for 1) control cultures and, 2) NCAC treatments at various doses.

XI. Transmission Electron Microscopy (TEM)

Four *E. coli* suspensions grown and prepared according to the INT assay protocol were treated with 0.2 ml INT stock solution and fixed with 3 % glutaraldehyde/0.1 M sodium cacodylate after reaction times of 0, 2, 5, and 12 minutes. Two further cultures were treated with 37 parts per million (ppm) quinoline-HCl and incubated along with a solvent control culture (containing the acidified H₂O supporting solvent in the absence of quinoline) for 60 min. at 37.5 °C. Afterwards, 0.2 ml of the INT stock was added to one quinoline-HCl treatment which was fixed as above after 2 minutes. The other quinoline-HCl culture and the solvent control were fixed without the addition of INT.

Fixation, mounting, cutting, and microscopy of samples were performed by Ms. Patrice L. Mason (Department of Histology, Virginia Institute of Marine Sciences, Gloucester Point, VA 23062). The fixation procedure was modeled after a standard glutaraldehyde/OsO₄ procedure [107]. Samples were cut on a Reichert-Jung Ultracut E and photographed on Hitachi HU-11B TEM and Zeiss CEM902 transmission electron microscopes.

XII. NADH-PMS-INT Assay

The non-enzymatic reduction of 0.2 mM INT by 5 μM NADH was measured spectrophotometrically at $\lambda = 490$ nm in PBS, pH 7.4. Assays were run in triplicate with and without addition of 0.02 μM phenazine methosulfate (PMS), a flavin analogue, in PBS. The effects of DMSO and 30 ppm quinoline

in DMSO on the rate of INT reduction were measured in all treatments.

XIII. Eukariotic Cell Systems and Cell Free Preparations

1. Macrophage INT Assay

Peritoneal macrophages were obtained from the toadfish *Opsanus tau* using a 50 ml glass syringe with a 18 guage spike [108]. The peritoneal cavity was flushed repeatedly with physiological saline (Hanks Balanced Salt Solution, HBSS; 6 ppt salinity, pH 7.6) and fluids from several fish were combined in sterile centrifuge tubes. These were centrifuged for 10 min at 550 *g*, followed by resuspension of the pellet in small amounts of buffer until cell numbers of $2 - 4 \times 10^8$ were achieved, based on cell counts of serial dilutions. The macrophages were stored in HBSS at

15 °C. Stock solutions of phorbol myristate acetate (PMA) and calcium ionophore A23187 (CI) in DMSO were diluted in HBSS to final concentrations of 0.16 μ M and 1.6 μ M, respectively [116]. 0.2 ml of macrophage suspension was treated with buffer, PMA, or CI, followed by addition of 0.2 ml of 10^{-4} M INT solution and absorbance at $\lambda = 490$ nm was monitored for 210 s in 0.5 ml optical glass cuvettes.

2. Marine Phytoplankton-INT Assays

Mature liquid cultures of two species of *Tetraselmis sp.*, *Chlorella sp.*, *Monochrysis sp.*, *Isochrysis sp* (Tahitian), *Dunaliella sp.* were provided by Mr. D. Abernathy (VIMS, Gloucester Pt., VA). Chlorophyll absorbance was measured at 560 nm and culture volume was adjusted with filtered York River water (salinity = 11 ppt) to provide a common chlorophyll density between

cultures. 15 ml of each culture was treated with 0.8 ml of INT stock, placed in sunlight for 6 hours and examined visually for INTF production every 2 hours.

3. Chemical Reduction of INT

NADPH in PBS was screened to determine its ability to directly reduce INT at physiological pH, and the time requirements for this process. Ascorbic acid was also tested in PBS and PBS adjusted to pH > 9.0 with 4 N NaOH. The reduction product(s) of the ascorbic acid treatment were subjected to FTNMR. Sterile solutions of NADPH solutions (pH 7.4, 5 mg/ml) were amended with 0.4 ml INT stock and absorbance spectra were recorded every 15 minutes for 3 h.

4. S-9 Preparations

Liver S-9 preparations from the spot *Leostomus xanthurus* were prepared by Mr. D. Sved from pooled corn oil- and 3-methyl cholanthrene (3-MC)/corn oil-injected (10 mg/kg body weight, IP) specimens kept in aquaria. To 50 μ L of the S-9 mix, 50 μ L of tris (1 μ M), 100 μ L NaCl (0.5 M), 0.400 mM NADH, and 33 μ L INT (0.1 mM) were added followed by monitoring of absorbance *vs.* time at $\lambda = 490$. Maximum ET for blanks (no S-9), carrier control S-9, and 3-MC-treated S-9 were recorded (N = 2).

XIV. Mutagenicity Evaluation of INT and INTF

Standard mutagenicity testing was performed on unpurified INT and INTF using the Ames/*Salmonella* assay according to protocols [106]. Strains TA97, TA98, TA100, and TA102 were used in spot tests and TA 98 and

TA 100 for preincubation tests. Test solutions were INT in PBS, INTF in 50% EtOH/PBS, and an equimolar INT/INTF mixture in 50% ethanol/PBS exposed to laboratory light for 3 hours. Phenobarbital induced rat liver S-9 (Litton Bionetics Inc., Charleston, S. C. 29405) was preincubated with the test solutions and bacteria for 20 minutes at 45^o C, followed by culturing.

In addition to the Ames assays, it was of interest to examine the ability of INT and INTF to interact with DNA *in vitro*. Two strains of *E. coli* containing the human oncogene plasmids PSV₂-neo or VERB-b (ATTC, Bethesda, MD) were grown in 50 ml ampicillin/tetracycline nutrient (LB) media (BRL, Bethesda, MD) and tested for the presence of plasmids by streaking onto ampicillin containing LB agar (the plasmids are coextensive with with the antibiotic resistance "R-factor" plasmid, PBR 322). Viable isolates were transferred to 500 ml LB nutrient broth and grown overnight at 37.5^oC with gyratory shaking (100 rpm). Aliquots of the S-phase culture were then transferred to 2 L flasks containing ampicillin/tetracycline and grown overnight under similar conditions. When cultures reached the midpoint of log phase (based on OD₆₄₀), multicopy plasmids were amplified by treatment of cultures with 3 ml of sterile chloramphenicol stock (34 mg/ml).

After 10 h incubation in the presence of chloramphenicol, cells were pelleted by repeated centrifugation (7-12 x 10³ g) and DNA was extracted and purified by standard phenol/chloroform/isoamyl alcohol methods [109]. Precautions for handling, storage, and disposal of human oncogenes were observed. After final ethanolic precipitation of plasmids, VERB-b extracts were given to Dr. L. Ellis for DNA probe work in *Crassostrea virginica*, and the 5.4 kB PSV₂-neo plasmid was retained for the present work. The plasmid pellet was resuspended in sterile TE buffer and stored at 0^o C. DNA

concentration and purity were estimated spectrophotometrically using absorbance at $\lambda = 260$ nm according to the following:

1 absorbance unit (@ $\lambda = 260$) \cong 50 $\mu\text{g}/\text{ml}$ DNA.

$\text{Abs}_{.260}/\text{Abs}_{.280} \cong$ % purity [117].

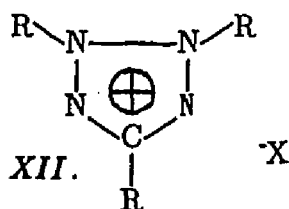
Hence, after correction for purity, plasmid DNA was estimated to be 476 $\mu\text{g}/\text{ml}$. The PSV₂-neo plasmid fraction was then assayed using submerged agarose gel electrophoresis (SAGE) with various starting dilutions of plasmid DNA, and agarose concentrations between 1.0 – 1.3%. 10 – 20 μl aliquots of plasmid and standards (1 kB supercoiled and linear ladder DNA standards; BRL Products, Bethesda MD) were placed in sterile wells and diluted to desired concentrations with a glycerol/EDTA/SDS stop solution. After many trial runs, the following parameters were used for all SAGE: 1% agarose (volume = 65 ml), 12 well comb, 20 μl injection volume, 2×10^{-2} stock dilution, $i = 11$ mA, $V = 24$ V, run time = 16 – 24 h, gels stained with approximately 1 mM ethidium bromide (EB, Sigma) in TEB [109] buffer and read using a Spretroline Model TR-302 Transilluminator (excitation $\lambda = 302$ nm, fluorescence $\lambda = 590$ nm). After conclusive identification of the supercoiled PSV₂-neo plasmid band, the supercoiled fraction was separated from a "nicked" circular population using preparative SAGE on low melting point 1% agarose followed by phenol/chloroform extraction (3 X) and NaCl/ethanol precipitation. Next, 20 μL of 1 mM INT, 1 mM INTF, and 1 μM EB stocks were amended to 1.4 μg 1 kB supercoiled ladder and 2.0 – 2.5 μg of purified PSV₂-neo plasmid extract and relative mobilities (cm) were recorded. Treatment of 1 – 20 kilobase (kB) plasmids with EB results in significant

unwinding of the supercoiled helix, causing changes in electrophoretic mobility. Any significant alkylation or intercalation of DNA by INT or INTF would cause molecular volume increases and concomitant reductions in mobility relative to untreated DNA. The magnitude of this reduction could be referenced to EB treatments and used to infer relative degrees of reaction between the tetrazolium salt and DNA. As a result of time and financial constraints, dose *vs.* mobility assays were not conducted.

RESULTS AND DISCUSSION

I. Chemical Structure and Solution Behavior of INT and INTF

Figure 3 contains the aromatic portion of the ^1H FTNMR spectra for INT, INTF, and the acetone extract from INT-treated *E. coli* cells along with consistent chemical structures. ^{13}C FTNMR spectra were run on all standards and were in agreement with elemental composition values provided by the manufacturers. The presented ^1H spectrum for INT is superior to a published ^1H INT spectrum, which was generated using a low field instrument containing no peak pick or integral data [110]. The poor resolution of the cited spectrum and the lack of supporting data made independent verification of postulated chemical structure impossible [110]. One author [93] has suggested the following structure for the tetrazolium ring:



The stated rationale for this structure [93] was that electronic resonance structures can be drawn with positive charges located at each tetrazolium ring position, and therefore representation XII is qualitatively superior to those with localized double bonds (*cf.*, structure X, above). A shortcoming of representation XII is that it suggests an equivalence of the tetrazole ring

FIGURE 3. Fourier Transform Nuclear Magnetic Resonance (FTNMR) Spectra. A. INT standard. B. INTF standard. C. Acetone extract from INT-treated *E. coli* cells.

FROM 8.62
TO 8.54 PPM
INTEGRAL= 7092.50

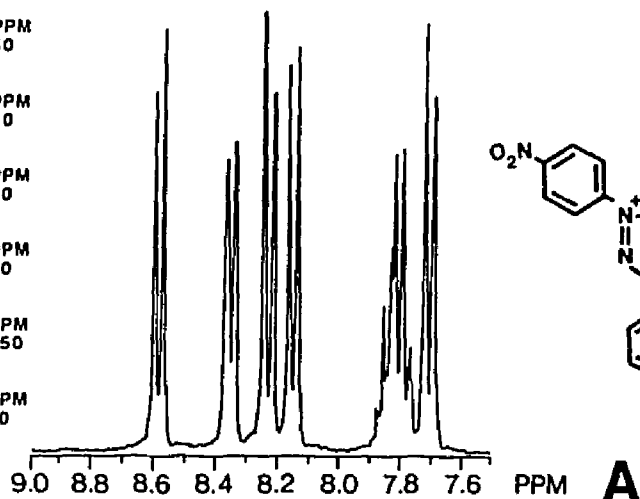
FROM 8.39
TO 8.31 PPM
INTEGRAL= 7127.50

FROM 8.26
TO 8.18 PPM
INTEGRAL= 7480.00

FROM 8.18
TO 8.10 PPM
INTEGRAL= 7342.50

FROM 7.89
TO 7.74 PPM
INTEGRAL= 11487.50

FROM 7.74
TO 7.66 PPM
INTEGRAL= 7385.00



FROM 8.29
TO 8.21 PPM
INTEGRAL= 2489.06

FROM 8.21
TO 8.17 PPM
INTEGRAL= 325.93

FROM 8.06
TO 7.99 PPM
INTEGRAL= 2234.68

FROM 7.93
TO 7.85 PPM
INTEGRAL= 2634.68

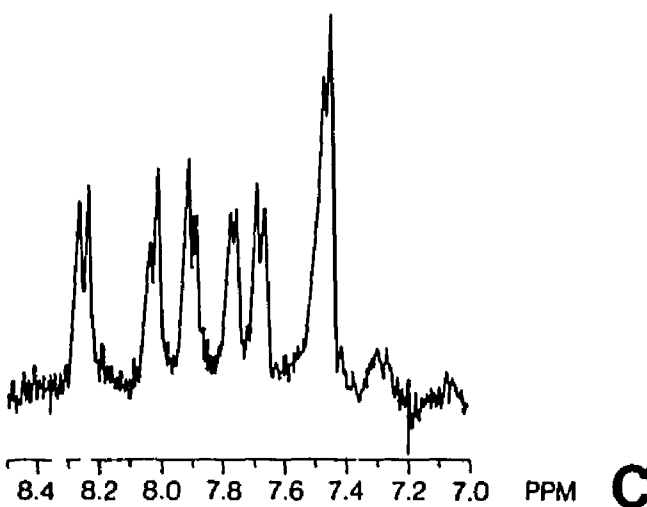
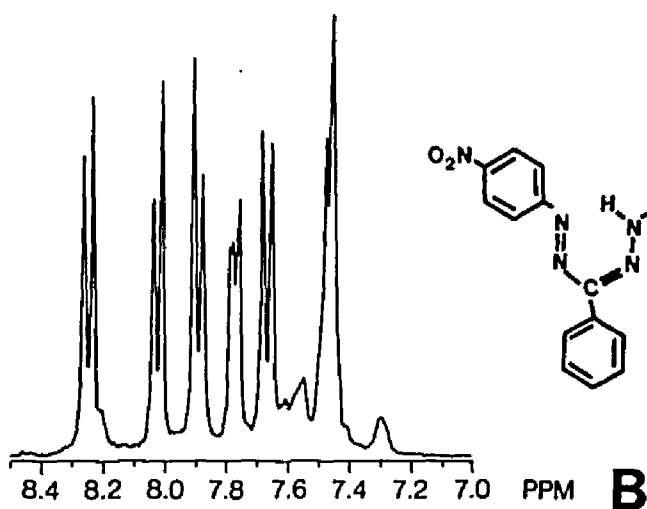
FROM 7.80
TO 7.73 PPM
INTEGRAL= 2349.68

FROM 7.70
TO 7.63 PPM
INTEGRAL= 2493.12

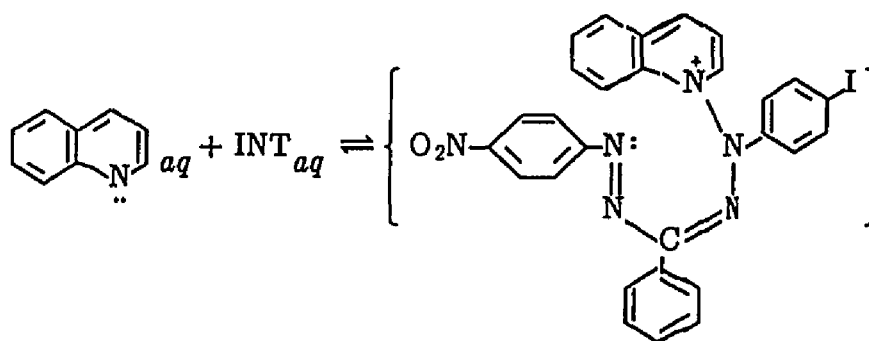
FROM 7.63
TO 7.52 PPM
INTEGRAL= 1508.75

FROM 7.52
TO 7.42 PPM
INTEGRAL= 4072.18

FROM 7.33
TO 7.25 PPM
INTEGRAL= 448.75



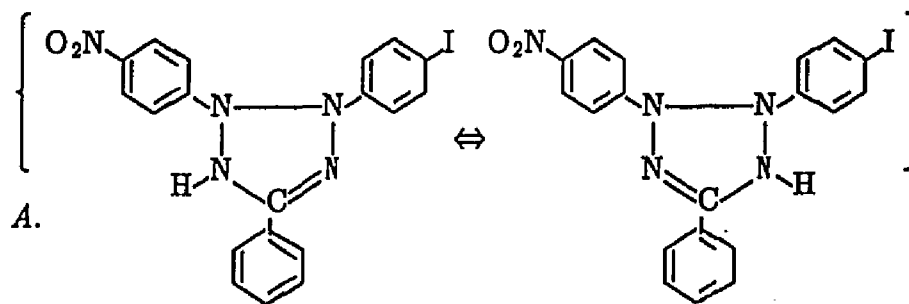
nitrogens that might lead to difficulties in the interpretation of reactivity or spectral data. Irrespective of representation, the following considerations are important and have been major sources of confusion regarding these compounds: 1) a quaternized nitrogen lends charge to the system and is a diagnostic feature of the entire class of compounds [73, 93, 97], 2) the iodo and nitro functionalities are electron-withdrawing and should increase the cationic character of the tetrazolium ring, enhance substantivity, and stabilize the hypothesized tetrazolanyl radical system relative to TPT, 3) the electron deficient tetrazole structure indicates that INT would be reactive towards nucleophiles, and this accounts for its documented resistance to acids and other oxidants, and, 4) there is no evidence for covalent association between the halide and the tetrazolium ring as previously suggested [80, 81]. With respect to INT reactivity toward nucleophiles, it might be expected that direct reactions such as the following between the test NCACs of this work and INT would be significant:



Experiments measuring absorbance spectra of quinoline and INT mixtures (this work), indicated that no such reactions occurred in aqueous media in the temperature range used in the bioassays. It is known that pyridine will react

with TPT in nonpolar media at elevated temperature, but apparently high activation energies are required [63]. Both INT and quinoline are hydroscopic (quinoline much more so) and it is probable that H₂O cage effects inhibit kinetic processes that would lead to direct NCAC-INT chemical reactions with even minimal yields.

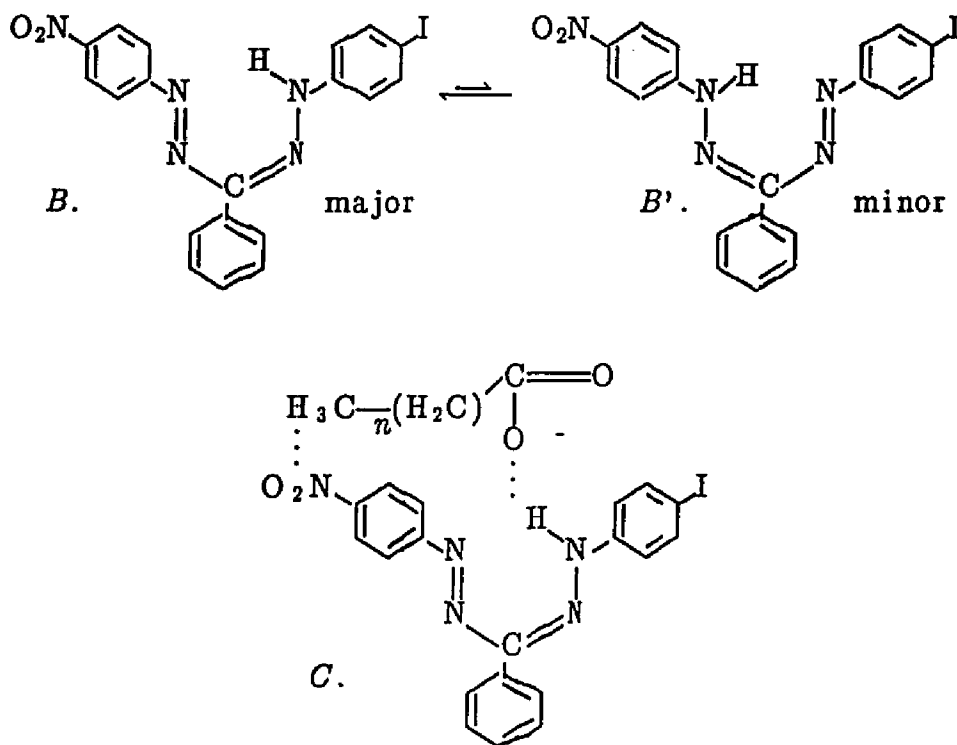
Spectra B and C (Fig. 3) show an acyclic, uncharged formazan system with the highest-order nitrogen being tertiary. This structure arises from the 2e⁻ reduction of INT and addition of one proton. In biological reductions, this is a hydride transfer route [65]. Apparently there are no published spectra demonstrating the *in vivo* reduction route from INT to INTF using extracts from treated organisms, and the examples in Fig. 3 (along with resonance and photochemical considerations) discount other conceivable structures for the formazan that could be postulated based on a hydride reduction (see resonance system A, below).



It can be seen from system A that use of tetrazole structure XII above [93] as a conceptual model might lead to erroneous INTF structures even when one has access to quantitative analysis such as NMR and the reaction route.

The simple acetone extraction gave good recovery of INTF from the INT-treated *E. coli* cells as indicated by decolorization of cell residues.

Interestingly, the INTF-*E. coli* extract spectrum appears subtly different than the INTF standard (*cf.*, Fig. 3 C and B, respectively), particularly with respect to the peaks at δ_{ppm} 7.52 – 7.63 (equivalent to 1.14 proton units) and the smaller signal at δ_{ppm} 7.33 – 7.25 (0.338 proton units). One wonders whether this difference resulted from stabilization of the 2H proton on the formazan by some cellular material, *e.g.*, a fatty acid carried over in the extraction. For instance, in d_6 -DMSO the 2H formazan proton might be free to exist in two resonance structures (*B* and *B'*, below), while under the influence of electrostatic forces of cellular materials in the extract, the statistical weight of the resonance is shifted overwhelmingly to the major structure (*B*, below);

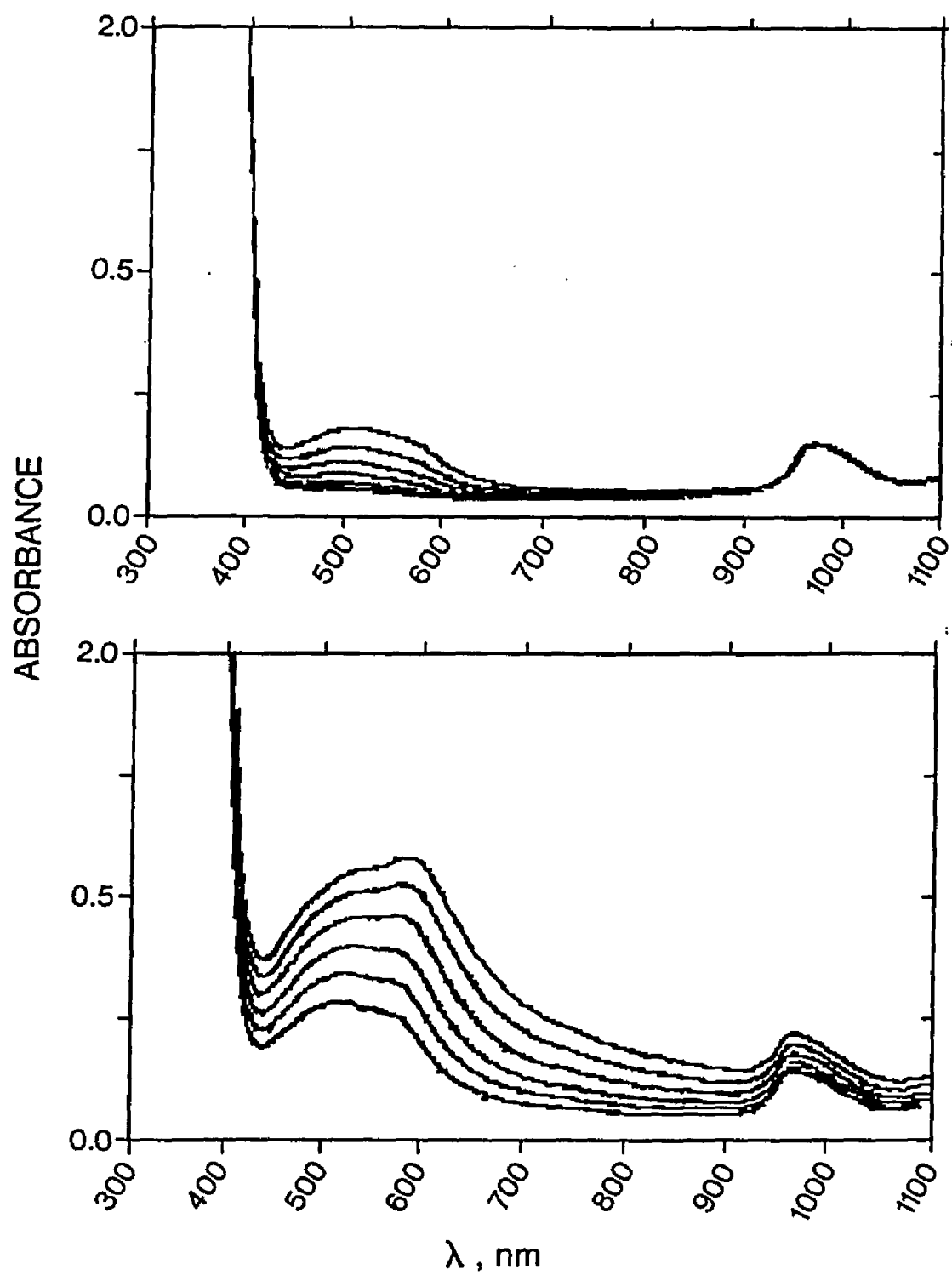


where *B* is NMR consistent, and *B'* and *C* are hypothetical with *C* showing a possible interaction of INTF (*B*) with a $\text{CH}_3-(\text{CH}_2)_n-\text{COO}^-$ fatty acid. Several

authors [63, 65] have suggested that mesomeric structures for tetrazolium compounds similar to *B* and *B'* above are likely, but only in systems with symmetric aryl groups (*e.g.*, TPT). But this is not entirely consistent with modern resonance theory [34, 35] and does not preclude skewed distributions of INTF resonance forms. The dipole moments of the 2- and 3- aryl groups (ignoring tetrazolium ring effects) are 1.71 D and 4.28 D [34, 35] and this would favor only a 2.5:1 statistical predominance of form *B* over form *B'*. Interestingly, the ratio of proton units between δ_{ppm} 7.52 - 7.63 and 7.33 - 7.25 in the FTNMR spectra (Fig. 3) is 3.4:1, whereas in the *E. coli* extract only the latter peak is apparent, with increased height. A shift in resonance distribution under the influence of a chemical interaction could account for the loss of the single proton signal at δ_{ppm} 7.52 - 7.63 in the *E. coli* extract. Hydrogen signals from the fatty acid in system *C* would not be detected in this region of the field, and since all other interactions are electrostatic with heteroatoms, shifting of the *C* ^1H signals relative to standards would be expected to be minimal.

The chemical reduction of tetrazolium compounds (especially TPT) with cellular reductants such as NADH, NADPH, and ascorbic acid (pH > 9.0) have been reported [65], but the time dependence of the reduced nicotinamide reactions and the endproducts of ascorbic acid reduction have not been well resolved. Figure 4, A and B shows absorbance spectra for the nonenzymatic INT reduction by NADPH at pH 7.4 ($\partial t = 15$ min). This suggests that direct nonenzymatic or acellular INT reduction by reduced nicotinamides is not a factor in assays involving INT incubation periods of less than 60 min. It has been claimed repeatedly (based on absorbance spectra) that ascorbic acid does not reduce tetrazolium compounds beyond the formazan. Nevertheless,

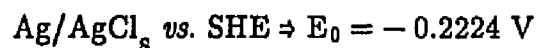
FIGURE 4. Direct Reduction of INT by NADPH. NADPH in PBS (5 mg/ml; pH 7.2), 0.05 mM INT. Scans at 15 min. intervals.



FTNMR spectra of ascorbic acid/INT solutions in water at pH 9 contained some 25 major peaks and many minor signals in the aromatic region, which indicated multiple reduction products. Proton signals from ascorbate itself were in the ranges δ_{ppm} 1.0 – 5.5 and 9.0 – 12.0, not in the aromatic range examined (δ_{ppm} 7.0 – 8.5).

II. Electrochemistry of INT

The rather complicated electrochemistry of INT in buffered aqueous systems was examined using several working and reference electrodes. Since the latter have different standard potentials relative to the SHE, the following standard potential values at 25^o C can be used to convert data from figures to a common scale:



Figures 5 and 6 show normal and differential pulse polarography (NPP and DPP respectively) of INT/PBS. NPP gave three resolved maxima (–0.168, –0.350, and –0.714 *vs.* Ag/AgCl) with $E_{1/2}^{\text{red}}$ of the first wave approximately –0.150 V *vs.* Ag/AgCl (or +0.073 V *vs.* SHE). DPP produced at least five resolved peaks (–0.096, –0.238, –0.328, –0.648, and –1.166 V *vs.* Ag/AgCl) (Fig. 6), but these peaks shifted with concentration in a nonlinear manner indicating product adsorption complications [*cf.*, 102]. To ameliorate adsorption difficulties, 100% ethanol was added to the PBS to increase solubilities of reactants and products and a vitreous carbon working electrode

FIGURE 5. Normal Pulse Polarogram; 0.133 mM INT in PBS with 2 drops of Triton X-100 maxima suppressor; Static Mercury Drop Electrode (Model 303A); 1 drop/s; 2 mV/s scan rate.

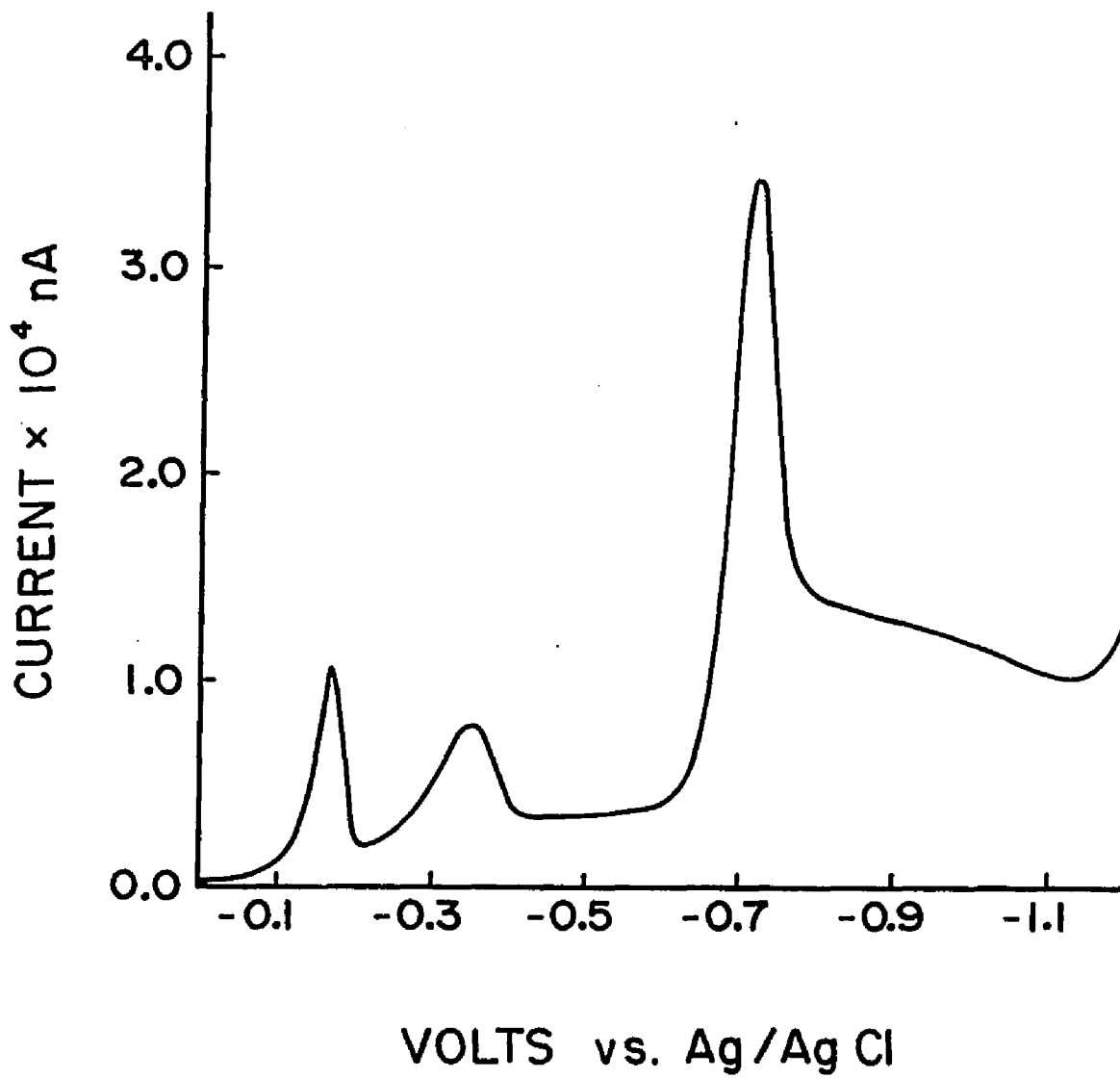
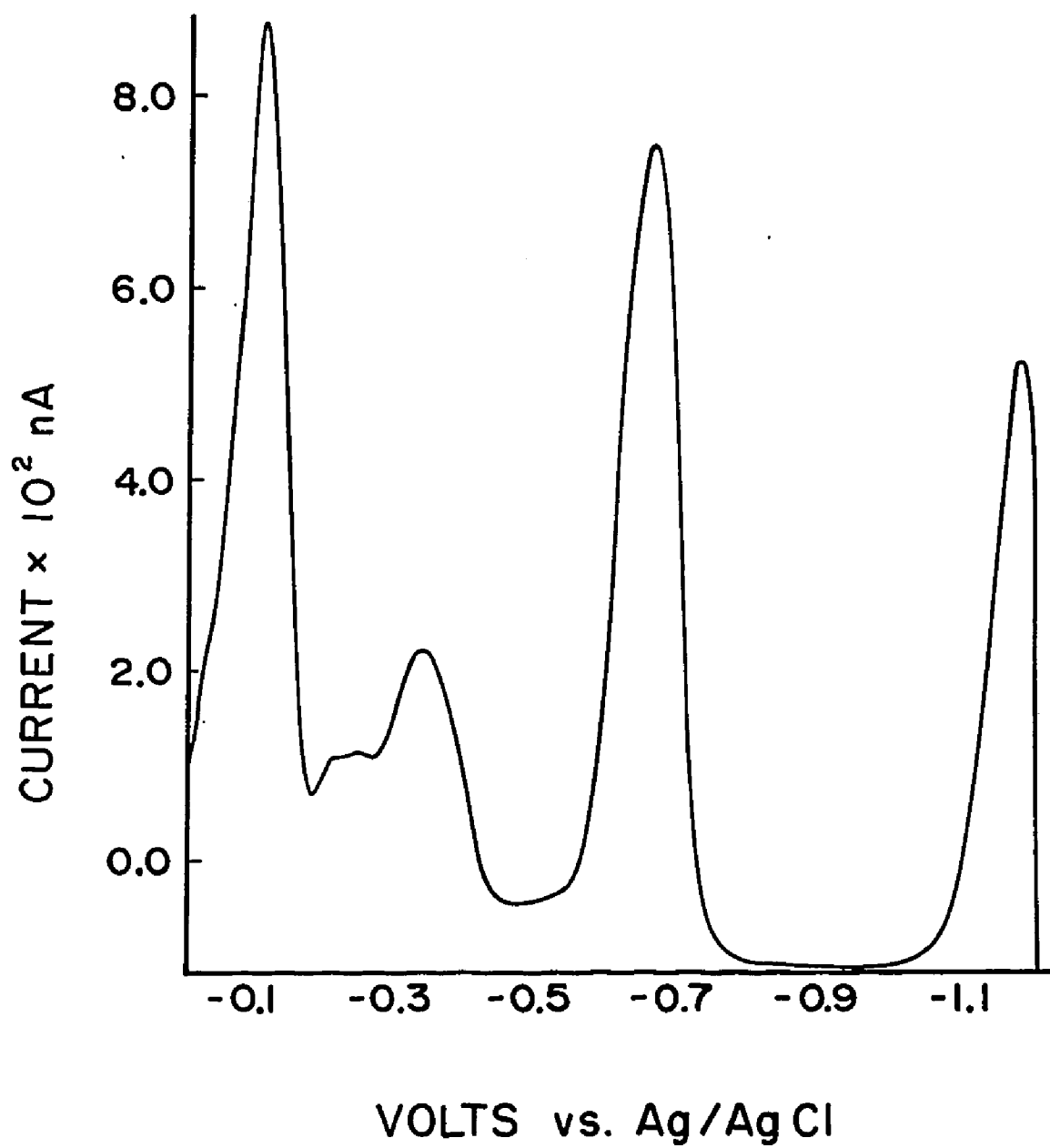


FIGURE 6. Differential Pulse Polarogram; 0.133 mM INT in PBS; 2 drops Triton X-100 maxima suppressor; Static Mercury Drop Electrode (Model 303A); 1 drop/s; 2 mV/s scan rate.



was substituted for Hg. Figure 7 shows a normal pulse polarogram of INT/PBS on vitreous carbon showing three waves (-0.17 , -0.52 , and -0.82 V *vs.* SCE) with much lower amplitudes than Hg. The first wave is broad and small, indicating irreversible electron transfer and interfering electrode processes, and the rising linear background is probably due to H^+ reduction and hydrogen filming on the electrode surface. Filming by a blue-green product was noted especially on carbon, but also on large area platinum electrodes. This suggested that radicals or dimerization reactions were occurring at some potential in the experimental range, but this was not pursued quantitatively. Theoretically, dimers could be formed *via* cathodic or anodic reactions of INT or INTF respectively (Fig. 9, below), and the fact that diformazans of nitrotetrazolium blue (NTB) and other compounds are blue to purple in aqueous media lends support to this conjecture [65]. Further, it is known that free radicals of several tetrazolium salts are green to black in organic media [65, 91]. Figures 8 and 9 show results of cyclic voltammetry (CV) at the same vitreous carbon electrode. In all CV, three peaks were well resolved and increases in scan rate caused peaks to shift slightly negative, again suggesting irreversible and complicated reduction processes. Figure 9 shows that each reduction peak gave rise to one or more oxidation waves on reverse scan indicating irreversibility as well as the presence of different pathways for oxidation and reduction on carbon. Similar mechanistic differences for oxidation and reduction have been reported for TPT on Pt [86]. In all CV's, the approximate peak ratios of the first two waves were 1:1 indicating a sequence of two one-electron reductions.

Since the apparent kinetics of the first wave could have been an artifact of many processes including heterogeneous mass transport, additional

FIGURE 7. Normal Pulse Polarogram; vitreous carbon electrode; 16.4 μM INT in 50 % ethanol:PBS (v/v); 2 drops Triton X-100 maxima suppressor; 2 drops/s; 5 mV/s scan rate.

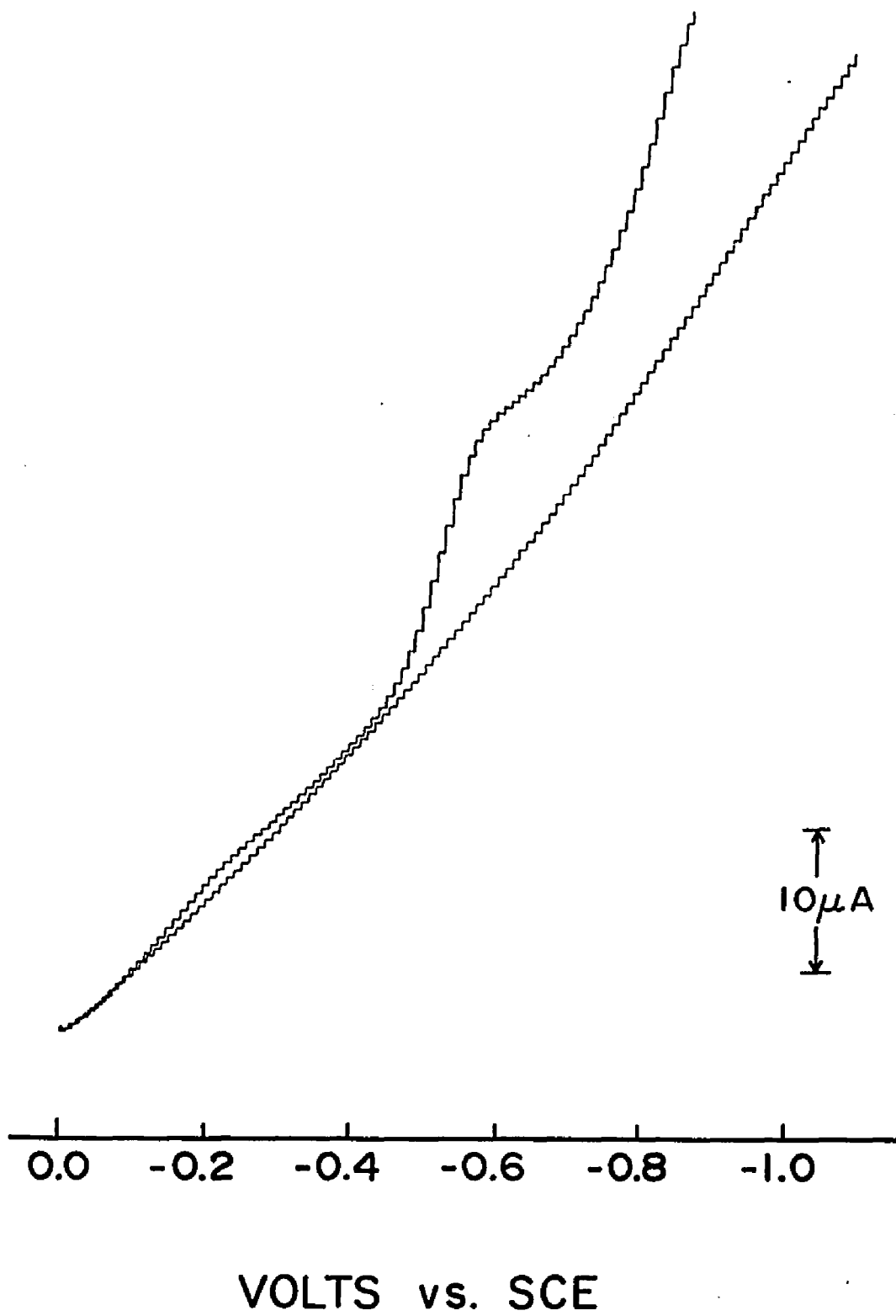




FIGURE 8. Cyclic Voltammogram on Vitreous Carbon Electrode. SCE reference electrode; 16.4 μM INT in 50 % ethanol:PBS (v/v); 2 drops Triton X-100 maxima suppressor; scan rates (bottom to top): 10, 50, 100, 200, 500, mV/s.

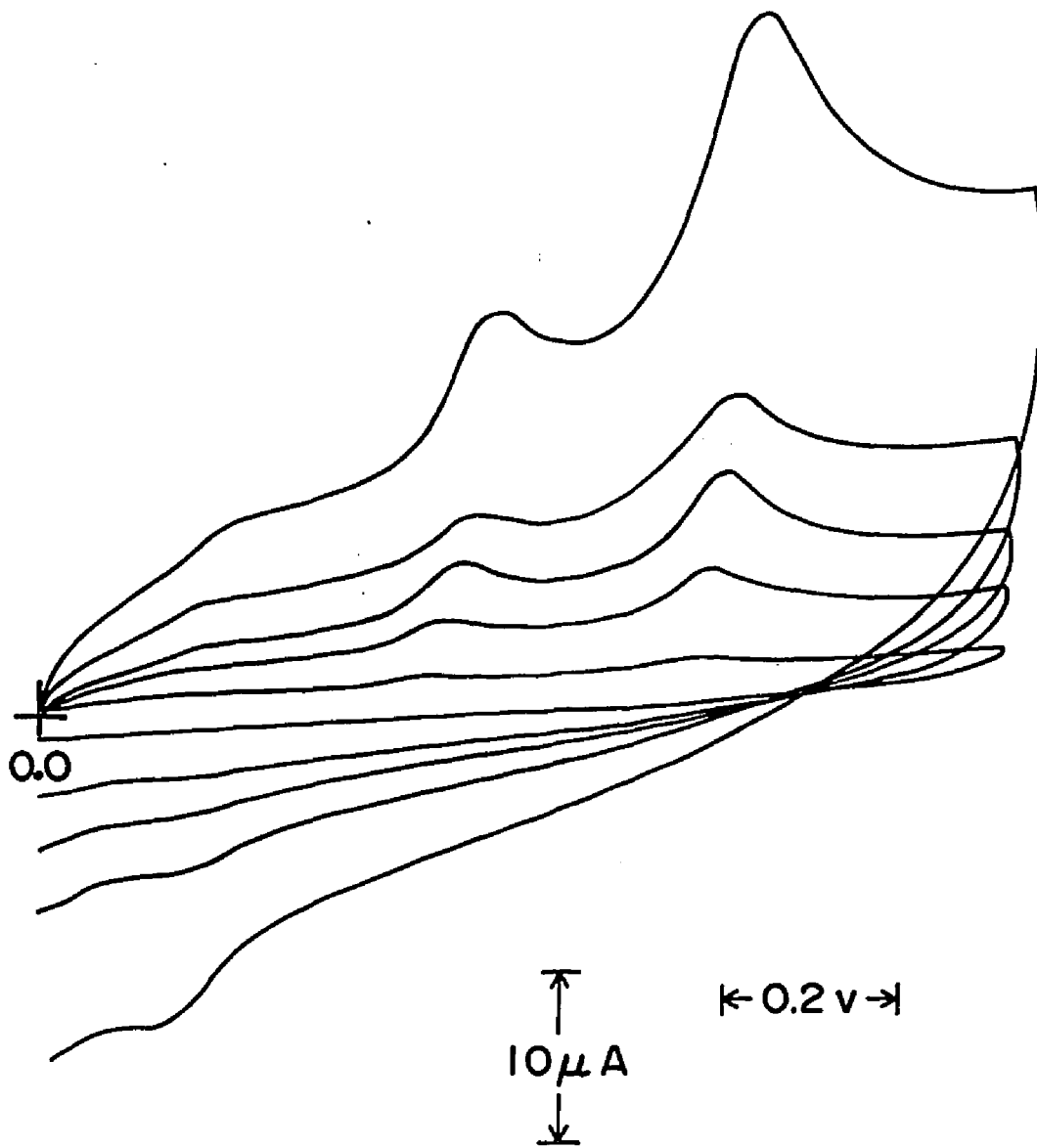
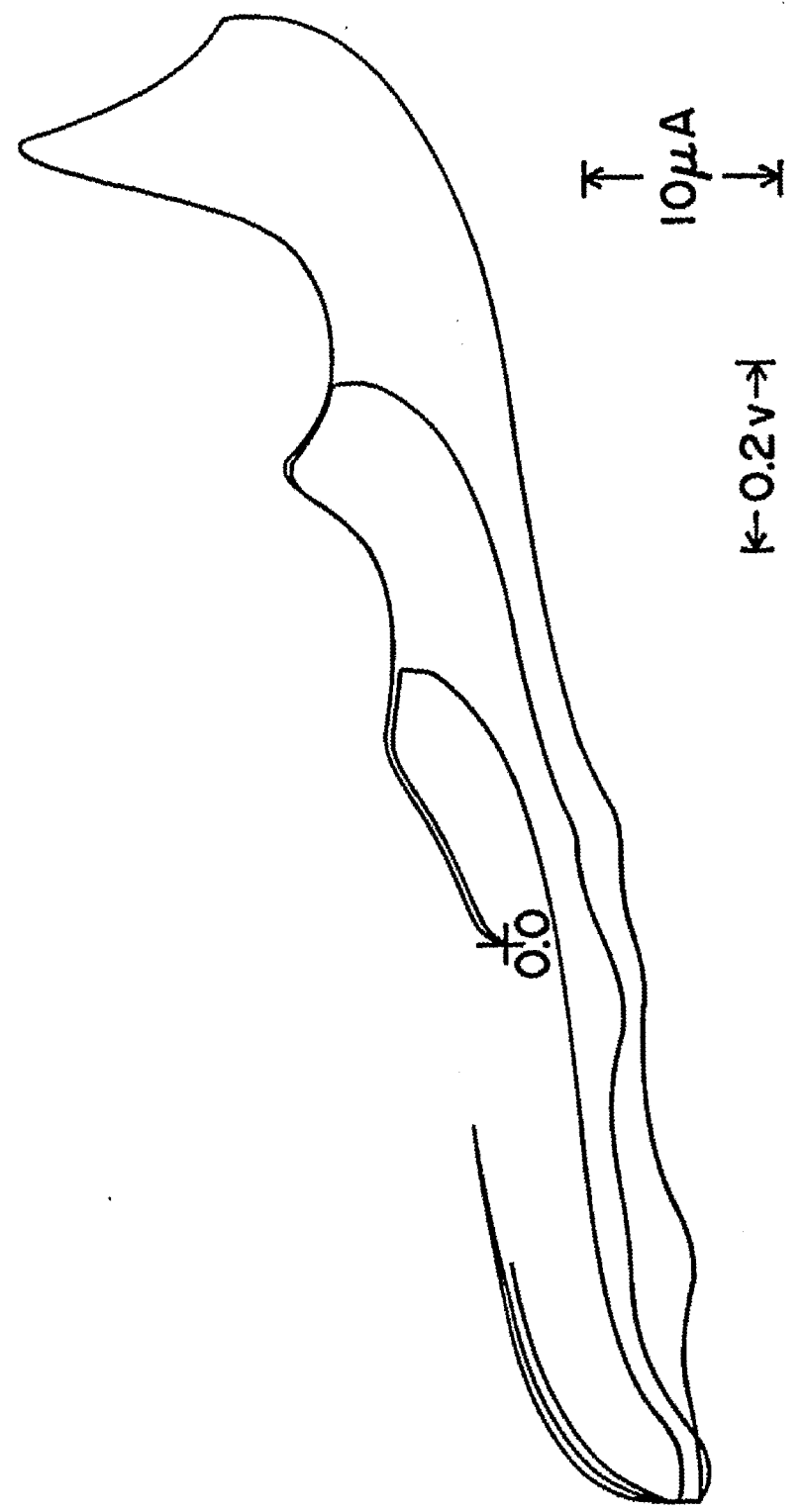


Figure 9. Cyclic Voltammogram on Vitreous Carbon Electrode.
SCE reference electrode; 66 μM INT in 50 % ethanol: PBS
(v/v); 150 mV/s scan rate.



experiments were conducted using the RRDE. Degassed solutions of 0.20×10^{-7} M INT in 1:1 PBS/ethanol (v/v) were analysed with respect to the first reduction wave, and data were used to solve the Levich equation, which provides a test that currents measured at the RRDE are faradaic [94, 102]. The RRDE experiments were run at a single rotation rate which gave a well controlled mass transfer regime. Solution of the Levich equation gave n values (number of electrons transferred) between 0.1 and 0.9, again suggesting irreversible one electron transfers in the first wave. DPP was also attempted in this system, but was subject to large startup transients especially at the faster sweep rates. As a result, data on the first wave were obscured.

Laser reflectance spectroelectrochemistry of INT reduction was unsuccessful in determining the minimum reduction potential for INT to INTF mainly because the changes in measured current from the photodetector were too small to be discerned from the background currents, which were some 2 – 3 orders of magnitude greater. Heavy deposits of INTF were noted on the electrode after all runs, indicating that reduction was occurring on Pt well positive of -1.0 V *vs.* SCE. This efficiency of this system could be optimized and modified by reducing the intensity of the incident beam, changing incident wavelength, and increasing the depth of the thin optical cell, but this was not done because of time constraints. A heavy particle recoil spectrometer also could be added to the thin cell system to detect potentials at which various sorption events occurred (*i.e.*, H^{ads} , INT, INTF, and any intermediates) and the effects of redox active pollutants (*e.g.*, quinoline) on reduction potential and sorption characteristics. The study of redox-active toxicants in such an experimental system would allow for interpretation of mechanisms and effects of these materials on biological ET processes.

FIGURE 10. Spectrochemical Identification of Minimum INT Reduction Potential on Pt Mesh Electrode. 10^{-2} M INT in 50 % ethanol:PBS (v/v); $\lambda = 490$ nm

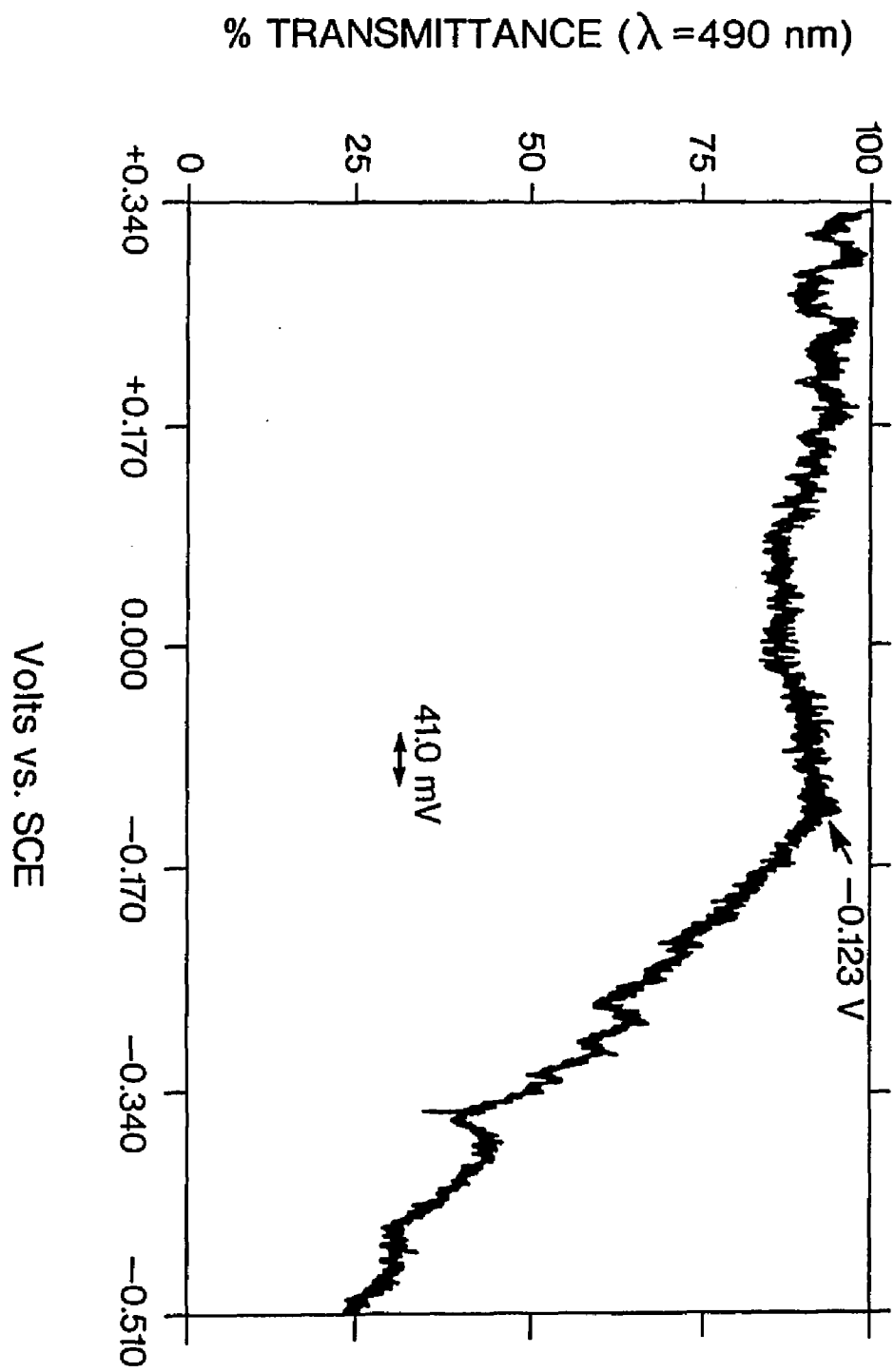
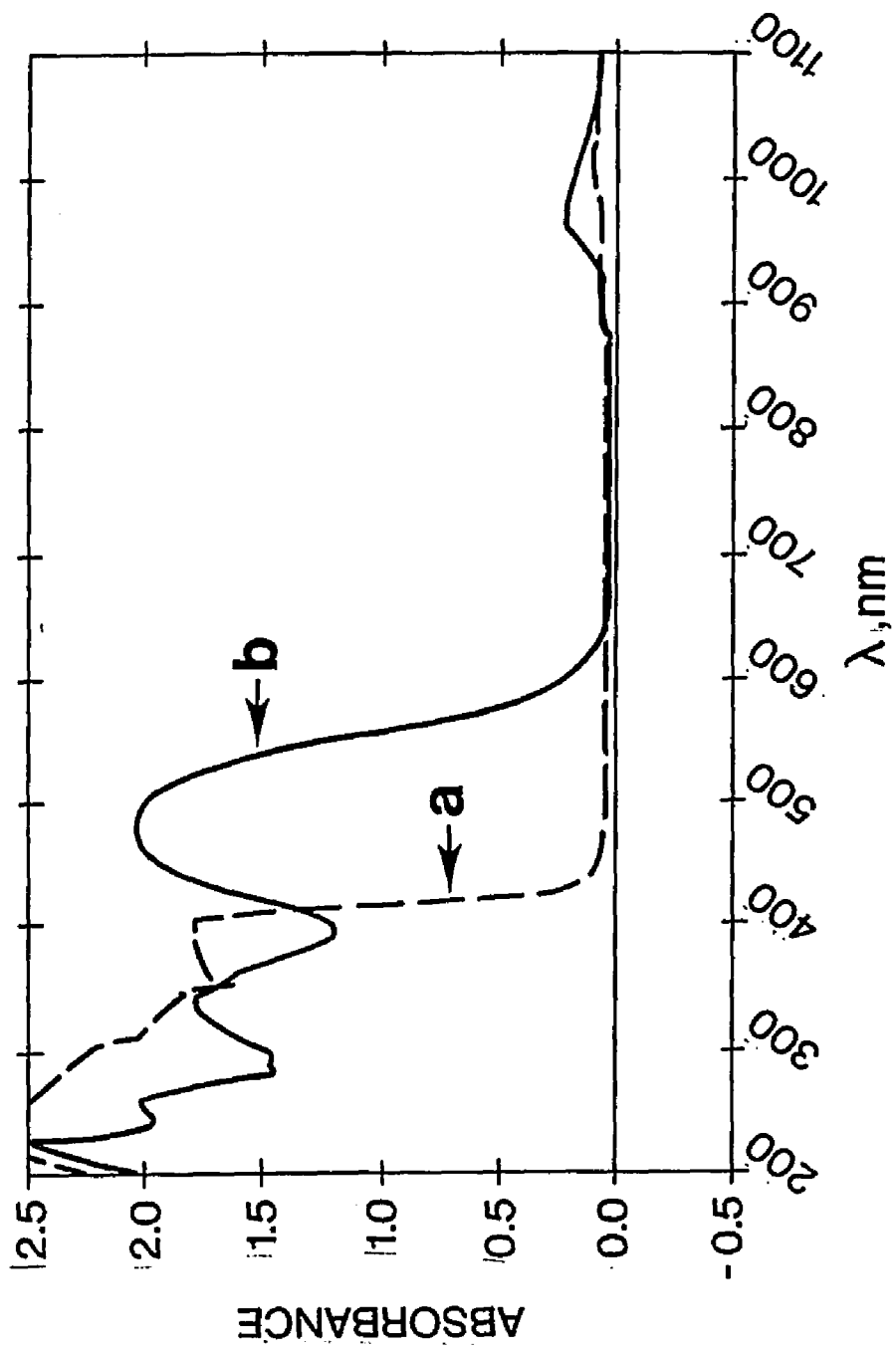


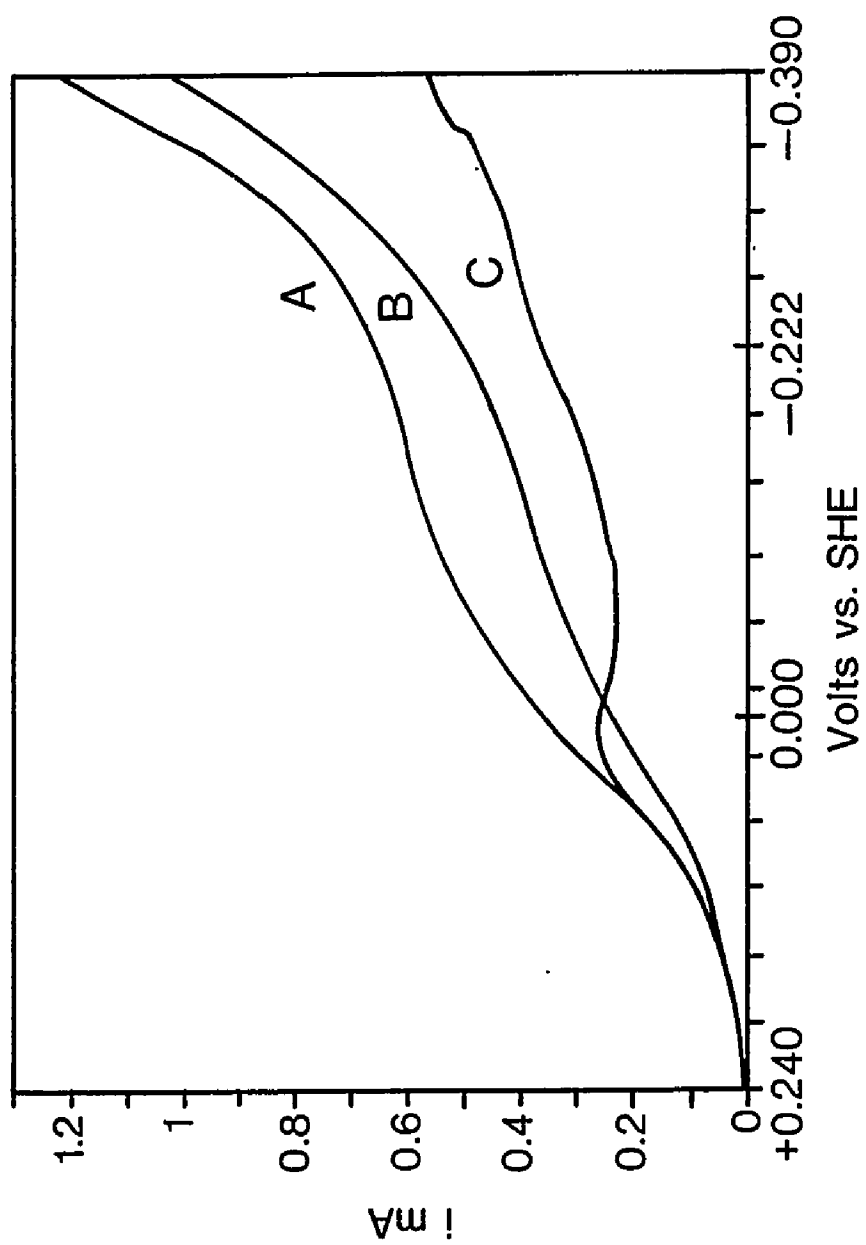
FIGURE 11. Electronic Absorbance Spectra of INT (a) and INTF (b)
Standards in 50 % ethanol:PBS (v/v).



Results of the spectrophotometric determination of the minimum reduction potential at which INTF could be detected optically on platinum mesh is shown in Figure 10. Production of INTF was monitored at $\lambda = 490$ nm because a prominent, unambiguous peak occurs at this wavelength in its solution absorption spectrum (Figure 11). The spectroelectrochemical system was able to detect the onset of INT reduction on Pt mesh. The reduction of INT apparently began at -0.117 to -0.126 V *vs.* SCE ($+0.116$ and $+0.125$ *vs.* SHE) and continued beyond -0.5 V *vs.* SCE. These results were reproducible, but as with mercury, adsorption of INTF was observed on the working and sometimes, counter electrodes. The onset of INT reduction occurred positive of the standard potential for H^+ reduction, and the results suggested the possibility of underpotential generation of reactive hydrogen species at the electrodes where filming occurred (see below). This spectroelectrochemical system is promising for future examination of redox effects of various pollutants in aqueous and simulated biological media (*e.g.*, a mixture of fatty acids) and for exploring the significance of such effects in simulated membrane systems.

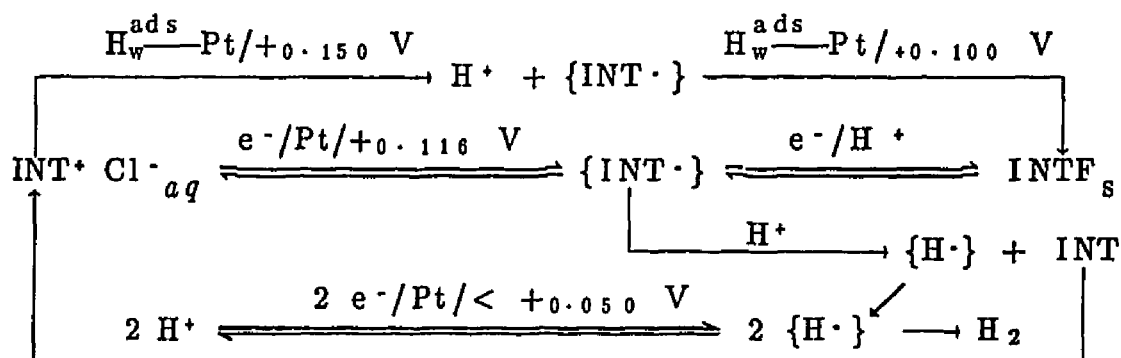
Figure 12 summarizes the results of numerous experiments addressing the pH dependence of the first wave on vitreous carbon using NPP. It can be seen that at pH = 3.0 the first wave peaks abruptly, whereas at pH = 9 and pH = 12, the waves are much broader. The differences in this wave at pH = 3 and pH > 7 on carbon as well as spectrochemical observations on Pt (Fig. 10) strongly suggested the possibility of competition for adsorbed hydrogen species by INT (or intermediates) and reactions resulting in the formation of molecular hydrogen. The exact nature of the INT interaction with the electrode and adsorbed hydrogen species is not known and could not be inferred from the data of the present work. The presence of 1) irreversible one electron reductions in

FIGURE 12. First Reduction Wave Characteristics as a Function of pH.
A. pH 11; B. pH 9.0; C. pH 3. 10^{-4} M INT in 50 % ethanol:PBS (v/v), NPP at vitreous carbon electrode, 100 mV/s scan rate.



the first wave, 2) presumed dimerization products, 3) pH effects, 4) approximate 1:1 peak current ratios from the first two reduction waves in CV and, 5) the very positive $E_{1/2}^{\text{red}}$ of INT on Pt suggested that INT is reduced *via* a direct slow one electron reduction, followed by a relatively fast one electron reduction and disproportionation (center route, below). It seems likely that the reduction to INTF proceeds through a tetrazolanyl radical intermediate. If the disproportionation step is limiting, as suggested in the literature [85, 86], it is not clear how the exponential inverse proportionality between formazan production and $[H^+]$ concentration can be explained without postulating interfering reactions involving hydrogen.

Given these data and that of previous authors, the following reaction scheme, shown as the uppermost route, cannot be ruled out (all potentials are *vs.* SHE):



The species $\text{H}_w^{\text{ads}}\text{-Pt}$ above represents weakly adsorbed hydrogen at a surface site on the Pt electrode, which gives a current maximum at approximately + 0.100 V *vs.* SHE [*cf.*, 94, 102]. It is significant that a TPT radical analogous to the $\{\text{INT}\cdot\}$ proposed above has been identified in TPT formazan oxidations at electrodes and as a reduction product in microsomal cytochrome P-450 preparations [65]. In the latter case, the tetrazolanyl radical reduced O_2 to

superoxide anion, thereby inhibiting the rate of formation of formazan and explaining the oxygen sensitivity of TPT reduction in biological systems. Under anaerobic conditions, the TPT tetrazolanyl radical further reacted to give TPTF. Conversely, the biochemical reduction of INT to INTF is not inhibited by oxygen [64, 65, 75] suggesting that, 1) INT does not form a tetrazolanyl radical, 2) the radical is generated in a rate limiting step followed by very rapid reduction and disproportionation to INTF that is favored over oxidation by O₂, or, 3) the radical is stable in the presence of oxygen either thermodynamically or through chemical sequestering in anaerobic microregions of the cell. According to the present data, it is likely that the INT tetrazolanyl radical species is formed at Pt electrodes and that the formation of INTF is inhibited by hydrogen ion concentrations above 10⁻⁷ M.

Experiments addressing the hypothesis of underpotential hydrogen evolution using DPP on the RRDE were inconclusive and further experiments using C fiber bundle electrodes are under consideration.

III. Mutagenicity Evaluation of INT and INTF

INT, INTF, and an irradiated solution of both compounds were not detected as mutagens in the Ames/*Salmonella* assay. In general, these compounds were toxic to the test bacteria, with culture lawns turning red upon incubation, and growth inhibition (*i.e.*, pindot colonies, reduced background lawns) observed at 100 μM doses in all treatments. In all strains tested except TA 98, complete inhibition of revertant colonies was observed at concentrations of 2 – 7 mM for all test solutions. Treatment of cultures with S9 caused rapid (< 10 min) reduction of INT to INTF and was therefore not used in INT

treatments. Otherwise, the S9 treatments gave no differences in reversion rate from controls. Despite the negative findings in these preliminary assays, very careful handling and disposal of these materials was observed. As with all bioactive compounds, especially those that are thought to form free radicals, obscure cellular and genetic interactions can occur that are not detected in single species tests. For example, results of binding assays using the PSV₂-neo plasmid and supercoiled ladder DNA suggested that INT could interact with DNA *in vitro*. Results of assays measuring electrophoretic mobility of plasmid DNA and supercoiled and linear DNA ladder standards are shown in Fig. 13. The mobility of the same materials treated with INT, INTF, and ethidium bromide (EB) are shown in Figure 14. The gel reproduced in Fig. 14 allows for the comparison of SAGE mobility for purified PSV₂-neo and 1 kB supercoiled ladder DNA controls *vs.* treatments with EB (a known intercalating agent), INT, and INTF (suspected intercalating agents). Pre-electrophoretic treatment of 1 – 20 kB supercoiled plasmids with EB is known to result in significant changes in mobility, with the intermediate weights (5 – 15 kB) showing the most pronounced effects [109]. It is evident from Fig. 14 that INT caused small mobility changes (smearing and distortion of terminal bands) in all treated samples relative to untreated controls, and the degree of mobility inhibition was related to MW of the plasmid for EB and INT treatments (*cf.*, lanes 7 – 14, Fig. 14). These mobility changes were similar to, but not as pronounced as those caused by EB. No mobility effects were observed for INTF which suggests that the interaction between INT and DNA was electrostatic. In native DNA, electrostatic repulsion between two monovalent phosphodiester groups is attenuated and dimensionally stabilized by one Mg²⁺ ion. This

FIGURE 13. SAGE Mobility of PSV₂-neo Plasmid DNA Relative to Linear and Supercoiled Ladder DNA Standards. 20 μ L injection.

Lane: 1, 6, 13: Supercoiled ladder*; 0.07 μ g/ μ l.
2, 9, 12: PSV₂-neo Stock; 0.24 μ g/ μ l.
3, 8: PSV₂-neo Stock; 0.08 μ g/ μ l.
4, 7, 11: PSV₂-neo Stock; 0.048 μ g/ μ l.
5, 10; Linear Ladder DNA Standard**.
14; Control.

Kilobase (kB) Size of DNA Ladder Standards (bottom to top):

* Supercoiled Ladder: 16.21, 14.17, 12.14, 10.10, 8.07, 7.05, 6.03, 5.01, 3.99, 2.97, 2.07.

** Linear Ladder: 12.216, 11.198, 10.180, 9.162, 8.144, 7.126, 6.108, 5.09, 4.07, 3.054, 2.036, 1.636, 1.018, 0.517, 0.506, 0.396, 0.344, 0.298, 0.220, 0.201, 0.154, 0.134, 0.075.

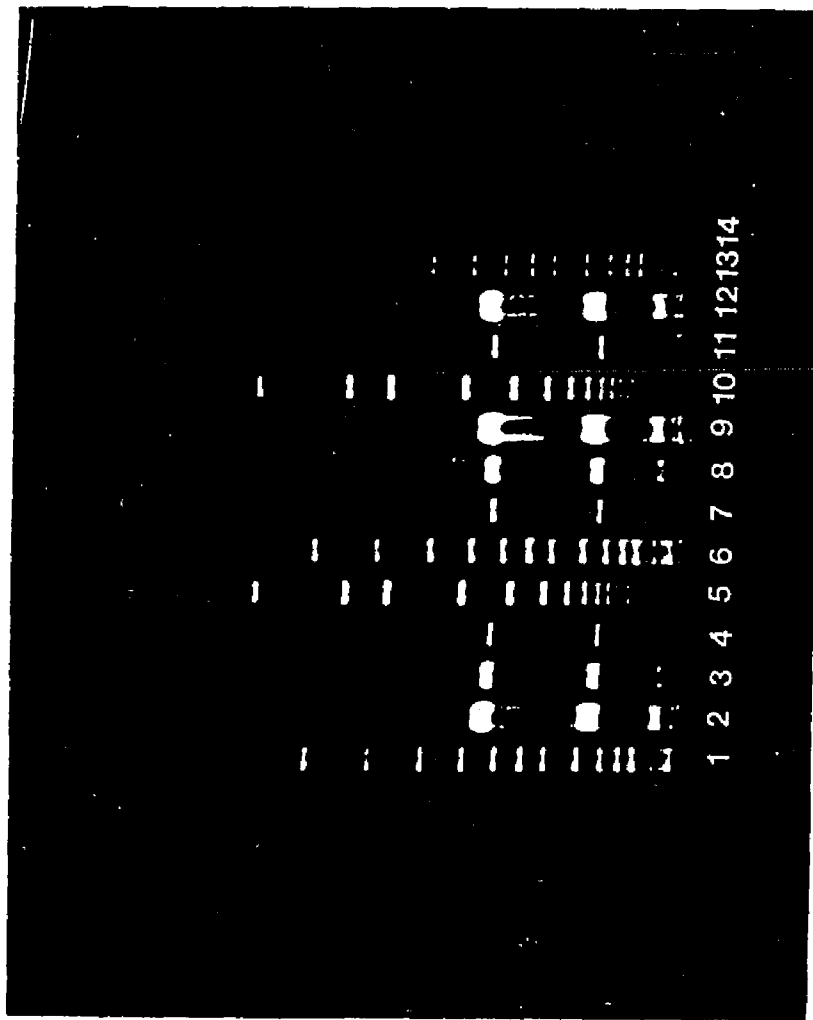
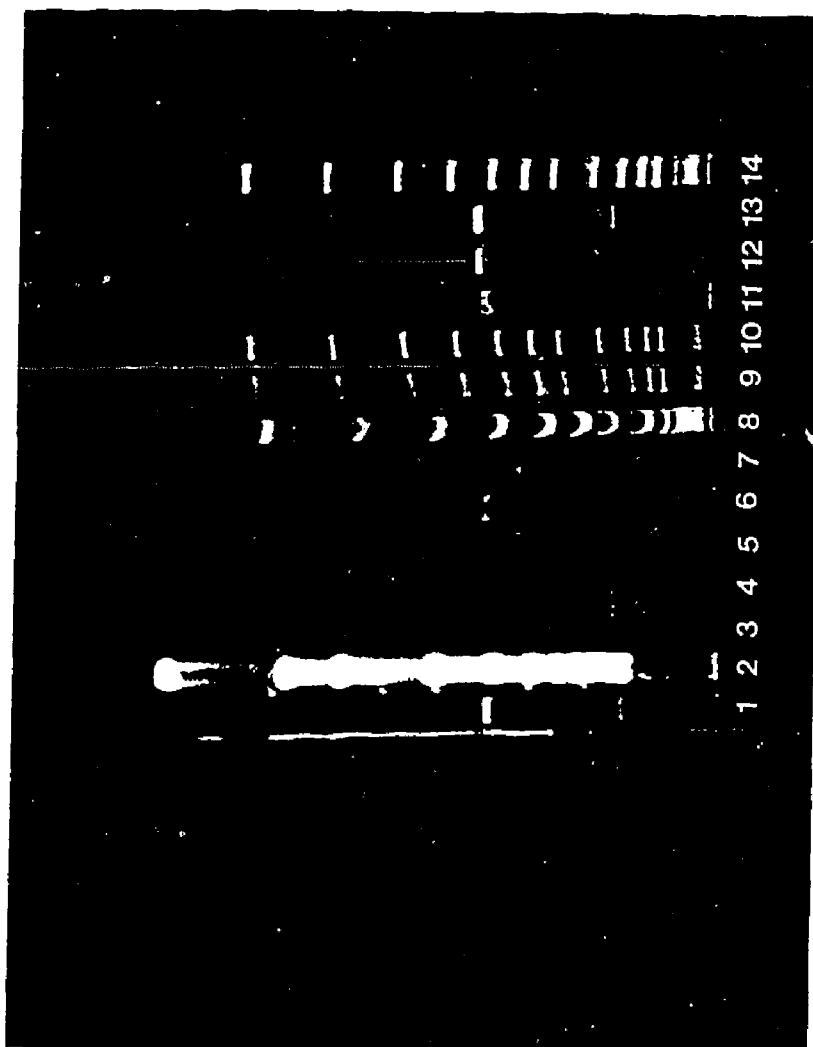


FIGURE 14. Effect of Ethidium Bromide, INT, and INTF on SAGE Mobility of PSV₂-neo Plasmids and Supercoiled Ladder DNA.

- Lane: 1, 6: PSV₂-neo Plasmid DNA, 0.025 $\mu\text{g}/\mu\text{l}$ †.
 2: Linear Ladder DNA; 0.5 $\mu\text{g}/\mu\text{l}$ ‡.
 3 – 5: PSV₂-neo DNA; 0.008 $\mu\text{g}/\mu\text{l}$ † (not detected).
 7: PSV₂-neo DNA + 30 μl ethidium bromide stock (1 μM).
 8: Supercoiled Ladder Stock + 30 μl ethidium bromide stock (1 μM)
 9: Supercoiled Ladder + 10 μL INT (1 mM stock).
 10: Supercoiled Ladder + 10 μL INTF (1 mM stock).
 11: PSV₂-neo DNA + 10 μL INT stock.
 12: PSV₂-neo DNA + 10 μL INTF stock
 13: PSV₂-neo Stock; 0.025 $\mu\text{g}/\mu\text{l}$ †.
 14: Supercoiled Ladder Standard.

† Approximate concentration.

‡ Lane Overloaded.



interaction is critical in maintaining the tertiary structure of the DNA helix [111]. If INT competes for negatively charged sites normally occupied by Mg or chelates the metal in a way similar to its chelation of Nb(V) [66], then the repulsion between phosphates would be greater, torsional effects and molecular volume would increase, and electrophoretic mobility would decrease. An increase in phosphodiester repulsion also would open the helix and increase its susceptibility to noncovalent intercalative binding (perhaps *via* one of the planar phenyl groups) [111]. In the INT-treated DNA bands (Fig. 14) the intensity of post electrophoretic EB staining was decreased relative to untreated controls and INTF treatments. This suggests an intercalative as well as electrostatic mechanism of INT/DNA interaction, or, conversely, a quenching of EB fluorescence by associated INT. It was not possible to conduct further experiments addressing this question, nor was it feasible to attempt to examine the tetrazolanyl species without analytical support. Like many free radicals, however, it is likely to have mutagenic properties and is a promising candidate for future electrophoretic studies of DNA binding. As an electrophile, the tetrazolanyl radical likely would possess the ability to dimerize or react covalently with nucleic acid bases.

As with the *Salmonella* mutagenicity results, the plasmid mobility assays were not conclusive by themselves, but did support reactivity predictions made solely on the basis of quantum mechanics and the documented behavior of analogous compounds. The potential for ionic associations between INT and DNA supports the conclusion that INT should be regarded as a potential carcinogen until comprehensive testing has been conducted.

IV. The Revised Direct INT Bioassay

As mentioned, it was necessary to modify the published direct INT assay [73] for the purposes of the present work. This was because the use of optimized cultures was thought to be essential for valid interpretation of toxicity and for an understanding of the full range of responses characteristic of the bacterium [60]. The latter was important because it was necessary to evaluate the technique with respect to its proposed use as a rapid toxicity assay, as well as in mechanistic work.

The INT assay procedure described in Materials and Methods was designed to correct for at least three sources of systematic error in the previously published method [73], *i.e.*, 1) obvious sources of uncontrolled toxicity (anaerobiosis, pH effects, and substrate limitation from using spent culture in the assays) were reduced, 2) problems with uneven delivery of cells to dose tubes (from random clumping/settling) were minimized by sonication and the use of 0.14 % agar in the PBS resuspension medium and, 3) ET estimates used in dose-response regressions and assays of different cell systems were optimized so that all salient information was included in comparisons.

With respect to 3) above, it was necessary to evaluate options for statistical handling of data. Published methods commonly have called for estimates of ET based on a terminal absorbance value for INTF after an extended incubation time (10 - 60 min.) of cultures with INT [73, 74]. More recently, the maximum slope of the "first-order" part of the INT reduction curve has been employed without a formazan extraction step [73]. Using data from 8 replicate samples of a control culture prepared according to revised

protocols of this work, the following methods of ET estimation were compared: 1) final INTF absorbance after 10 min incubation of cultures with INT, 2) "first order" rate of INTF *vs.* time per 30 s interval, 3) probit slope values for the total ET response surface for a 210 s run and, 4) an integrated value of total INTF absorbance after 210 s (given instrumentally as "activity"). It was found that use of the final absorbance value after 10 min. incubation of bacteria with INT was more reproducible (c. v. = 3.5 %) than any of the shorter (210 s) rate estimates, but the method tended to obscure important differences in the treatments, and gave no information on kinetics (below). The long run time per sample was also prohibitive in terms of benchlife of the incubated test suspensions, which showed decreases in INT activity after 3.5 h. The maximum slope, probit slope, activity value estimates for ET showed more variability than did values of final absorbance but had comparable c.v.'s (13.2 %, 10.0%, and 13.6%, respectively). The response surfaces of these were indicative of the variability between treatments and were thought to be better for discerning subtle or gradient changes in ET response with toxicant treatment. Linearizing the total absorbance *vs.* time function using a probit transform was time consuming and did nothing to improve comparability between runs (the maximum slope estimates were equivalent) and obscured small variations in lag time response. Hence, it was decided that maximum slope and lag time values conveyed all salient information available, and were most appropriate terms of time and experimental flexibility. The computed activity value was not used because it was insensitive to nonlinearities and gave erroneous values if a run was terminated before the 210 s time had elapsed. The latter was sometimes necessary when, in threshold doses (below), lag time was not observed and absorbances were off scale before completion of the 210 s run. The use of

activity values under these circumstances would have given inaccurate and unusable data. The published method [73] was nebulous on these points, and the results included only EC_{50} values that had been generated by regressing INT slope values on dose. The meaning of "first order", method of calculation of maximum slopes, length of the run period, and considerations pertaining to kinetic variations were not reported or mentioned. The run time of 210 s for the present work was chosen because it became clear that 1) lag times before response in controls and most toxicant treatments were between 60 – 100 s, and these were followed by rapid absorbance increases at $\lambda = 490$ nm for the remainder of the run and 2) by 200 – 210 s, virtually all absorbance *vs.* time functions were outside the linear range of the spectrophotometer.

With respect to the sources of stress within the growth culture medium, Figure 15 summarizes the results of comparative INT assays run using the published method [73] *vs.* the revised method of the present work. The INT assays were run in tandem after initial growth periods of 8, 16, and 36 h. The long incubations were used because the published method used 20 – 24 h post S-phase cultures of the aerobe *Pseudomonas alcaligenes*, and the revised protocol of this work calls for incubation times corresponding to the early stages of S-phase (Figure 16). Figure 15 shows that the use of spent growth medium as a dosing medium and substrate for INT work gave lower ET rates at all incubation times relative to the the method used for this study. The very long lag periods before response and low pH values of suspensions from the published method [73] indicated that acidic and oxygen-limited conditions gave rise to altered respiratory states (anaerobic respiration and/or resting states). The bacteria prepared using the revised method showed vigorous INT responses and short lag times (70 – 90 s) at all incubation times. Variance in the INT

FIGURE 15. Comparison of INT Reduction Assays. Maximum INTF Response *vs.* Incubation Period (8, 16, 36 h)

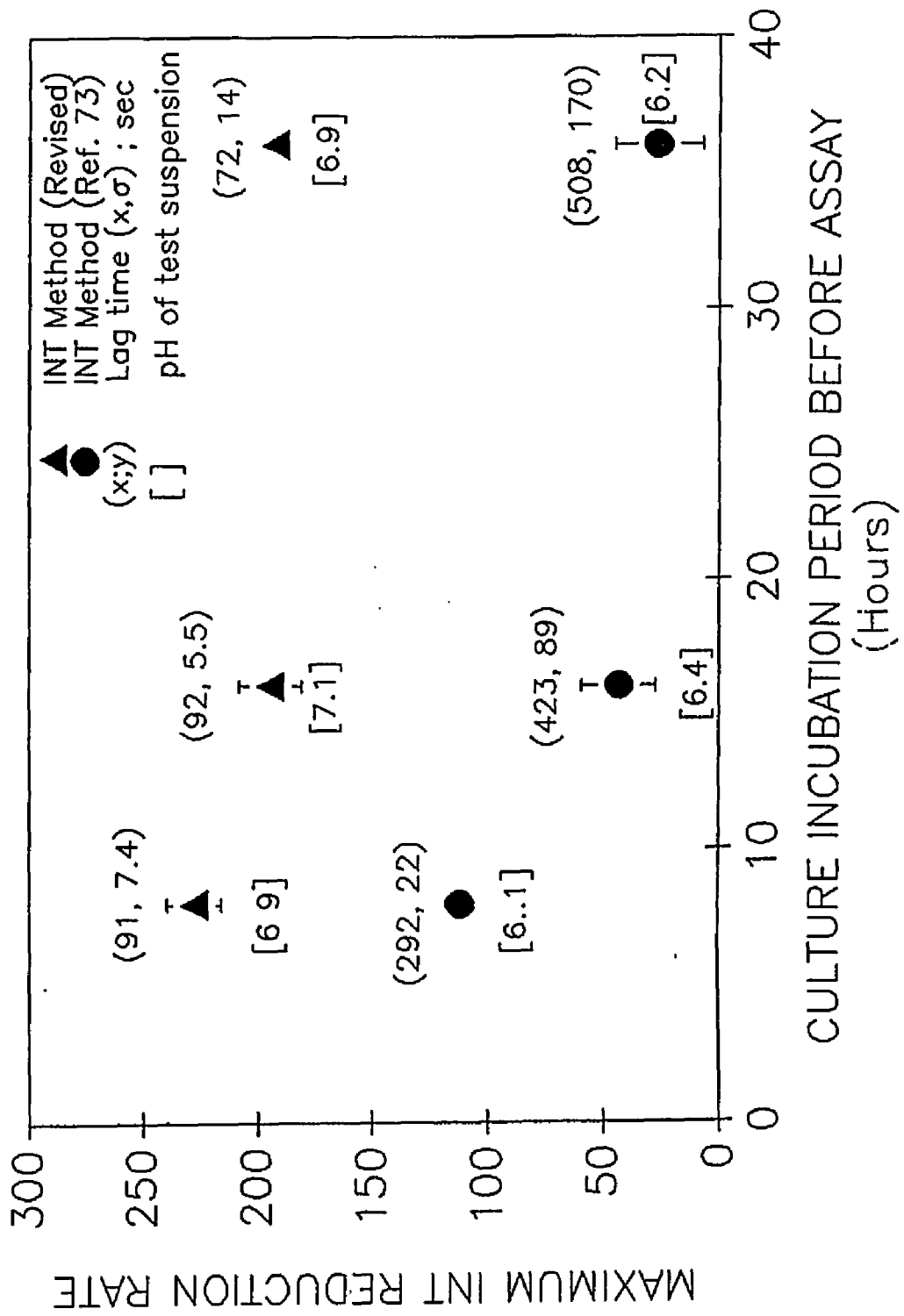
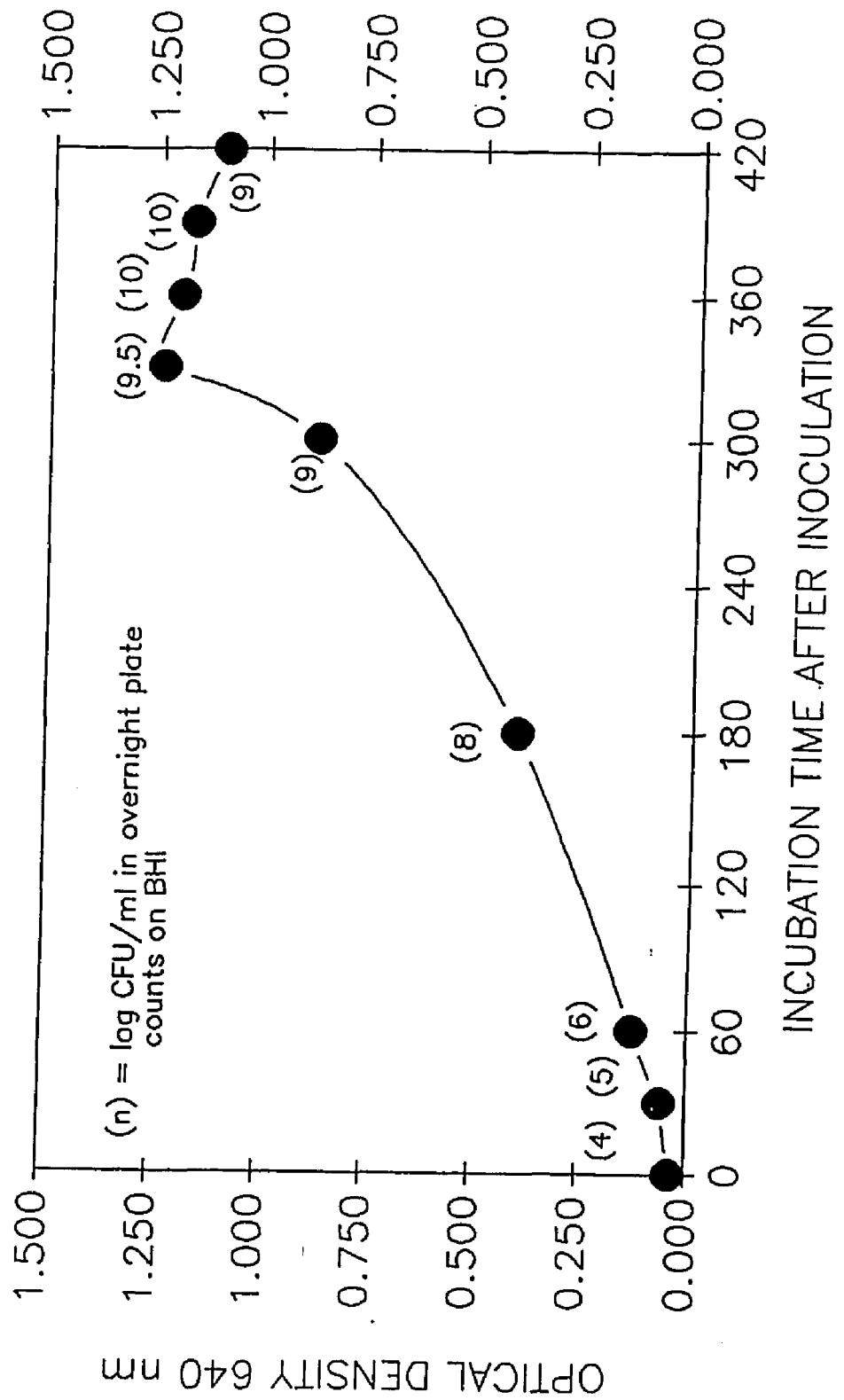


FIGURE 16. *Escherichia coli* Growth Curve.



response of the two treatments appeared similar, but lag time c.v.s were between 4.7 – 20% over the entire test period for the revised method, and 7.6 – 74 % for the published . Assuming that results derived from *E. coli* can be compared to those for a *Pseudomonas sp.*, it is not surprising that the toxicity work in the published method had very low variability. The effect of toxicants would amplify those of medium toxicity and limit the range of ET responses in treatments.

The agar/PBS resuspension and sonication steps were designed to 1) raise pH values characteristic of the spent medium (measured range = 6.0 – 6.5) to optimum values in the resuspension (measured range = 6.9 – 7.3) and, 2) facilitate separation of cell clumps without deleterious effects on the bacteria. Sonication was initiated because cell sedimentation and clumping during pipeting was observed when normal (unthickened) PBS was used as the resuspension medium. Visual observations of sonicated cells in DAPI procedures indicated that the light sonication step was successful in separating the cell aggregates. Further, INT responses were stimulated in the suspensions relative to unsonicated cultures (Table 2). The light sonication had a stimulatory effect on *E. coli* with treatment times of < 30 s. Sonication for more than 30 s caused reduction in INT response, probably because of heating of the medium. Therefore the length of preparative sonication of *E. coli* test suspensions was limited to 5 one second bursts at low fequency.

V. Solution Behavior of the NCAC Reagents

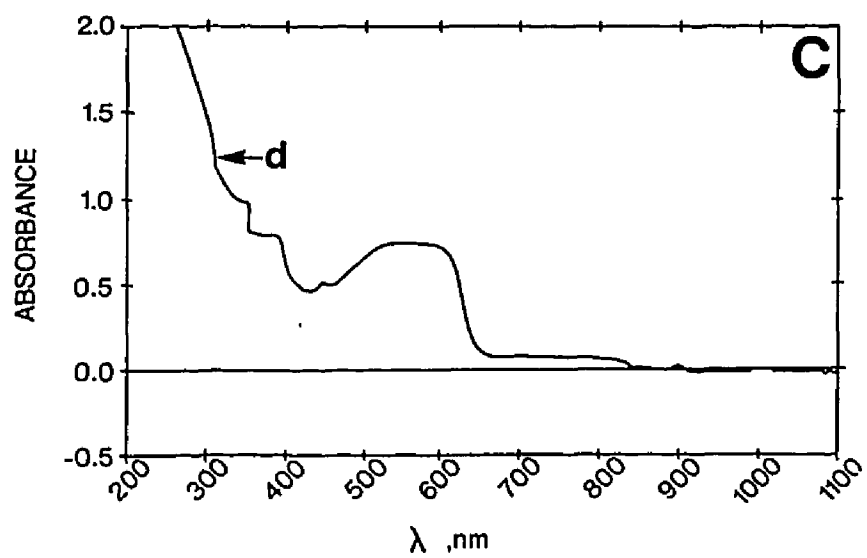
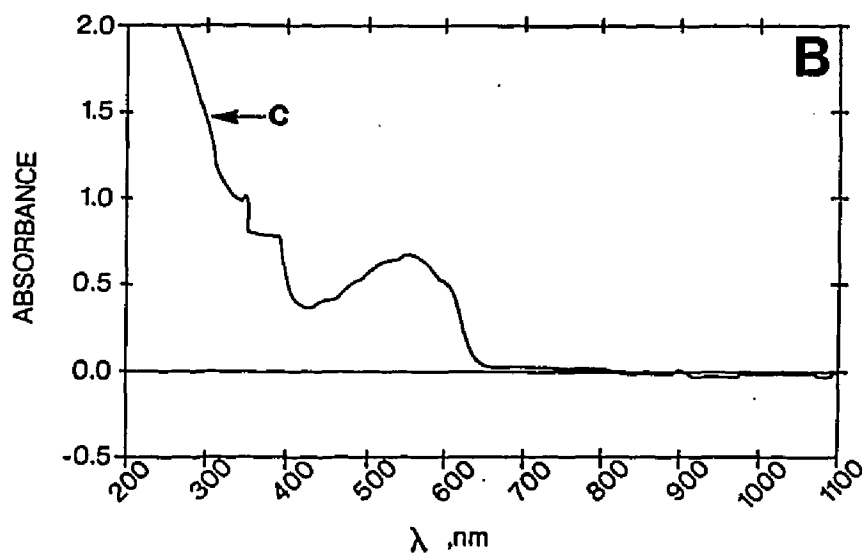
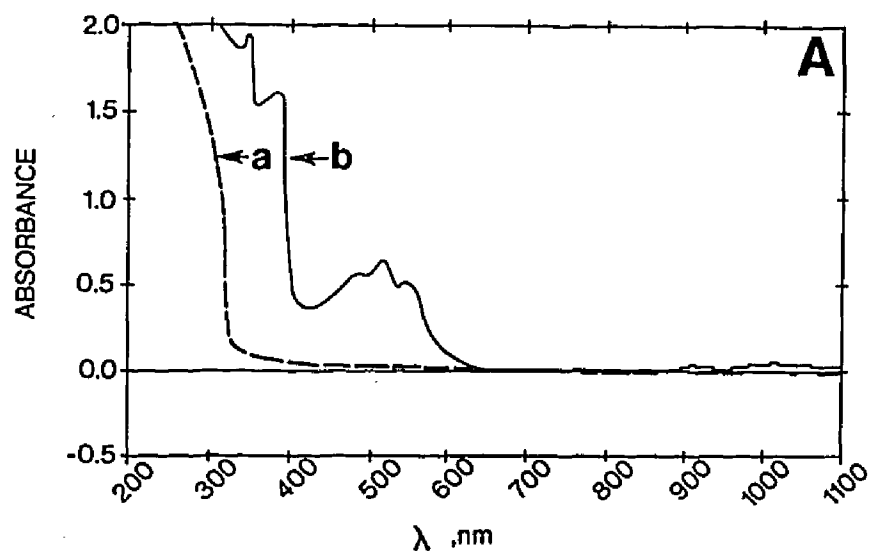
Quinoline master stock solutions in DMSO exhibited indefinite shelf life under nitrogen at 0 °C, with no significant degradation products observed in

TABLE 2. Effect of Sonication Time on INT Response and Viable Cell Density in *E. coli*.

Sonication Time (sec)†	Lag Time (sec)	Max. INT Slope	CFU/ml (BHI agar)
0	50 (4)*	255 (3)*	10 ⁹
5	87 (5)	253 (11)	10 ⁹
10	57 (5)	366 (18)	10 ⁹
20.0	63 (6)	420 (17)	10 ⁹

† Instrument on low setting (setting = 2).
* Population standard deviation; N = 3

FIGURE 17.A. Electronic Absorbance Spectra of 4-AF (a) and 4-AF Degradation Products (b) After Reaction With DMSO (5 min.). B. 4-AF Degradation Products (c); 15 min. reaction with DMSO. C. 4-AF Degradation Products (d); 25 min. reaction with DMSO.



routine checks of absorbance spectra and occasional analysis by capillary column GC. This was not the case with 4-AF, which degraded under these conditions to a chromogenic product that reacted with the DMSO:PBS carrier to form a red solution, which gradually turned crimson, violet, and then green-black. Absorbance spectra of 4-AF and the degradation product(s) are presented in Fig. 17. As a result of this degradation problem, data from several INT assays, cell counts, and oxygen consumption studies had to be discounted because the red reaction product obviously was not the test compound of interest. Thereafter, 4-AF master stock solutions were checked immediately before each dose application in the bioassays to make certain that degradation had not occurred. Also, 4-AF crystals were dissolved directly in DMSO rather than first dissolving them in small amounts of hot EtOH followed by DMSO. Interestingly, the 4-AF degradation product did not appear to be photolytic in origin. Exposure of quinoline and 4-AF solutions in 1:2 (v/v) EtOH/PBS in borosilicate flasks to natural and artificial sunlight (GE Quartzline Lamp, Q500T 3/cc) for relatively extended periods suggested that quinoline had a low Φ , while 4-AF was more photoreactive. The latter estimates were semiquantitative and based on product absorbance spectra (Fig. 18). Although presumptive 4-AF photoproducts and altered absorbance spectra were observed after 30, 60, and 90 min irradiation periods with the Quartzline lamp, these products were red-brown in solution and showed no propensity to react with DMSO. It was concluded that chemical oxidation was responsible for the 4-AF products.

VI. Identification of a 4-AF Oxidation Product

Normal phase HPLC analysis of the green-black 4-AF degradation mixture in DMSO showed that at least 5 different compounds and/or isomers were present. Thin layer chromatography of this mixture resolved two major bands. One band was fluorescent (excitation $\lambda = 254$ nm and 350 nm) and the other was non fluorescent at both wavelengths. The non fluorescent product was less polar than the fluorescent material (inferred from chromatographic mobility) and was red-brown in color. This product gave a mass spectrum with a molecular ion at $m/z = 151$ and fragments at 139 and 93. The mass spectrum of the fluorescent product was consistent with 4-azafluorene-9-one (Figure 19). The other products in the mixture were assumed to be isomers of the 4-azafluorene standard reagent.

VII. NCAC/INT Bioassay Results with Mechanistic Interpretations

Treatment of aerobically grown *E. coli* cultures with increasing doses of quinoline and 4-AF gave nonlinear responses in electron transport (ET) as measured by the reduction of INT to INTF (Figures 20 and 21). With both NCAC's, dose *vs.* ET functions decreased linearly to around 50% inhibition (*i.e.*, the EC_{50}), increased to levels near or above the controls, and then decreased rapidly to background levels. The "threshold" dose range where stimulation of ET was noted was more discrete with quinoline (22 - 40 ppm) than with 4-AF (400 - 600 ppm), but in both cases the apparent ET kinetic response in this range differed markedly from controls and lower doses. In the controls and low doses, both NCAC's gave ET rate functions that were characterized by lag periods of 60 - 100 seconds (no INTF formation), followed

FIGURE 18. A and B. Electronic Absorbance Spectra of 4-AF (1) and Photodegradation Products. Irradiation Times: 30 min (2); 60 min (3); 90 min (4); 360 min (5).

C. Electronic Absorbance Spectra of Quinoline (1) and Quinoline Irradiated for 12 h. (2).

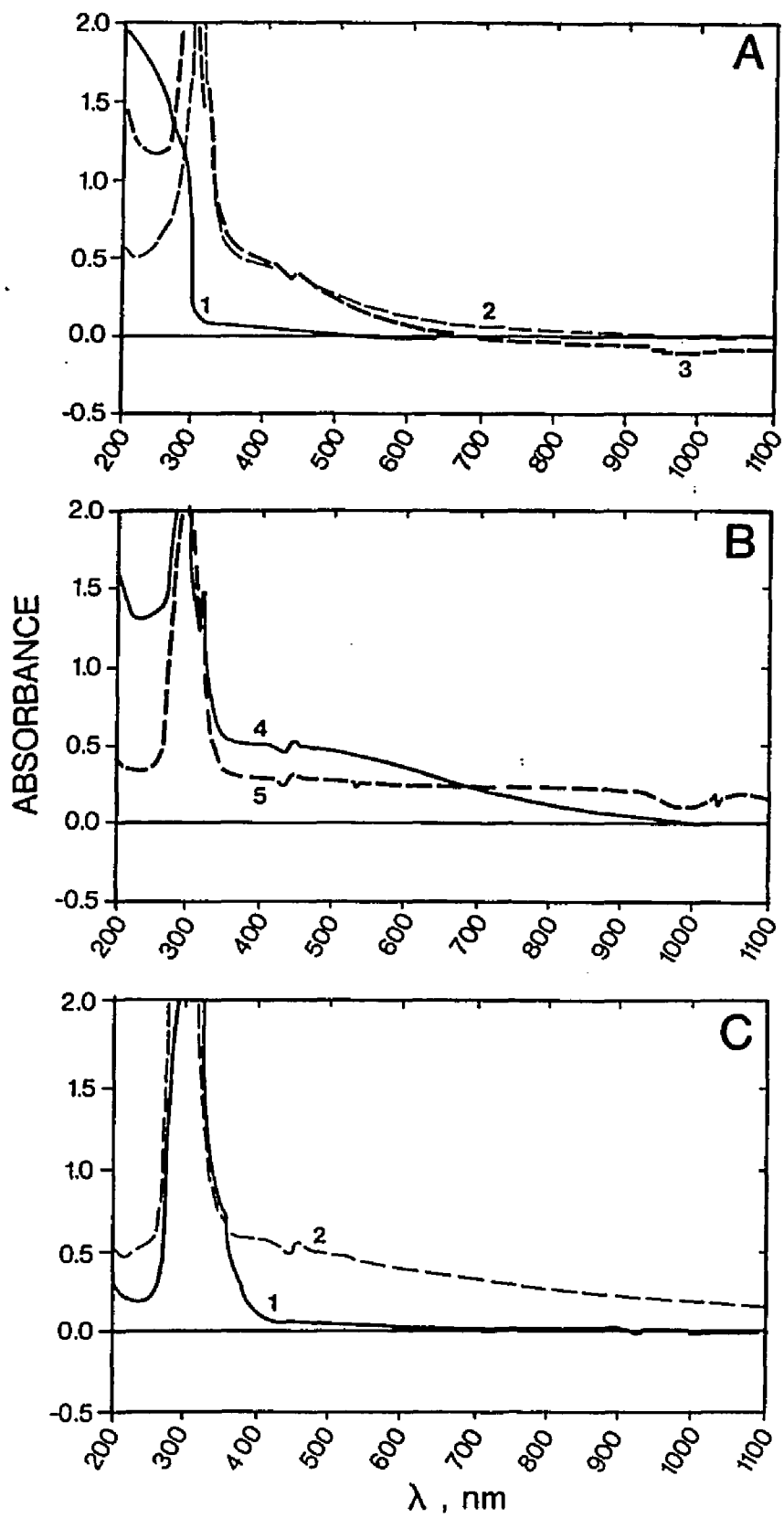
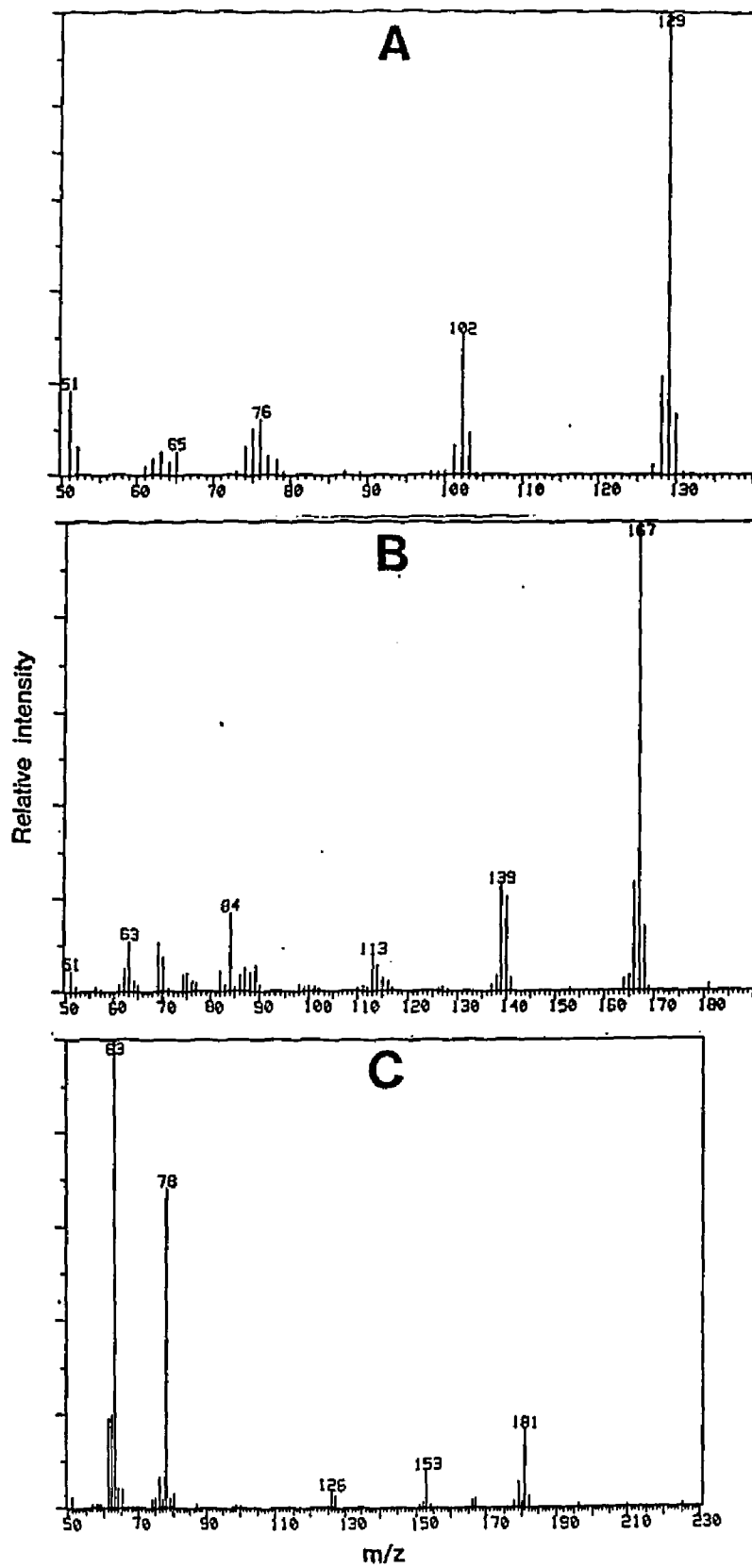


FIGURE 19. Mass Spectra. A. Quinoline standard. B. 4-azafluorene standard. C. 4-azafluorene degradation product in DMSO (4-azafluorene-9-one).



by rapid linear increases in absorbance at $\lambda = 490$ nm (reduction of INT to INTF by ET). This lag period, which showed a temperature dependence, was assumed to be the diffusion time of INT molecule across the outer membrane of the bacteria. At threshold doses, lag periods were not observed, the ET function was parabolic, and ET rates were stimulated (Figures 22 and 23). Assays conducted with other toxicants such as tributyl tin chloride (TBT; Figure 24) yielded expected dose-response functions with constant lag times. TBT was chosen for comparative purposes because 1) it was available in high purity, 2) it is membrane-active [112] and, 3) at threshold doses it is known to inhibit respiratory ET and oxidative phosphorylation *via* hydrophobic associations with ET enzyme complexes [112].

It can be seen from Figures 20 and 21 that the nonlinearities in electron transport were more pronounced with quinoline than 4-AF, and these occurred in a range of concentrations that might be encountered environmentally. For this reason and the degradation problems with 4-AF mentioned above, additional experiments were conducted using quinoline as the model toxicant. It was hypothesized that threshold doses of quinoline caused alterations of outer membrane (*i.e.*, the "cell envelope" surrounding the plasma membrane) permeability that allowed for instantaneous diffusion of the INT molecule to inner membrane reduction sites. To examine this, INT reduction was monitored in gram(+) cells (*i.e.*, cells naturally deficient in outer membrane lipids; *e.g.*, *S. salivarius*), and gram(-) cells that had diminished outer membranes from chemical or genetic manipulation (*E. coli* spheroplasts and *S. typhimurium* rfa mutants, respectively). These data were referenced to wild type gram(-) cells with intact outer membranes and are presented in Figures 25 and 26. These figures illustrate a gradient of ET kinetic response types ranging

FIGURE 20. **Effect of Quinoline Concentration on INT Reduction Rate**
in *E. coli*.

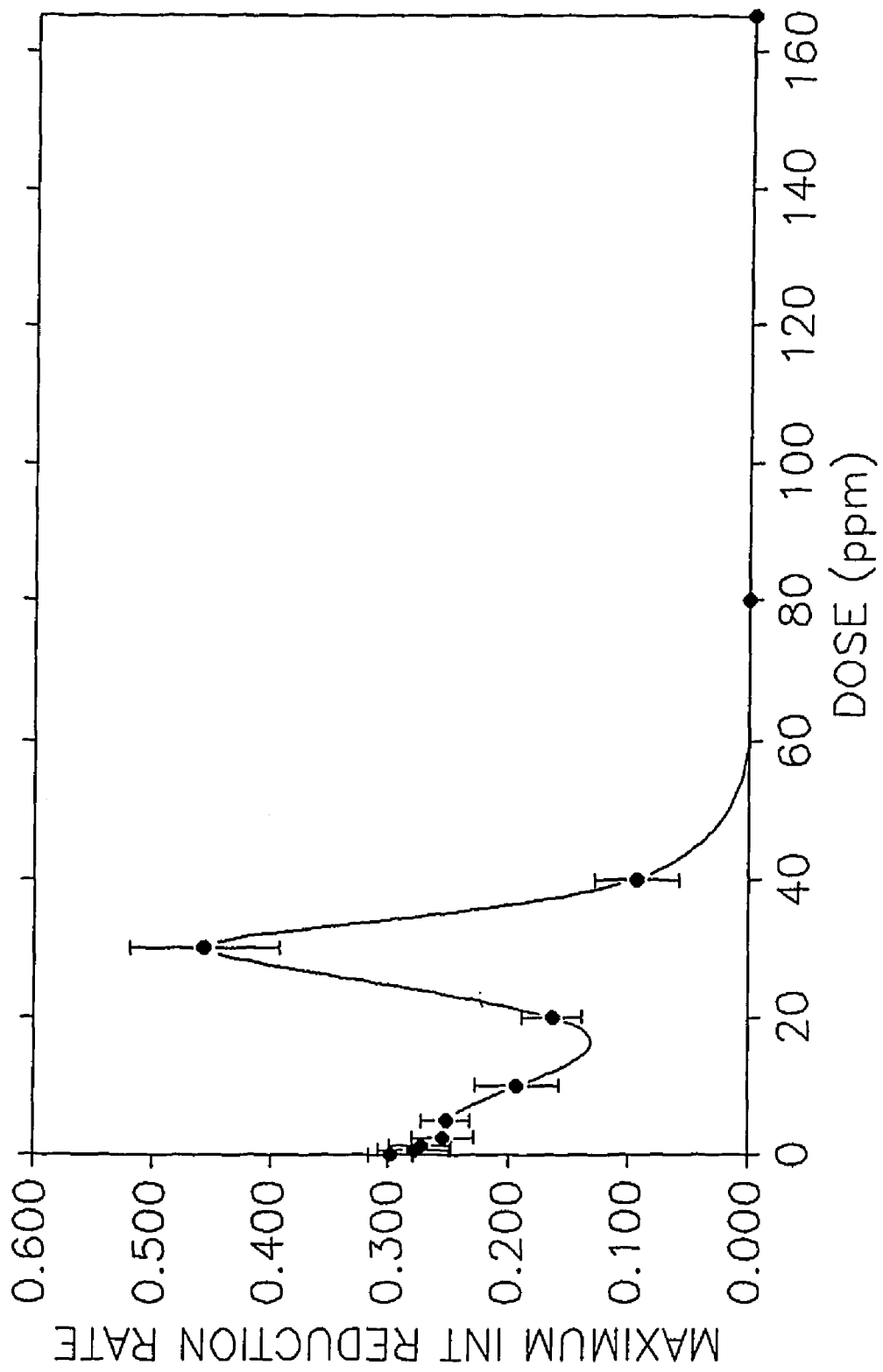


FIGURE 21. Effect of 4-azafluorene Concentration on INT Reduction Rate in *E. coli*.

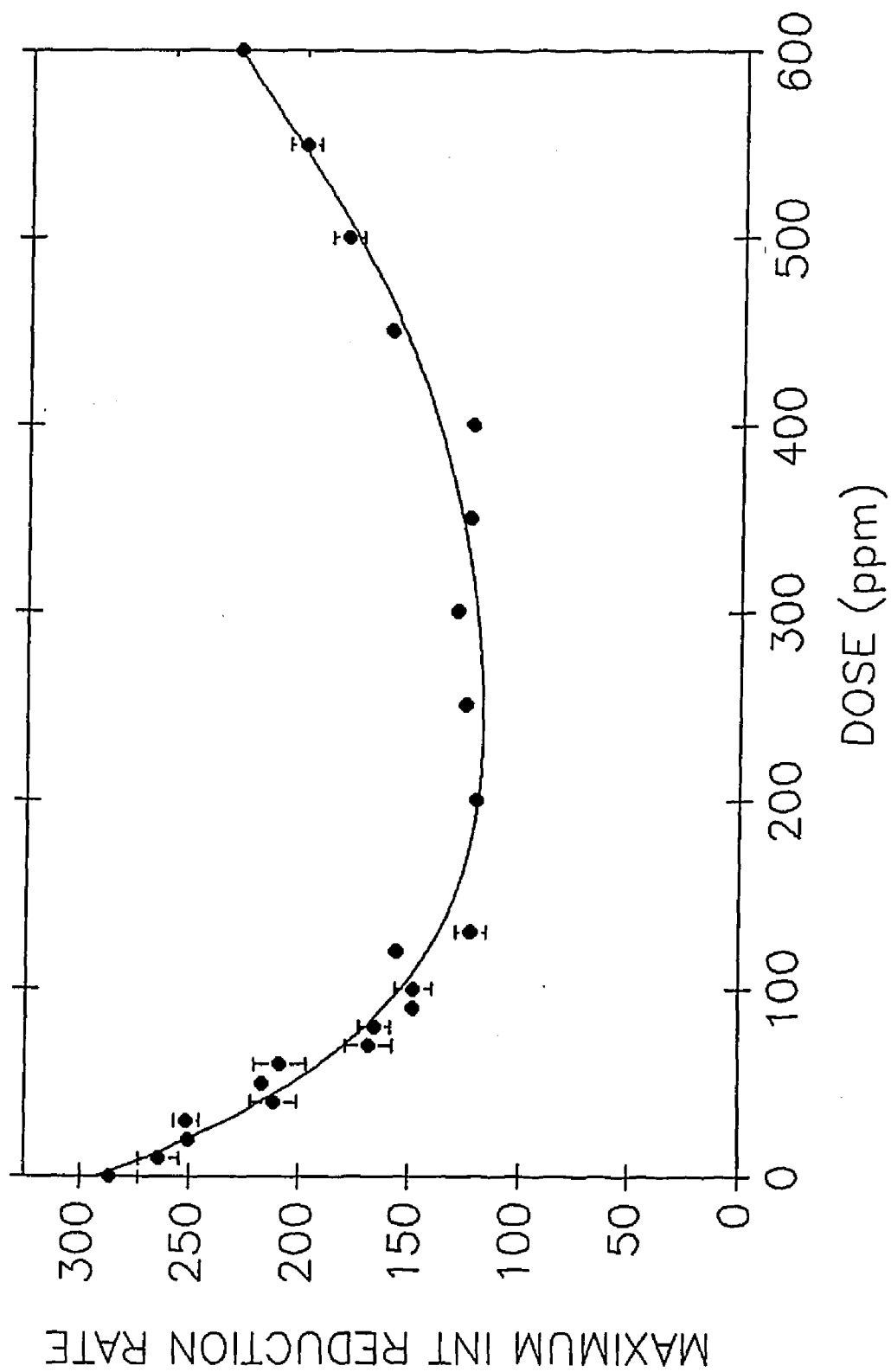


FIGURE 22. Effect of Quinoline Concentration on INT Reduction Kinetics in *E. coli*.

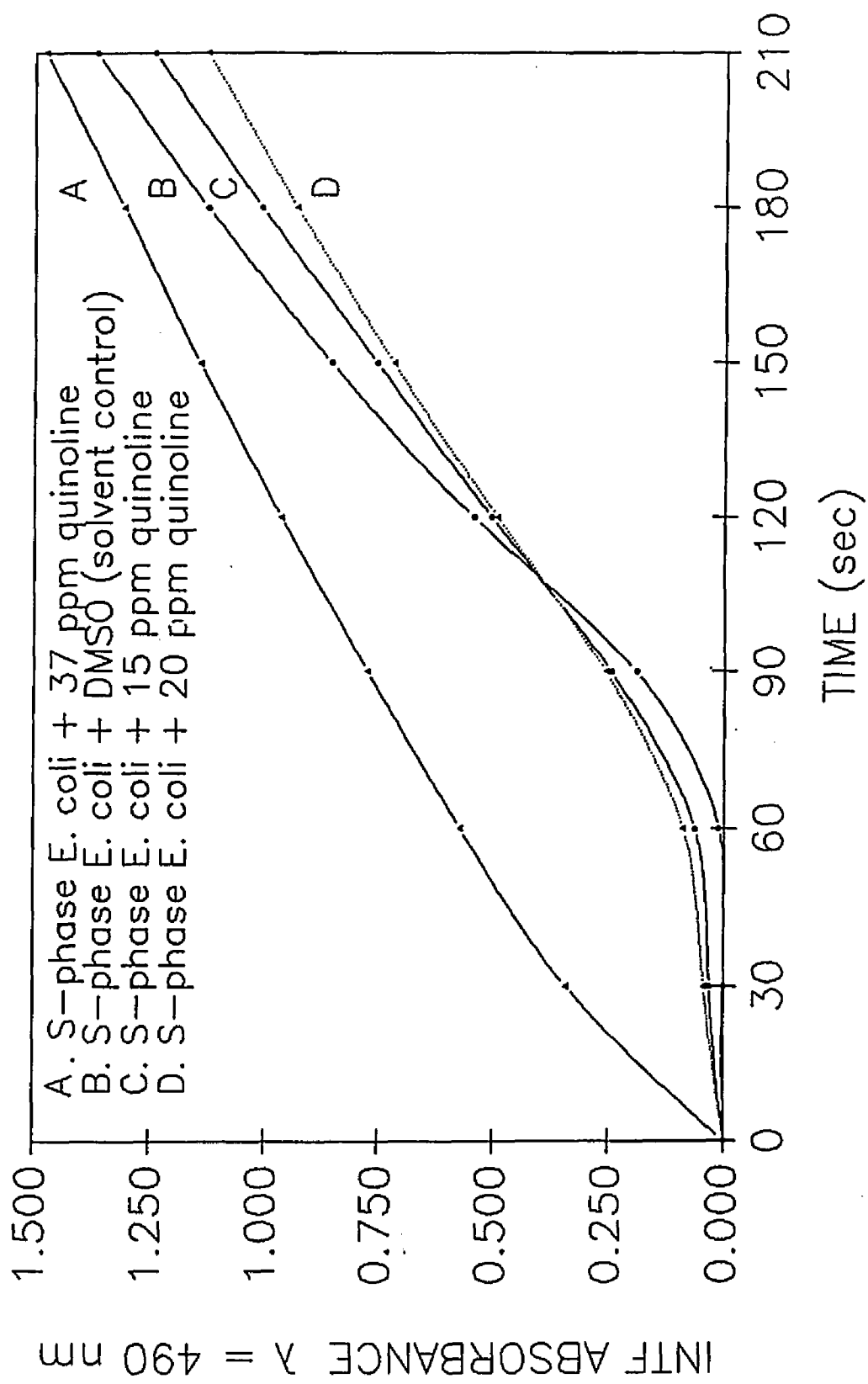


FIGURE 23. Effect of 4-azafluorene Concentration on INT Reduction Kinetics
in *E. coli*.

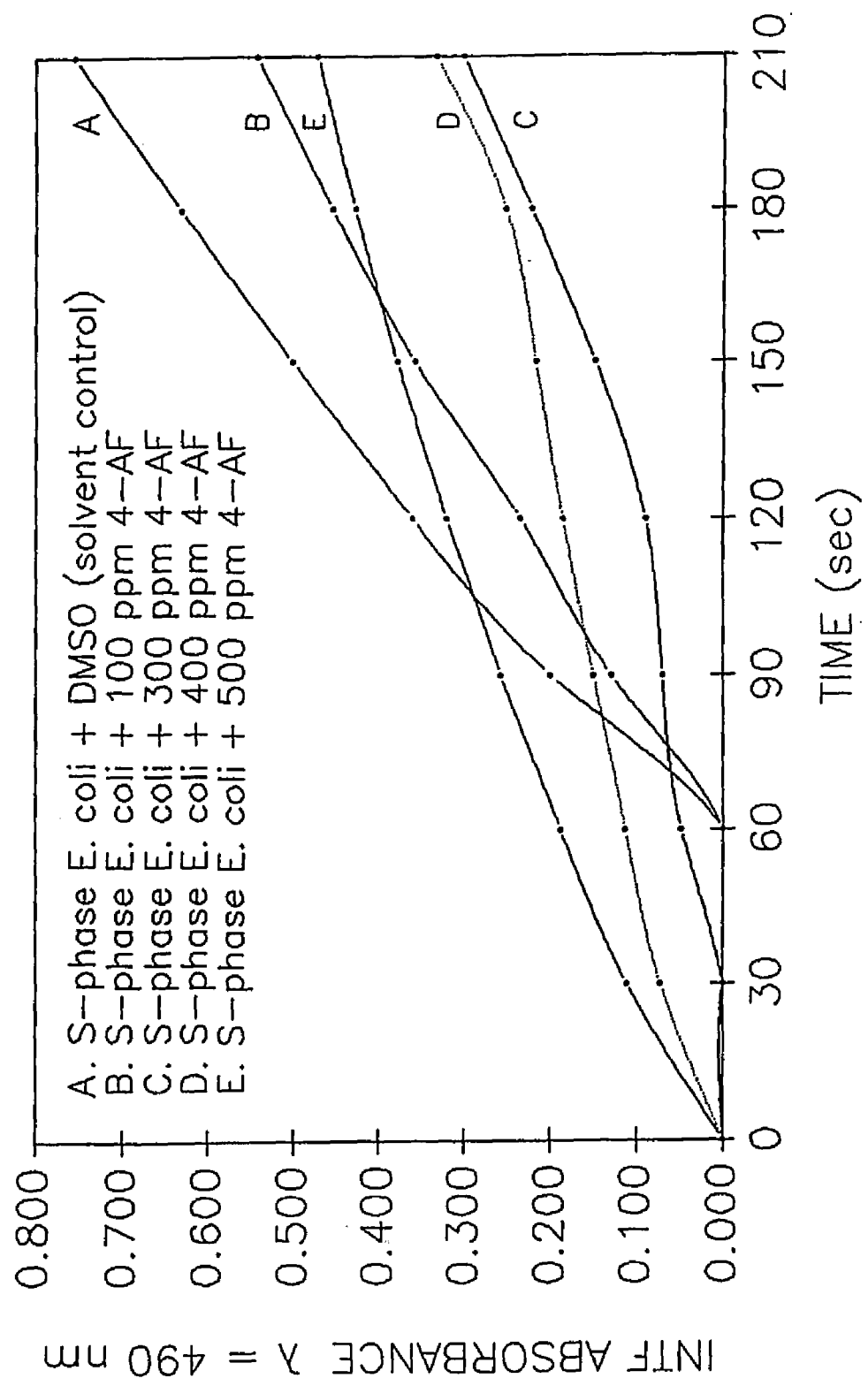
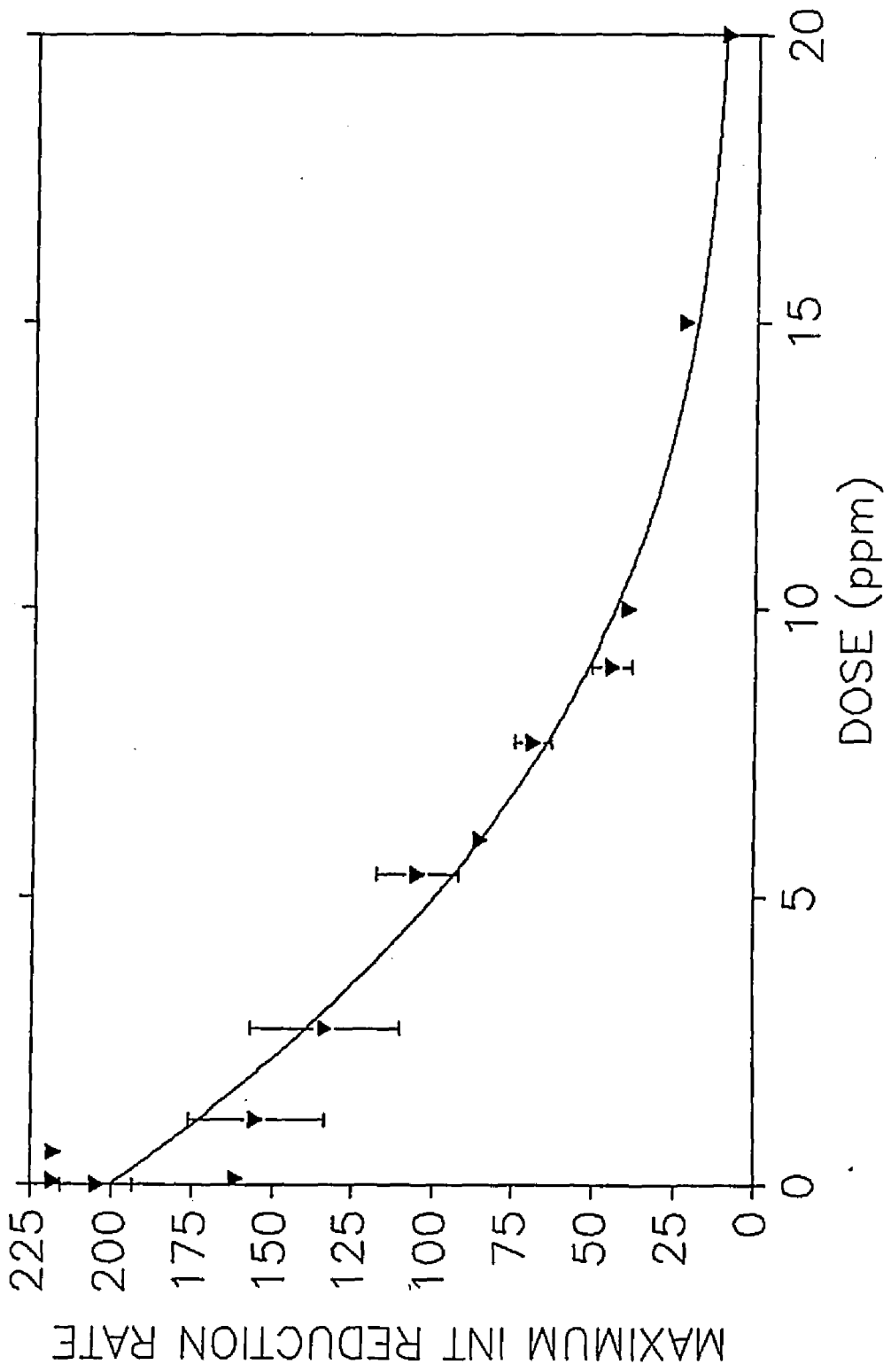


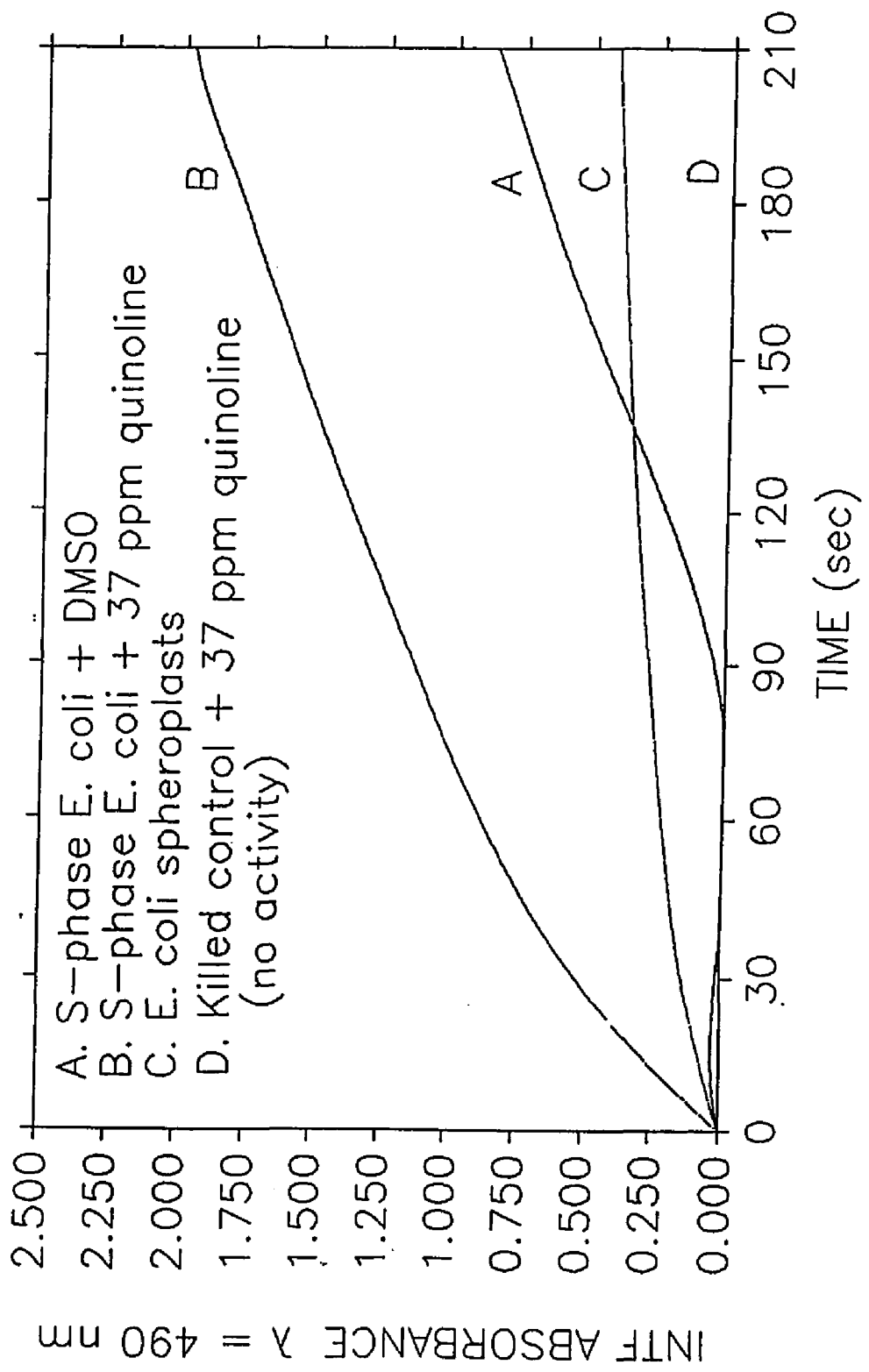
FIGURE 24. Effect of Tributyltin Chloride Concentration on INT Reduction Rate in *E. coli*.



from roughly sigmoidal (with lag periods before response) in gram(−) systems, to instantaneous linear and parabolic responses in cell systems with diminished or no outer membranes. Treatment of wild type *S. typhimurium* and *E. coli* with a threshold dose of quinoline (37 ppm) caused the ET response to change from sigmoidal to parabolic, and resemble the response of the gram(+) cells. This corresponds to the predicted diffusional behavior of INT in the presence of lipoidal outer membranes. In general, as lipoidal outer membrane character was decreased (wild type *E. coli* and *S. typhimurium* > *rfa* mutants > spheroplasts > gram(+) *S. salivarius*), the penetration time of INT was decreased as well. The decrease in lag time corresponds to a decreased interaction between INT and outer membrane structures, presumably lipids, and increased rates of access to inner membrane catalytic sites. In the threshold NCAC doses, the data suggest a similar increase in access to these sites, and the increased rates indicate an increased degree of reduction in the respiratory chain (discussed further below).

Questions arose as to whether the stimulated ET noted in the threshold doses was occasioned by increases in cell number (*via* adaptation or stimulated growth on the NCAC) or respiratory oxygen consumption. Table 3 shows that incubation of cultures with threshold doses of quinoline (35 ppm) for 60 minutes caused reductions in DAPI counts and much larger reductions in overnight viable counts. In 4-AF treated cells, overnight viability was reduced 7 – 9 orders of magnitude in doses much below the threshold range. These findings showed that while threshold doses gave stimulated ET responses after an hour of incubation, this was unrelated to cell number at the time of analysis and was inversely related to overnight viability. Figure 27 illustrates the effects of various doses of quinoline on oxygen consumption in treated *E. coli*. Cultures

FIGURE 25. INT Reduction Kinetics in Various *E. coli* Cell Systems.



A. S-phase E. coli + DMSO
B. S-phase E. coli + 37 ppm quinoline
C. E. coli spheroplasts
D. Killed control + 37 ppm quinoline
(no activity)

INTF ABSORBANCE $\lambda = 490 \text{ m}$

FIGURE 26. INT Reduction Kinetics in Deep Rough Mutants (*rfa*) and Gram(+) Cell Systems.

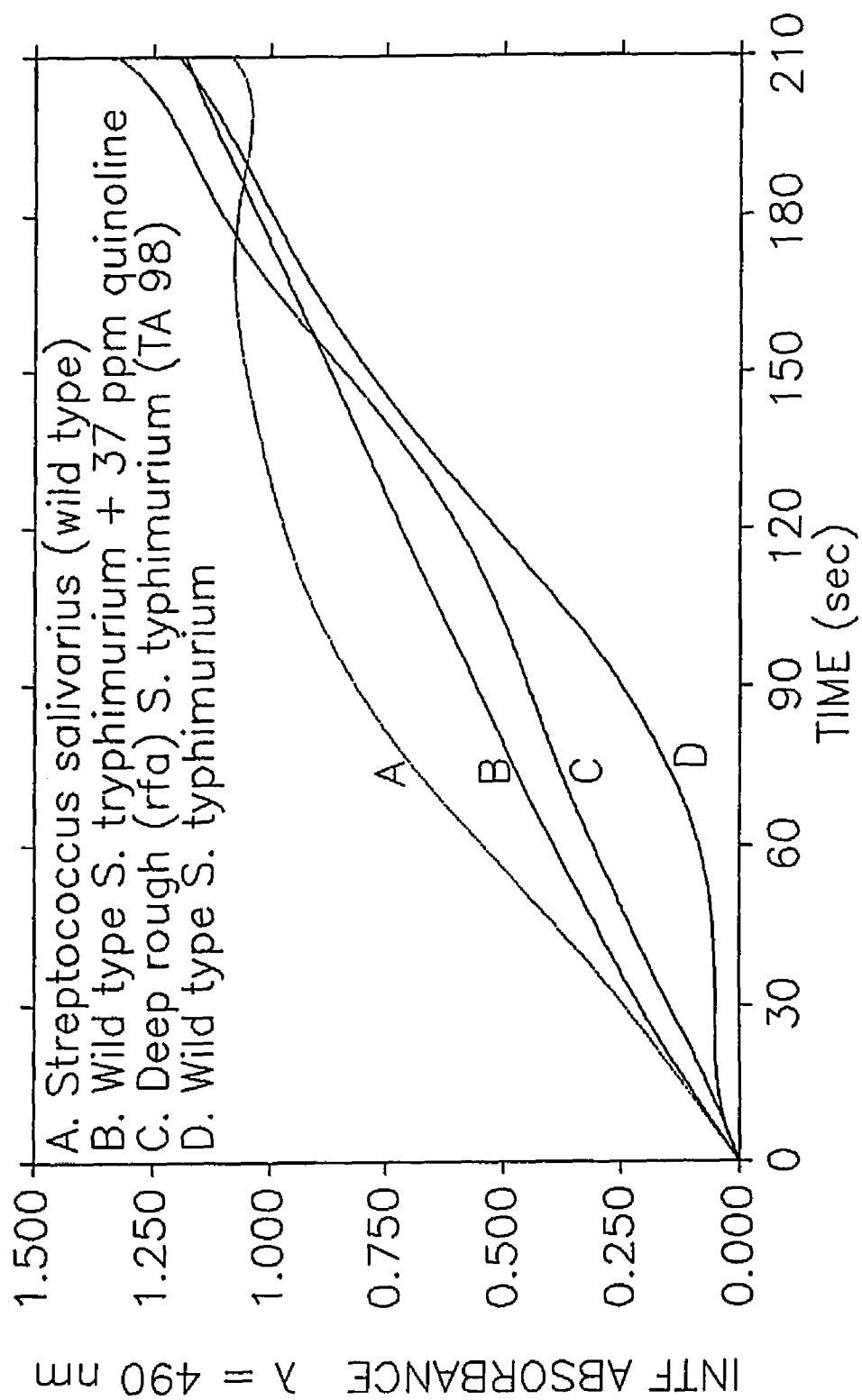


TABLE 3. Effect of Quinoline and 4-azafluorene Concentration on Overnight Viability and Direct Count Cell Densities in *E. coli*.

NCAC	Concentration (ppm)	Overnight Plate Count*	Direct DAPI Count*
Quinoline	0.0	$10^9 - 10^{10}$	10^9
	0.0(s)†	10^9	10^9
	5.0	$10^8 - 10^9$	
	10.0	$10^8 - 10^7$	
	15.0	$10^8 - 10^7$	
	20.0	$10^2 - 10^3$	10^9
	25.0	$10^1 - 10^2$	
	30.0	$10^1 - 10^2$	
	35.0	$10^1 - 10^2$	$10^7 - 10^9$
	40.0	$10^1 - 10^2$	
	50.0	$< 10^1$	
	80.0	$< 10^1$	
4-azafluorene	0.0	10^9	10^9
	0.0(s)†	10^9	10^9
	10.0	10^8	
	20.0	$10^7 - 10^8$	
	30.0	$10^5 - 10^6$	
	40.0	$10^3 - 10^4$	
	50.0	$10^3 - 10^4$	
	90.0	$10^2 - 10^3$	10^8
	100.0	$10^1 - 10^2$	10^8

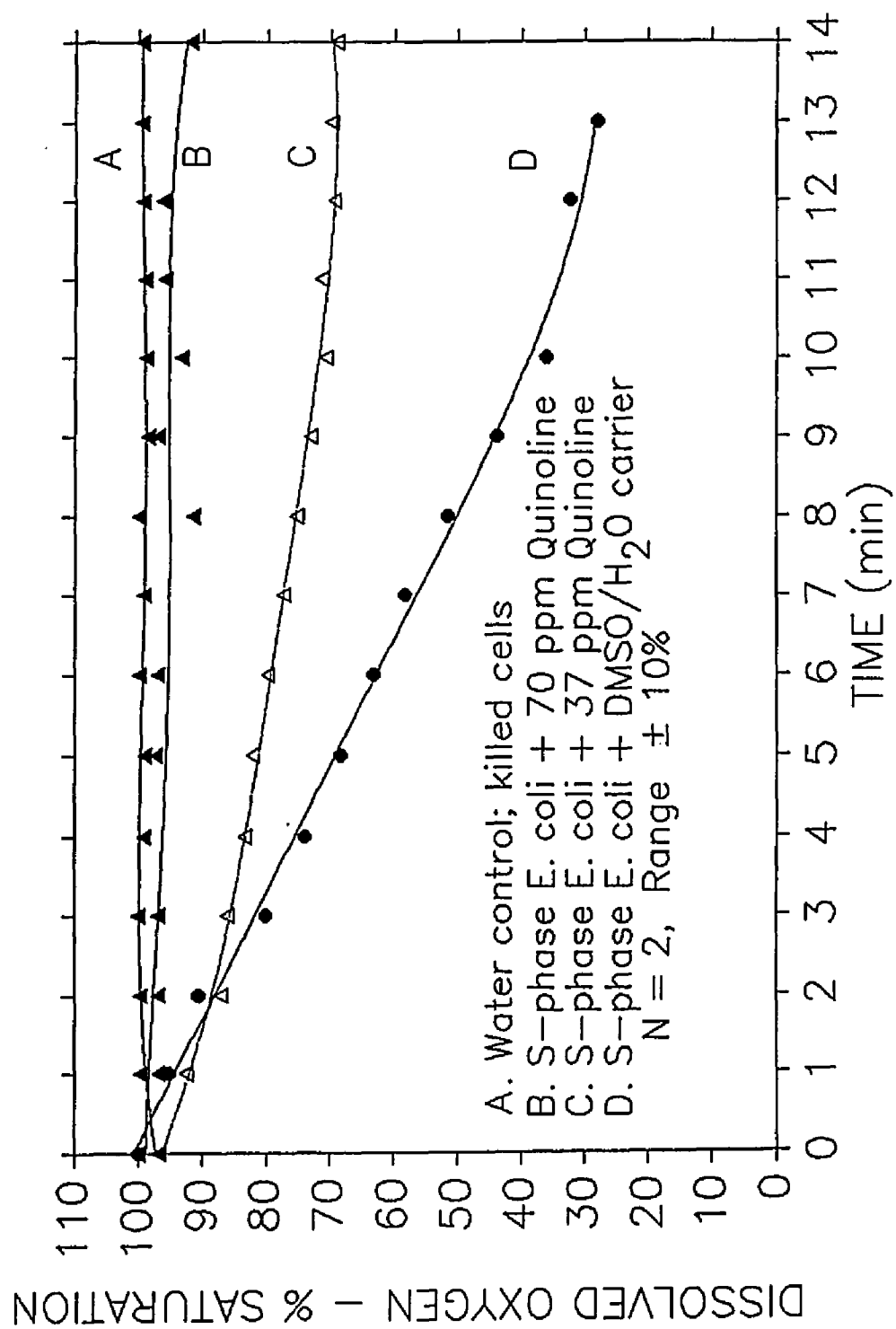
* colony forming units per ml.

† DMSO solvent control.

incubated with 37 ppm quinoline showed decreased oxygen demand relative to controls. ET analysis of these cultures gave the typical lag time before INT reduction in controls, while at 37 ppm quinoline, the response was parabolic with no lag, and INT reduction was stimulated above controls by a factor of 1.96. It is known that approximately 90% of total oxygen demand in *E. coli* is accounted for by cytochrome oxidases, which are tightly bound to the inner cell membrane, and conduct electrons from reduced terminal cytochrome(s) to oxygen [59, 60]. The ET and oxygen demand data suggest that the activity of these oxidases (or some other intermediate electron carriers) were inhibited at threshold doses of quinoline. In general, inhibition of terminal electron transport in the presence of adequate substrate is accompanied by accumulation of reducing equivalents (*e.g.*, ubiquinol) in the respiratory chain [60] and decreases in respiratory ATP production [113, 114]. The resultant decrease in cytosolic $[ATP]/[ADP][Pi]$ ratios gives rise to stimulated respiratory ET to O_2 [60, 113, 114]. Under conditions of chemical inhibition, however, this homeostatic compensation for [ATP] decreases cannot occur. Other oxidants, *e.g.*, tetrazolium compounds, can be reduced in the presence of ET inhibitors and frequently exhibit stimulated rates in inhibited *vs.* uninhibited systems [115, 116].

Theoretically, NCACs such as quinoline and 4-AF could inhibit electron transport either through terminal blocking of electron transfer (protein denaturation as with TBT, chemical oxidation of electron carriers) or by scouring of electrons followed by redox cycling with some other material present in the cell. The latter process has been observed with certain PAH quinones,

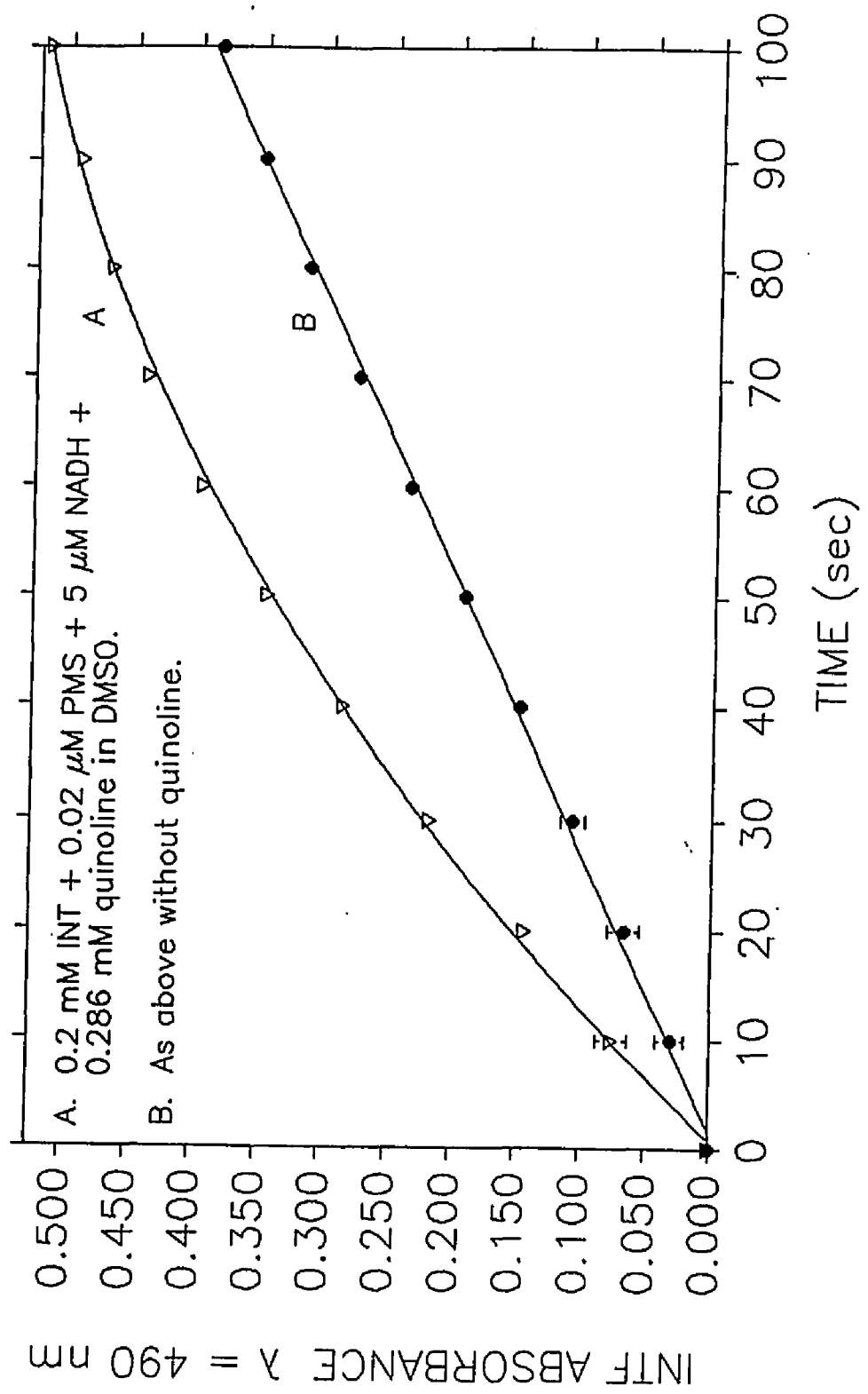
FIGURE 27. Effect of Quinoline Concentration on Cellular Oxygen Demand in *E. coli*.



which are able to oxidize NADH, reduce cytochrome c and oxygen, and nonenzymatically oxidize very stable aromatic systems such as benzo(a)pyrene [117, 118]. Further, several dialkyl pyridine and quinoline compounds have been shown to inhibit cytochrome P-450 activity and heme biosynthesis *via* a redox mechanism proceeding through radical cation intermediates [119]. In the present work, the accumulation of reducing equivalents, redox cycling of electrons *via* NCAC intermediates, and an increase in outer membrane permeability could account for the observed NCAC threshold effects in the absence of increased cell number and oxygen reduction. The data suggest that multilevel toxic effects of the NCACs gave rise to conditions of reduced homeostatic ability that were manifested in ET anomalies and reduced cell viability. Also, it appears that the primary assumption of the INT rate assay (*i.e.*, direct proportionality between INTF production rate and metabolic "health" of a cell system) was not supported with respect to NCAC-treated *E. coli* [65, 69 - 74, 79 - 83]. This is significant because tetrazolium reduction has long been proposed as a reliable method for monitoring the health of wastewater microorganisms subjected to contamination [79] and for monitoring polluted environments. The responses observed in this work could easily apply to other contaminants and species, and would be especially significant in real world treatment facilities, where effluent composition and toxicity typically is highly variable from day to day.

Results of assays measuring nonenzymatic reduction of INT by NADH as effected by PMS, DMSO, and 37 ppm quinoline are summarized in Figure 28. In the time period of the assay (100 sec.), direct INT reduction by NADH was not observed (*cf.*, NADH results, Fig. 4). The addition of PMS, however, catalyzed rapid electron transfer from NADH to INT. At 37 ppm quinoline the

FIGURE 28. Effect of Threshold Concentration of Quinoline on PMS-Mediated Reduction of INT by NADH. Noncellular system, pH 7.2, N = 3.

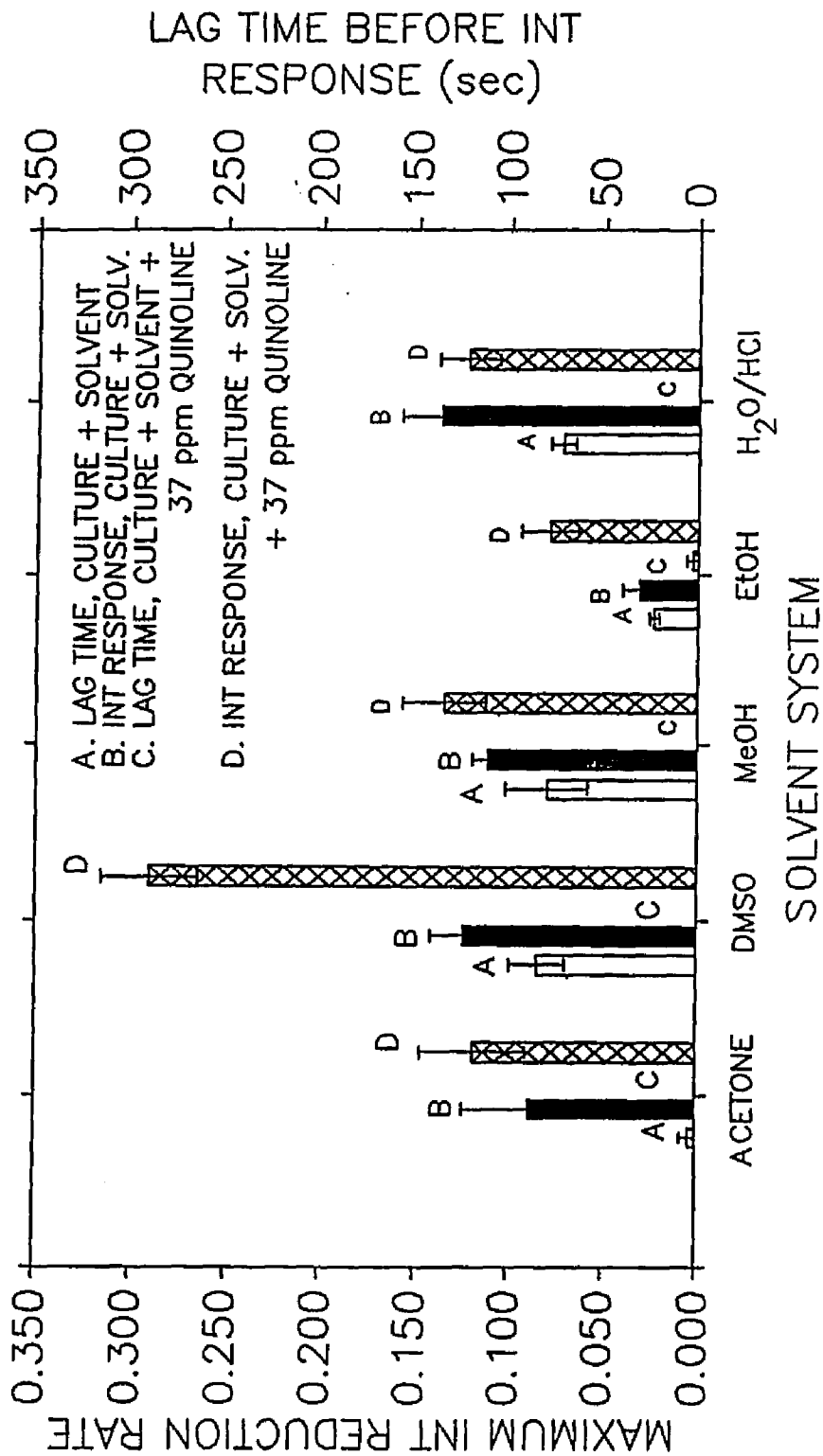


NADH/PMS reduction of INT appeared to be further stimulated. No attempt was made to demonstrate quinoline concentration effects on stimulation of ET. For the threshold runs reported, quinoline caused marked stimulation of ET rate and total INT reduction per 100 s interval relative to the DMSO controls. The stimulation of ET from NAD(P)H to oxidants such as tetrazolium salts and oxygen by flavin analogues (*e.g.*, PMS) has been well established. It is also known that reduced flavin dehydrogenase systems (containing a PMS-like catalytic center) can be directly oxidized by tetrazolium salts but not by oxygen, because the catalytic moiety is shielded in the native state [59]. This gives an important insight to the reasons for depressed oxygen reduction in the threshold NCAC treatments while, at the same time, INT reduction indicated vigorous ET: inhibition of ET reaching terminal oxidases would cause the O₂ binding sites to saturate. At the point of saturation, O₂ consumption (binding followed by reduction) would be curtailed. Opportunistic (*i.e.*, non enzymatic) O₂ reduction at flavin centers also would not occur for reasons already given. This leaves open the possibility of oxidation of pyridine-linked systems, which can be oxidized by oxygen directly, albeit at slow rates relative to enzymatic reduction. The results from Figs. 27 and 28 indicate that appreciable levels of nonenzymatic oxidation of pyridine linked systems are not occurring and this further suggests that redox cycles are operating that inhibit the ability of O₂ to oxidize molecules in the respiratory chain. The lack of detected threshold anomalies in TBT treated *E. coli* further reinforces the redox hypothesis because TBT causes ET inhibition by denaturing proteins, not by redox cycling, and oxidation of pyridine-linked systems can still occur in TBT treated systems [112].

VIII. Effects of Solvents on INT Reduction Kinetics

Although the characteristic ET response in solvent controls was identical to untreated controls in terms of lag time and apparent kinetics, it was of interest to examine potential interactions between the quinoline and the DMSO solvent system. Stimulated, parabolic ET responses at critical doses of quinoline had been observed in other solvents systems, *viz.* Tween 80: ethanol: water (1:5:94 % v/v/v), so a range of different solvents were examined. Figure 29 summarizes the effects of five solvent carriers (8 % final concentration) and 37 ppm quinoline treatments on lag time and ET rate in *E. coli* suspensions. Acetone and, to a lesser degree, ethanol caused reductions in lag times in the absence of quinoline. In the case of acetone, the addition of quinoline did not significantly alter the electron transport response relative to the solvent alone. In other solvents however, addition of quinoline caused electron transport kinetics to change from sigmoidal to parabolic and gave stimulated ET rates. In the absence of organic solvents (*i.e.*, the H₂O/HCl treatment), quinoline-HCl gave similar results. Apparently, there was a significant degree of synergism between quinoline and DMSO in terms of ET rate, but not lag time. Work with mitochondria and submitochondrial particles has shown that high levels of DMSO (5 – 20 %) increase membrane permeability and facilitate electron transfer between thiol groups on dehydrogenases and tetrazolium acceptors [121]. But there are numerous problems in comparing mitochondria with gram(-) bacteria, and even greater difficulties in comparing submitochondrial particles with anything else. For example, mitochondria lack an outer membrane and peptidoglycan sacculus characteristic of gram(-) bacteria, and have porous, highly specialized catalytic inner and outer "plasma"

FIGURE 29. Effect of Solvent System (8 % final) and Threshold Concentration of Quinoline on Lag Period and INT Reduction Rate in *E. coli*.



membrane systems. Submitochondrial particles are inside-out relative to the intact organelles and assays are frequently conducted in augmented, decidedly nonphysiological, media. Data on DMSO-ET effects in these systems can therefore be used only in a heuristic sense when interpreting bacterial data. A DMSO-mediated stimulation of ET was suggested by the results of one bacterial-INT reduction study in which the toxicity of various herbicides was found to be depressed in DMSO relative to acetone and ethanol [73] (*cf.*, the INT response in these solvents in Fig. 29). Although there was no discussion of specific rates or presentation of graphic data in this study, the increase in herbicide dose needed to reach the EC_{50} in DMSO could have resulted from a solvent stimulation of ET. In the INT assays of this work, however, these effects were not observed in solvent controls, NCAC doses outside the threshold range, or in the PMS assay described above. The results presented in Figure 29 were obtained using solvent concentrations above those used in the INT assays, which were kept between 2.5 - 4%. Assays with increasing levels of DMSO (0, 6%, 20%, 30%, and 50%) did not evidence lag time changes or significant toxicity until concentrations were greater than 20 %, at which point significant ET activity was not detected in 210 s runs. The reduction of lag time and stimulation of INT response by quinoline in several different solvents, including water, indicates that the chemical characteristics of the NCAC, not the solvent, accounted for the observed ET anomalies at the threshold doses.

IX. Ultrastructural Evidence of NCAC-Mediated Membrane Effects

The effects of quinoline-HCl on *E. coli* membrane structure as evidenced by transmission electron microscopy (TEM) are presented in Figure 30, A - G.

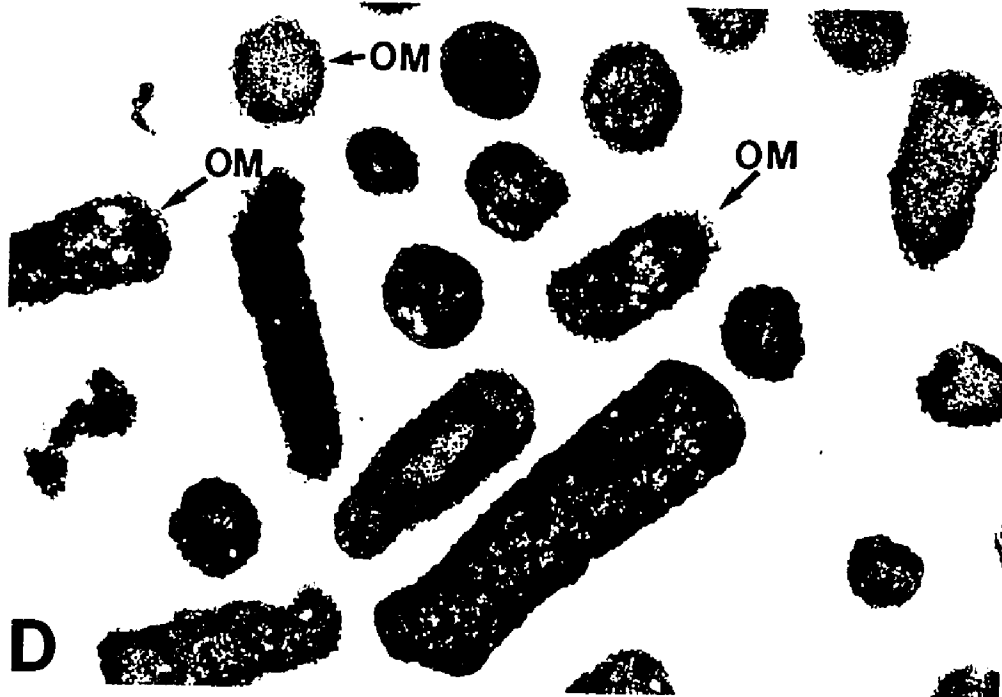
Figure 30 A shows the solvent control with cells appearing morphologically normal and showing no signs of structural distortion. Parts B and C show the same cells after 2 minutes and 12 minutes of incubation with INT (respectively). In both, INTF deposits can be seen extending from periplasmic regions into the cytoplasm, with apparently undisrupted outer membrane layers surrounding the inclusions. Fig. 30 D and E give two perspectives on quinoline-HCl treated cells in the absence of INT. The presence of outer membrane wrinkles and topological distortion relative to the controls can be readily seen (note periplasmic space and outer surface). Parts F and G show the quinoline-HCl treatments after incubation with INT for 2 minutes. INTF inclusions are very prominent in these treatments and fill the periplasmic space and cytoplasm to a larger extent than control cells incubated with INT for 12 minutes (*cf.*, Fig. 30 C, F, G). The outer membranes appear fragmented and overall cellular shape is highly distorted. The difference in INTF inclusions between the quinoline-HCl cells and control cells after 2 and 12 min incubation with INT (respectively) supports the results of the spectrophotometric rate assay.

It is interesting to note that the inner membranes in Fig. 30 D and E also appear to be affected by the outer membrane distortions, and this suggests that in addition to permeability problems, additional secondary effects may have occurred. ET molecular complexes operate by concerted creation and destruction of macromolecular wavefunctions [58] which open and close catalytic centers through protein conformational changes. Many of the ET complexes are embedded in the membrane and accept electrons from diffusable carriers such as ubiquinone. It can be clearly seen that physical and chemical inner membrane integrity is therefore essential for proper functioning. Departure from normal membrane topology would result in decreased efficiency

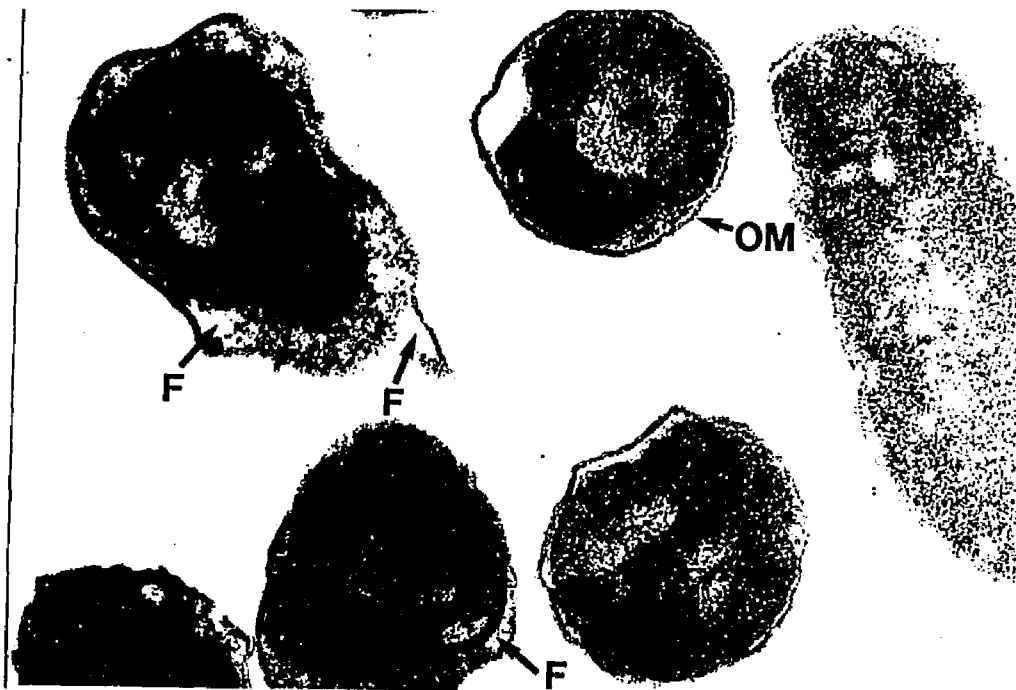
FIGURE 30. Transmission Electron Micrographs of Control and Quinoline-HCl Treated *E. coli*.

- A. Solvent Control (34,660 X). PS = periplasmic space; OM = outer membrane.
- B. Solvent Control + 0.3 ml INT Stock (12,600 X). 2 min. incubation with INT. F = INT-formazan deposit.
- C. Same as B.; 12 min incubation with INT.
- D. NCAC Treatment, 37 ppm quinoline-HCl (12,600 X).
- E. Same as D. (21,000 X).
- F. Same as D., with 0.3 ml INT stock (17,280 X).
- G. Same as F. (21,000 X).









of electron transport (*e.g.*, sequestering or distorting of active sites, increasing energy of activation for conformational changes, increasing distances between sites), and this would reinforce the redox effects of the NCACs. The high degree of connectance between the outer and inner membrane structure and function makes differentiating these processes difficult. Resolution of these processes would require a much higher degree of analytical sophistication than was available for this study.

INT activity was not detected in 0.22 μm filtrates of *E. coli* treated with 37 ppm quinoline, and there was no detected change in UV/visible absorbance spectra of these filtrates. Similarly, freeze-thaw and spheroplast lysis filtrates did not reduce INT. Sucrose-mediated osmotic shock and lytic ultrasonication for 8 min. eliminated INT activity, in both test suspensions and filtrates. This indicated that the threshold membrane effects were not lytic in nature and did not involve the liberation of detectable amounts of free lipid or protein from outer membranes. Treatment of *E. coli* with 37 ppm quinoline dose and equimolar amounts of Mg^{2+} (60 min) did not cause a decrease in the threshold response as might be expected if the NCAC were weakening of the outer membrane *via* chelation of coordination ions between the lipopolysaccharide layers. The chemical environment surrounding divalent cations in a lipid membrane *vs.* that in aqueous suspension are highly disparate, so addition of cations to the suspension does not constitute a conclusive falsification of the chelation hypothesis. For example, treatment of *E. coli* with EDTA gave a parabolic response, but it was depressed relative to untreated cells. The lack of increased ET in the EDTA treatment would be expected since EDTA does not enter the respiratory chain and cause accumulation of reduced equivalents *via* redox cycling as postulated for the NCACs.

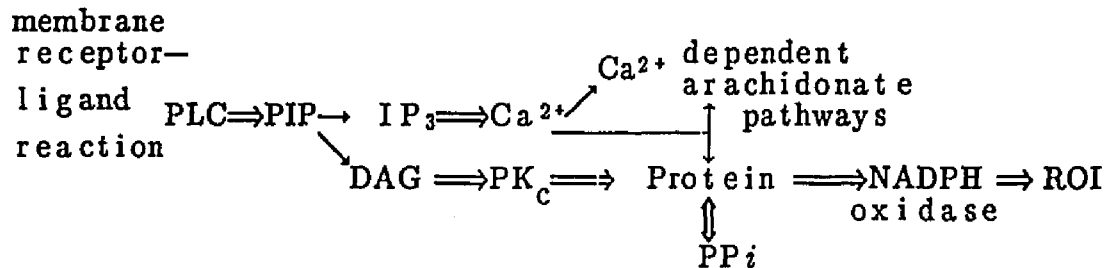
IX. Results of INT Reduction Assays in Assorted Eukaryotic Systems

1. Macrophage INT Assay

Macrophages from *Opsanus tau* have been used to examine pollutant effects on immune systems of fish, and recently, to elucidate molecular mechanisms of toxicity from membrane active toxicants such as TBT [108]. The latter procedure involved examination of "oxidative burst" electron transport, which, under normal circumstances, is the mechanism by which macrophages kill phagocytized microorganisms. In general, when leucocytes, including macrophages, are stimulated, they may undergo a CN⁻ insensitive respiratory burst resulting in secretion of reactive oxygen intermediates (ROI) *via* a membrane bound NADPH-dependent oxidase complex. Concomitantly, a smaller metabolic burst may be initiated in which arachidonates are cleaved from bound phospholipid pools and liberated for prostaglandin metabolism—a process also giving rise to ROI [108, 112, 122]. These processes can be modulated by artificial means (including toxicant treatment) and the deviation from normal behavior can be used in mechanistic toxicology. For example, in the presence of certain effectuators (phorbol esters, calcium ionophore), the oxidative burst can be triggered artificially, and the resulting "chemiluminescent" response quantified using a superoxide-activated luminol reaction system in a scintillation counter [123]. Pollutant treatments can depress or stimulate this response, or, in the case of TBT, give threshold spikes over an extended dose range [108].

The interaction of macrophage membrane receptors with bacterial or particulate ligands is thought to give rise to buildup of superoxide anion during

phagocytosis *via* the following "second messenger" mechanisms (*cf.*, review, ref. 122).

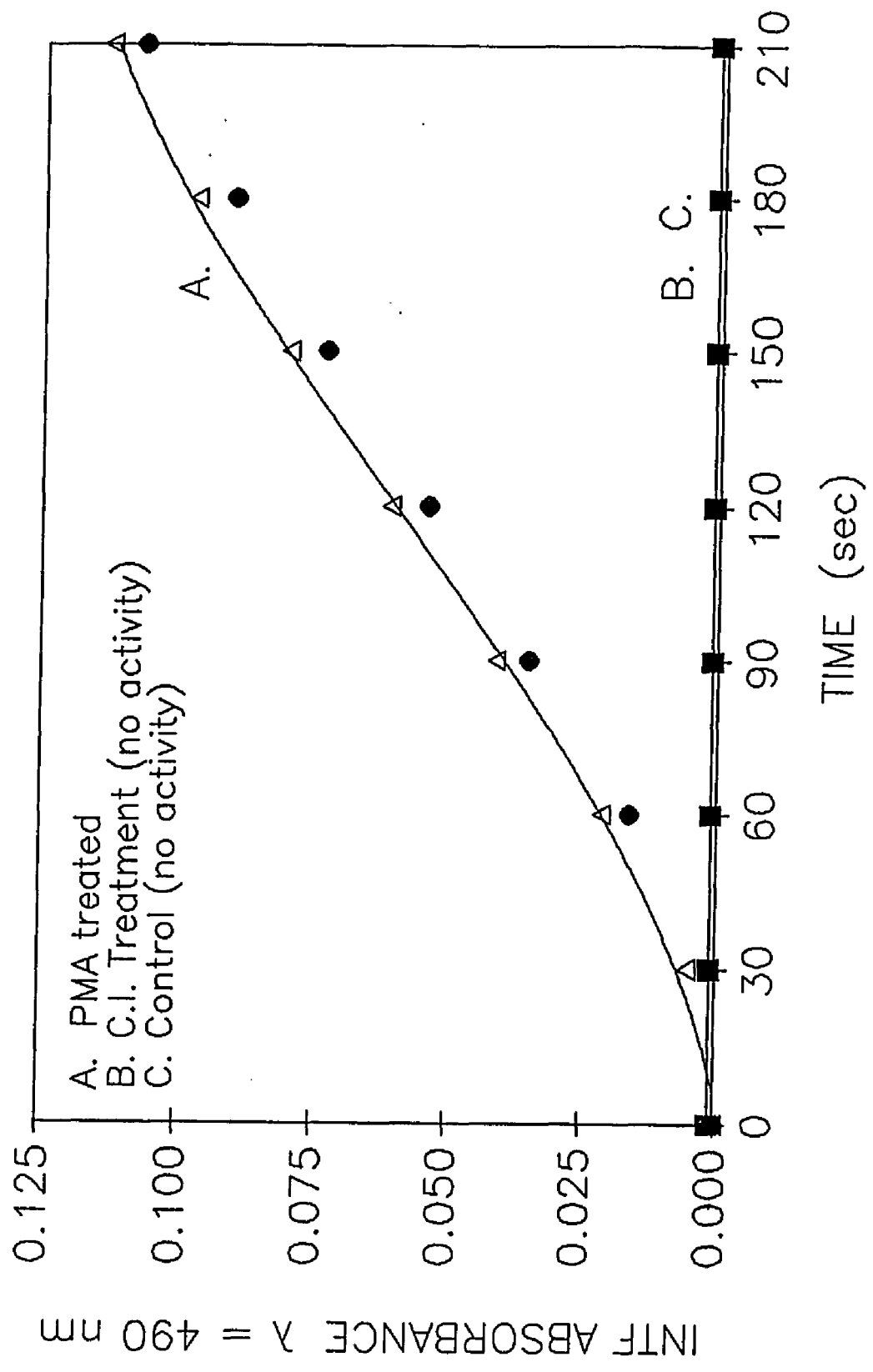


where PLC is phospholipase c; PIP phosphatidylinositol-bis-phosphate, DAG is diacylglycerol, IP₃ inositol triphosphate, and PK_c is protein kinase c.

The significance of these pathways to the present work is that metabolically dormant ("resting") macrophages can be induced to begin ET leading to ROI by chemicals that mimic various steps in this natural process. Calcium ionophore (CI), for example, mimics the effect of elevated levels of soluble IP₃ which are normally only present after receptor interaction at the membrane signalling immanent phagocytosis. The effect of CI and IP₃ is to increase Ca²⁺ and feed forward the arachidonate pathway (uppermost path). PMA (a cancer promoter derived from plants of the genus *Euphorbia*) mimics the effects of DAG, which interacts with PK_c, lowering its affinity for Ca²⁺ and thus "uninhibiting" PK_c. PK_c thereupon becomes activated and activates the NADPH oxidase system in the membrane, which produces the superoxide used to destroy the phagocytized materials. The macrophage will turn on superoxide generating systems *via* second messengers soon after the membrane ligand-receptor reactions have occurred, but superoxide concentrations will not rise to peak levels for up to 20 minutes after induction, as quantified by

scintillation counting [123]. It would seem that this lag corresponds to the time it would take the cell to complete phagocytosis and for all second messenger pathways to become fully activated. These mechanisms of NADPH oxidase activation are not well resolved and it was of interest to know whether oxidative burst as measured in chemiluminescence studies was the effect of both postulated pathways (*i.e.*, arachidonate and PK_C activation) or whether one pathway operated rapidly, while the other behaved more as a long term system which became constitutive over an active period and then slowly tapered off. Based on the number of postulated steps involved in these pathways, it was expected that the PK_C pathway would "spike" rapidly (DAGs are readily formed and transported) while the arachidonate pathway would operate more gradually and indirectly. The ability to differentiate these pathways has obvious implications for the interpretation of mechanisms in macrophage-pollutant assays. The purpose of this experiment was to take a few preliminary steps toward resolving this problem, and evaluate the use of INT for estimating electron transport in a novel system. Referring to Fig. 31, it was found that untreated macrophages did not reduce INT in the 210 s treatment period and this response was not effected by additions of CI at levels found to be optimal in chemiluminescence studies [108]. Although not presented in Fig. 31, the CI assays were monitored for 630 s and no activity was observed. Treatment with PMA, however, stimulated a rapid and continuous reduction of INT over the entire period of the runs. Although further work is needed, these results suggest that 1) INT can be used to examine activated macrophage electron transport and to differentiate between the various possible pathways leading to ROI and, 2) the effect of DAG-mimicing agents appears to include immediate stimulation of NADPH oxidase \rightarrow O₂ ET in treated

FIGURE 31. Effect of Calcium Ionophore A23187 (CI) and Phorbol Myristate Acetate (PMA) on INT Reduction in Resting Peritoneal Macrophages From The Toadfish *Opsanus Tau*.
N = 2.



macrophages. Liberation of intracellular Ca^{2+} pools by IP_3 -mimicing agents has a delayed effect probably leading through arachidonate pathways (as indicated by chemiluminescence). The instantaneous induction of the "activated" state for PMA-treated macrophages does not appear to have been reported. It would be interesting to evaluate the threshold oxidative burst reaction mediated pollutants such as TBT [108] with respect to both of these pathways using INT.

2. Liver S-9 INT Assay

S-9 fractions from 3-MC treated spot appeared to have greater ET rates relative to corn oil controls, but since only two replicates were available, statistical tests were not conducted. The maximum $d(\text{INTF})/(30 \text{ s})$ rate results are as follows: blanks = no activity; corn oil controls = 40, 52; and the 3-MC treatments = 54, 72 (values are change in absorbance/30 s x 100; $\lambda = 490 \text{ nm}$). The means of these estimates are close to 2σ units apart, and exhibit c.v.s around 13 - 14 %, which would probably decrease to an acceptable range (< 10 %) with more replicates. At the time of writing, experiments are being designed to optimize the S-9/INT assay. Hopefully an S-9/INT assay of increased sensitivity can be developed for use in environmental screening.

3. Marine Phytoplankton INT Assay

The behavior of INT in phytoplankton cultures was much less dynamic than in the bacterial cultures, even in the presence of sunlight. It was therefore decided that phytoplankton would not be acceptable for further examination of

the ET anomalies and membrane effects described above for bacteria, or as test organisms in toxicity assays using INT reduction. Within 4 hours of INT exposure, the *Tetraselmis sp.* and *Isochrysis sp.* had observable quantities of INTF, while the *Monochrysis sp.*, *Dunaliella sp.*, and *Chlorella sp.* were less active or inactive. The INTF deposits appeared to be cytoplasmic and localized in dark bodies. Based on visual observation, the plankton showed the following INT reactivities: *Tetraselmis* (both species) > *Isochrysis* > *Monochrysis* > *Chlorella*, *Dunaliella*. It would seem that assays using INT for enumeration or metabolic assessment of natural plankton assemblages would have to include removal of all bacteria, including nanobacteria, which would reduce INT much more rapidly than was observed for these cultures and confute the data.

SUMMARY OF CONCLUSIONS

There has been both inaccuracy and inconsistency in the presentation of structural, electrochemical, and mechanistic data on TPT, INT and their formazans in the published literature. This is due, in part, to the difficulties of working with these materials in complex environments such as electroanalytical and biological systems. As a result of the heterogeneity and physicochemical disparity between these systems, sites and mechanisms of biological reduction of TPT, INT, and related compounds cannot be directly inferred from data generated at electrodes. The presented chemical structures of INT and INTF standards as well as INTF extracted from treated bacterial cells are supported by quantitative analysis. Other possible structures of INTF have been considered and are counterindicated based on spectrophotometric and FTNMR data. These results and the hydride reduction route supported by the electrochemical and FTNMR studies should help to resolve some of the basic representational difficulties found in the literature.

Electrochemical data presented showed a) NPP and DPP of INT gave $E_{1/2}^{\text{red}}$ of the first wave between +0.126 and +0.073 V *vs.* SHE, b) the minimum reduction potential for formation of INTF on Pt was between +0.116 and +0.125 V *vs.* SHE (*cf.*, Table 1), and the values on C electrodes were comparable, c) INT \rightarrow INTF reductions at Pt and C electrodes appeared to be mediated by two direct one-electron reductions and disproportionation by one proton (hydride transfer), and d) the presence of interfering reactions involving adsorbed H species or radicals were indicated on Pt and C. Observations from a thin cell spectroelectrochemical system were inconclusive, but optimization of the system and addition of recoil spectrometry would probably aid in

interpreting reactions of adsorbed species during reductions. The spectrophotometric system was sensitive and reproducible in detecting the minimum reduction potential of INT on Pt mesh and holds promise for further work elucidating the effects of toxicants on ET. Results with all analytical systems indicated that further work is needed to fully understand INT electrochemistry at electrodes and *in vivo*. Hopefully, this work has provided a quantitative basis for future study.

Although not detected as mutagens in the Ames test, INT, INTF, and mixtures of the two were handled with caution. Based on the positive results in electrophoretic DNA unwinding assays, it would appear prudent to regard these materials as mutagens until conclusive multispecies tests have demonstrated that no cancer risk exists.

The INT reduction assay used in this study for NCAC toxicity estimation apparently did not fulfill the assumption of a direct proportionality between INTF formation and cell viability or metabolic status as suggested in recent work. The method did, however, give information on membrane effects and prompted further experiments addressing related phenomena and mechanisms of toxicity. The INT assay showed a threshold dose transient in ET that corresponded to an altered respiratory state in cells treated with threshold levels of the NCACs. The use of optimized cell suspensions was an important factor leading to the observation of NCAC threshold effects. At threshold doses, estimates of ET *vs.* oxygen consumption/cell viability gave opposing pictures of the status of treated cells. It would seem, therefore, that tetrazolium reduction assay results from wastewater or natural environmental systems should be interpreted with caution. Perhaps the most fitting use of this kind of assay is to study the behavior of toxicants or other materials with

respect to membranes and redox pathways in whole bacterial or microeukaryotic (*e.g.*, macrophage) cells. The preliminary results of INT reduction assays in S-9 fractions were encouraging, but many procedural questions need to be explored before conclusions on the applicability of the method to rapid environmental screening of organisms can be reached.

Results of the NCAC bioassays strongly suggest that the test NCACs disrupted several homeostatic processes in *E. coli*. Respiratory ET systems, oxygen reduction, and membrane permeability and structural topology all evidenced NCAC threshold effects. Results of ET rate assays in cells with differing degrees of outer membrane lipid content, NCAC oxygen consumption assays, noncellular NCAC-PMA-INT assays, and transmission electron microscopy supported the following conclusions: a) NCACs acted in some way to increase outer membrane permeability, b) impacts on the outer membrane probably caused periplasmic and inner membrane processes to be affected either chemically or structurally, c) the NCACs entered the respiratory chain and inhibited ET to oxygen probably by redox cycling, and d) the cumulative impacts on membrane and respiratory systems was sufficient, in the threshold doses, to cause significant reductions in viable cell counts of overnight cultures. It was not possible to differentiate between processes suggested in b and c above.

An important characteristic of organisms is that they become dynamically unstable when processes approach or exceed critical boundaries. Cellular and organismic homeostasis is mediated by superimposed and interdependent systems of nonlinear feedback processes. In such nonlinear complex systems, the observed responses to multilevel effects such as intoxication are frequently threshold in nature [*cf.*, 49, 50, 108]. Toxicological

thresholds are being increasingly noticed in subcellular and cellular systems [108], and it would seem logical to begin looking for them at higher levels of organismic and ecological organization.

The membrane and electrochemical effects observed in this work suggested that NCACs may be important in determining the toxicity of complex mixtures. This is particularly applicable to the processes of membrane transport of lipophilic species (such as high molecular weight PAHs), free radical toxicity and intracellular redox buffering, cocarcinogenesis, and membrane-mediated developmental effects.

Environmental PAH-NCAC mixtures contain an abundance of chemical species that likely possess interesting and unexplored toxicological properties. Of particular interest to the author are materials such as PAH and azaarene nitriles, NCAC organometallic complexes, photooxidized species, N-oxides and radicals, and N- substituted azaarenes and carbolines. These and other constituents of mixtures (*e.g.*, O- and S- containing aromatics and polar oxidation products) should be addressed with a view towards uncovering novel pathways and effects while simultaneously upgrading our existing models.

As mentioned previously, the physiology and electrochemistry of tetrazolium salts have been somewhat oversimplified, and a great deal of relevant and interesting work remains to be done. Apparently, the use of tetrazolium salts for demonstrating threshold state transitions and pollutant membrane effects has not been reported elsewhere. In the course of this work, the use of microscopic imaging systems [124] in monitoring the reduction of INT by NCAC treated and pristine *E. coli* was explored and important qualitative data were gathered on INT physiological effects. At present, the feasibility of

expanding these applications to other organisms and populations is under consideration.

LITERATURE CITED

- [1] Blumer, M., J. Sass, G. Souza, H. Sanders, F. Grassle, and G. Hampson (1970). "The West Falmouth Oil Spill", Woods Hole Oceanographic Institution reference # 70-44, 42 pp.
- [2] Blumer, M. (1975). "Organic Compounds in Nature: Limits of Our Knowledge", *Angewandte Chemie*, 14(8):507-514.
- [3] Blumer, M. (1976). "Polycyclic aromatic hydrocarbons in nature", *Scientific American*, 234:34-44.
- [4] Wolfe, D. A. (ed.). *Fates and Effects of Petroleum Hydrocarbons in Marine Organisms and Ecosystems*, Pergammon Press, 1977, NY, NY, 478 pp.
- [5] Lopez-Avila, V., and R. A. Hites (1980). "Organic compounds in an industrial wastewater. Their transport into the sediments." *Environ. Sci. Technol.*, 14(11):1382-90.
- [6] Farrington, J. W., J. M. Teal, and P. L. Parker. "Petroleum Hydrocarbons", in: *Strategies for Marine Pollution Monitoring*, E. D. Goldberg (ed), 1976 Wiley, NY, pp. 3 - 34.
- [7] Neff, J. M. *Polycyclic Aromatic Hydrocarbons in the Aquatic Environment*. 1979 Applied Science Publishers, London, 261 pp.
- [8] National Academy of Science (USA). *Particulate Polycyclic Organic Matter*, 1972, NAS, Washington D.C., 361 pp.
- [9] Kinghorn, R. R. F. *An Introduction to the Physics and Chemistry of Petroleum*. 1983 Wiley, NY, 420 pp.
- [10] Farrington, J. W., and B. W. Tripp (1977). "Hydrocarbons in western North Atlantic surface sediments", *Geochim. Cosmochim. Acta* 41:1627-1641.
- [11] Farrington, J. W. (1977). "The biogeochemistry of oil in the ocean", *Oceanus*, 20(4):5-14.
- [12] Blumer, M., and W. W. Youngblood (1975). "Polycyclic aromatic hydrocarbons in soils and recent sediments", *Science*, 188:53-55.
- [13] Blumer, M., T. Dorsey, and J. Sass (1977). "Azaarenes in recent maine sediments", *Science*, 195(4275):283-285.
- [14] Youngblood, W. W., and M. Blumer (1975). "Polycyclic aromatic hydrocarbons in the environment: homologous series in soils and recent sediments", *Geochim. Cosmochim. Acta*, 39:1303-1307.

- [15] Hites, R. A., R. E. LaFlamme, and J. W. Farrington (1977). "Sedimentary polycyclic aromatic hydrocarbons: the historical record", *Science*, 198(4319):829-831.
- [16] Blumer, M., W. Blumer, and T. Reich (1977). "Polycyclic aromatic hydrocarbons in soils of a mountain valley: correlation with highway traffic and cancer incidence", *Environ. Sci. Technol.*, 11:1082-1084.
- [17] Malins, D. C., and H. O. Hodgins (1981). "Petroleum and marine fishes: a review of uptake, disposition, and effects", *Environ. Sci. Technol.*, 15:1272-1280.
- [18] Malins, D. C., B. B. McCain, D. W. Brown, S. L. Chan, M. S. Meyers, J. T. Landahl, P. G. Prohaska, A. J. Friedman, L. D. Rhodes, D. G. Burrows, W. D. Gronlund, and H. O. Hodgins (1984). "Chemical pollutants in sediments and diseases of bottom-dwelling fish in Puget Sound, Washington", *Environ. Sci. Technol.* 18(9):705-713.
- [19] Malins, D. C., Krahn, M. M., Meyers, M. S., Rhodes, L. D., Brown, D. W., Krone, C. A., McCain, B. B. and Chan, S. -L. (1985). "Toxic chemicals in sediments and biota from a creosote-polluted harbor: relationships with hepatic neoplasms and other hepatic lesions in English sole (*Parophrys vetulus*)", *Carcinogenesis*, 6(10):1463-1469
- [20] Krahn, M. M., M. S. Meyers, D. G. Burrows, and D. C. Malins (1984). "Determination of metabolites of xenobiotics in the bile of fish from polluted waterways", *Xenobiotica*, 14(8):633-646.
- [21] Malins, D. C., Myers, M. S. and Roubal, W. T. (1983). "Organic free radicals associated with idiopathic liver lesions of English sole (*Parophrys vetulus*) from polluted marine environments", *Environmental Science and Technology*, 17(11):679-685.
- [22] Roubal, W. T. and Malins, D. C. (1985). "Free radical derivatives of nitrogen heterocycles in livers of English sole (*Parophrys vetulis*) with hepatic neoplasms and other liver lesions", *Aquatic Toxicology*, 6:87-103.
- [23] White, C. M., A. G. Sharkey, M. L. Lee, and D. L. Vassilaros. "Some analytical aspects of the quantitative determination of polynuclear aromatic hydrocarbons in fugative emissions from coal liquifaction processes", In: *Polynuclear Aromatic Hydrocarbons 3rd International Symposium*, P. W. Jones and P. Leber (ed). 1980 Ann Arbor Science Publishers, Ann Arbor, MI, pp. 261 - 276.
- [24] Nishioka, M., H. -C. Chang, and M. L. Lee (1986). "Structural characteristics of polycyclic aromatic hydrocarbon isomers in coal tars and combustion products", *Environ. Sci. Technol.* 20(10):1023-1027.

- [25] Krone, C. A., Burrows, D. G., Brown, D. W., Robisch, P. A., Friedman, A. J. and Malins, D. C. (1986). "Nitrogen-containing aromatic compounds in sediments from a polluted harbor in Puget Sound", *Environmental Science and Technology*, 20(11):1144-1150.
- [26] Yamauchi, T. and Handa, T. (1987). "Characterization of aza heterocyclic hydrocarbon particulate matter", *Environmental Science and Technology*, 21(12):1177-1181.
- [27] Schmeltz, I., and D. Hoffmann (1977). "Nitrogen containing compounds in tobacco smoke." *Chem. Rev.* 77:295-311.
- [28] Dong, M. W., D. C. Locke, and D. Hoffmann (1977). "Characterization of aza-arenes in basic organic portion of suspended particulate matter", *Environ. Sci. Technol.*, 11(6):612-618.
- [29] Grimmer, G., Jacob, J. and Naujack, K. W. (1983). "Profile of the polycyclic aromatic compounds from crude oils. Part 3. Inventory by GC/MS. PAH in environmental materials", *Analytical Chemistry*, 55(11):2398.
- [30] McKay, J. F., Weber, J. H., and Latham, D. R. (1976). "Characterization of nitrogen bases in high boiling point petroleum distillates", *Analytical Chemistry*, 48:891-898.
- [31] Mohr, D. H., and C. J. King (1985). "Identification of polar organic compounds in coal-gasification condensate water by gas chromatography-mass spectrometry analysis of high-performance liquid chromatography fractions", *Environ. Sci. Technol.*, 19(10):929-935.
- [32] Sawicki, E., Meeker, J. E. and Morgan, M. J. (1965). "The quantitative composition of air pollution source effluents in terms of aza heterocyclic compounds and polynuclear aromatic hydrocarbons", *Air Water Pollution*, 9(5):291-298.
- [33] Kleindienst, T. E., P. B. Shepson, E. O. Edney, L. D. Claxton, L. T. Cupitt (1986). "Wood smoke: measurement of the mutagenic activities of its gas- and particulate phase photooxidation products". *Environ. Sci. Technol.* 20(5):493-501.
- [34] Streitwieser, A. and Heathcock, C. H. *Introduction to Organic Chemistry, 2nd Ed.* Macmillan Co., NY, 1981, pp. 1061-1109.
- [35] Carey, F. A., and R. J. Sundberg. *Advanced Organic Chemistry, 2nd Ed.* 1984 Plenum Press, NY, NY. Part A: 711 pp.
- [36] Smith, J. H., W. R. Mabey, N. Bohonos, B. R. Holt, S. S. Lee, T. -W. Chou, D. C. Bomberger, and T. Mill (1977, 1978). "Environmental pathways of selected chemicals in freshwater systems", Parts I and II, EPA 600/7-77-113 and 600/7-78-074, respectively.

- [37] Stetter, J. R., Stamoudis, V. C. and Jorgensen, A. D. (1985) "Interactions of aqueous metal ions with organic compounds found in coal gasification: Process condensates". *Environmental Science and Technology*, 19(10):924-928.
- [38] Ames, B. N. "Carcinogens and anti-carcinogens", in: *Mutagens in Our Environment*, 1982 Alan Liss, Inc. NY, NY, pp. 3 - 19.
- [39] Moore, H. W., and Czerniak, R. (1981). "Naturally occurring quinones as potential bioreductive alkylating agents", *Med. Res. Rev.* 1:249-252.
- [40] Malins, D. C., and W. T. Roubal (1985). "Free radicals derived from nitrogen-containing xenobiotics in sediments and liver of bile from English sole from Puget Sound, Washington", presented paper, *Third International Symposium on Responses of Marine Organisms to Pollutants*, Plymouth, U.K., 7 pp.
- [41] Calvert, J. G., and J. N. Pitts. *Photochemistry*, 1966 Wiley, NY, NY, 899 pp.
- [42] Tjessem, K., and A. Aaberg (1983). "Photochemical transformation and degradation of petroleum residues in the marine environment", *Chemosphere*, 12(11):1373-1394.
- [43] Zepp, R. G. (1978). "Quantum yields for reaction of pollutants in dilute aqueous solution", *Environ. Sci. Technol.*, 12:327-29.
- [44] Rostad, C. E., W. E. Pereira, and S. M. Ratcliff (1984). "Bonded phase extraction column isolation of organic compounds in groundwater at a hazardous waste site", *Anal. Chem.*, 56:2856-2860.
- [45] Laseter, J. L. and DeLeon, I. R. *The Bayou Bonfouca Creosote Spill*, Report to the Captain of the Port of New Orleans, Center for Bio-organic Studies, University of New Orleans, New Orleans, LA, 70122, 1981, pp. 1-44.
- [46] Fabacher, D. L., C. J. Schmitt, J. M. Besser, and M. J. Mac (1988). "Chemical characterization and mutagenic properties of Polycyclic aromatic compounds in sediment from tributaries of the Great Lakes". *Environ. Toxicol. Chem.* 7:529-543.
- [47] Electric Power Research Institute (1980). "Inventory of organic emissions from fossil fuel combustion for power generation". EPRI EA-1394-TPS 78-820, 44 pp.
- [48] Tomkins, B. A., and C. -h. Ho (1982). "Determination of polycyclic aromatic amines in natural and synthetic crudes", *Anal. Chem.* 54:91-96.
- [49] Moore, M. N. (1986). "Molecular and cellular indices of pollutant effects". *NATO ASI Series*, G9, pp. 417-435

- [50] Bayne, B. L. "Measuring the effects of pollution at the cellular and organism level". In: *The Role of the Oceans as a Waste Disposal Option*, G. Kullenberg, Ed., Reidel Publishers, NY, 1986, pp. 617-634.
- [51] Lyman, W. J., Reehl, W. F., and Rosenblatt, D. H. *Handbook of Chemical Property Estimation Methods*. McGraw-Hill, NY, 1982, Sect. 17, pp. 1-24.
- [52] Leo, A. J. "Hydrophobicity, the underlying property in most biochemical events", in: *Environmental Health Chemistry*, J. D. McKinney (ed.). 1981, Ann Arbor Publishers, Ann Arbor, MI, pp. 323-334.
- [53] Rapaport, R. A., and S. J. Eisenreich (1984). "Chromatographic determination of octanol:water partition coefficients (K_{ow}) for 58 polychlorinated biphenyl congeners". *Environ. Sci. Technol.* 18(3):163-170.
- [54] Bean, R. M., D. D. Dauble, B. L. Thomas, R. W. Hanf, and E. K. Chess (1985). "Uptake and biotransformation of quinoline by rainbow trout", *Aquatic Toxicol.* 7:221-239.
- [55] Lewis, W. H. and Elvin-Lewis, M. P. F. *Medical Botany*, Wiley Interscience, NY, 1977, pp. 1-449.
- [56] Kingsbury, J. M. *Poisonous Plants of the United States and Canada*. 1964, Prentice-Hall, Englewood Cliffs, NJ, 625 pp.
- [57] Chuaqui, C. A., and A. Petkau (1987). "Chemical reactivity and biological effects of superoxide radicals", *Radiat. Phys. Chem.*, 30(5/6):365-373.
- [58] Dreyer, J. L. (1984). "Electron transport in biological systems: an overview". *Experientia*, 40(7):653-776.
- [59] Lehninger, A. L. *Biochemistry, 2nd Ed.* 1975 Worth Publishers, NY, NY, 1077 pp.
- [60] Neidhardt, F. C. (Ed.) *Escherichia coli and Salmonella typhimurium. Cellular and Molecular Biology*. ASC, Washington, D. C., 1987, 1649 p.
- [61] Jambour, B. (1954). "Reduction of tetrazolium salt", *Nature*, 173(4408):774-775.
- [62] Kuhn, R. and Jerchel, D. (1941). "Uber Invertseifen. VII Mitteil: Tetrazoliumsalze. *Ber. Dtsch. Chem. Ges.*, 74(6):941-948.
- [63] Nineham, A. W. (1955). "Chemistry of formazans and tetrazolium salts", *Chemical Reviews*, 65(2):355-483.

- [64] Smith, F. E. (1951). "Tetrazolium salt", *Science*, 113:751-754.
- [65] Altman, F. P. (1976). "Tetrazolium salts and formazans", *Prog. Histochem. Cytochem.*, 9:1-56.
- [66] Aleksandrov, A., Kostova, S., and Navratil, O. (1985). "Extraction of triple ion-associated niobium(V) complexes with polyphenols and 2-(p-iodophenyl) -3- (p-nitophenyl)-5-tetrazolium chloride", *Collected Czech. Chem. Commun.*, 50(11):2369-2374.
- [67] Raggio, M., and De Raggio, N.M. (1951). "Recientes aplicaciones biologicas y quimicas de derivados del tetrazole", *Ciencia e Investigacion. (Buenos Aires)*, 7(35):35-39.
- [68] Kenner, R. A. and Ahmed, S. I., (1975). "Correlation between oxygen utilization and electron transport activity in marine phytoplankton", *Marine Biology*, 33:125-133.
- [69] Zimmermann, R., Iturriaga, R., and Becker-Birke, J. (1978). "Simultaneous determination of the total number of aquatic bacteria and the number thereof involved in respiration", *Applied and Environmental Microbiology*, 36(6):926-935.
- [70] Packard, T. T., Healy, M. L., and Richards, F. A. (1971). "Vertical distribution of the activity of the respiratory electron transport system in marine phytoplankton", *Limnology and Oceanography*, 16(1):60-70
- [71] Packard, T. T. *Advances in Aquatic Microb.*, Vol. 3, H. W. Jannasch and P. J. Williams Eds., Academic Press, NY, 1985, pp. 207-261.
- [72] Trevors, J. T. (1984). "Dehydrogenase activity in soils: a comparison between INT and TTC", *Soil Biology and Biochemistry*, 16(6):673-674.
- [73] Bitton, G., Khafif, T., Chataingner, N., Bastide, J., and Coste, C.M. (1986). "A direct INT-dehydrogenase assay (DIDHA) for assessing chemical toxicity", *Toxicity Assessment*, 1(1):1-12.
- [74] Dutton, R. J., Bitton, G., and Koopman, B. (1986). "Rapid test for toxicity in wastewater systems", *Toxicity Assessment*, 1(1):147-158.
- [75] Atkinson, E., Melvin, S., and Fox, S.W. (1950). "Some properties of 2,3,5, triphenyl tetrazolium chloride and several related iodo derivatives", *Science*, 111:385-387.
- [76] Wagner, H. and Grossmann, H. (1976). "Thin layer chromatographic and spectrophotometric testing of tetrazolium salts and thier formazans for use as quantitative redox indicators", *Z. Med. Labortech*, 16(2):94-103.

- [77] Trevors, J. T. "A Method for Assessing the Effect of Pollutants on Electron Transport System (ETS) Activity in Soil and Sediment". In: *Toxicity Screening Procedures Using Bacterial Systems* (Liu and Dutka, Eds.), pp. 163 – 173, 1984, Dekker, NY
- [78] Reid, W. V. (1952). "Formazan und tetrazoliumsalze, ihre Synthesen und ihre Bedeutung als Reduktionsindikatoren und Vitalfarbstoffe", *Angewandte Chemie*, 64 Jahrg. No. 14:394.
- [79] Jones, P. H. and Prasad, D. (1969). "The use of tetrazolium salts as a measure of sludge activity", *Journal WPCF*, Vol. 41(11), Part II, pp. R441–R449.
- [80] Packard, T. T. (1971). "The measurement of electron transport activity in marine phytoplankton", *Journal of Marine Research*, 29(3):235–244.
- [81] Bitton, G. (1983). "Bacterial and biochemical tests for assessing chemical toxicity in the aquatic environment: a review", *CRC Critical Reviews of Environmental Control*, 13(1)51–67.
- [82] Malicky-Schlatte, G. (1973). "Über die dehydrogenaseaktivität in Sediment des Lunzer Untersees", *Archives of Hydrobiology*, 72:525–532.
- [83] Itturiaga, R. v, Rheinheimer, G. (1975). "Eine einfache Method zur Auszahlung von Bakterien mit aktivem Electronentransportsystem in Wasser- und sedimentproben", *Kielor Meeresforschungen*, 31(2):83–85.
- [84] Jambour, B. *Tetrazoliumsalze in der Biology*, 1960, Fisher-Verlag, Jena, Germany, 151 pp.
- [85] Jambour, B. (1958). "Problems involved in the polarography of triphenyltetrazolium chloride", *J. Chem. Soc.(London)*, 604:1604 – 1609.
- [86] Tabakovic, I., Trkovnik, M., and Grujic, Z. (1979). "Electrochemical synthesis of heterocyclic compounds. Part 6. The redox behavior of the formazan-tetrazolium salt system in acetonitrile", *Journal of the Chemical Soc. Perkin Trans. 2*(2):166–171.
- [87] Karmarkar, S.S., Pearse, A. G., and Seligman, A. M. (1960). "Preparation of nitrotetrazolium salts containing benzothiazole", *J. Org. Chem.* 25:575–578
- [88] Campbell, H. and Kane, P. O. (1956). "Tetrazolium compounds. Part V. Polarography of triphenyltetrazolium bromide and some of its substituted derivatives", *J. Chem. Soc.(London)*, 603:3130– 3139.
- [89] Kivalo, P. and Mustakallio, K. K. (1956). "A polarographic study of some tetrazolium compounds", *Suomen Kemi. B.* 29:154–157.

- [90] Ladanyi, L., Farsang, Gy., and Balogh, S. (1975). "Electrochemical oxidation reduction mechanism of some organic systems of biological interest. Redox properties of 2,3,5, triphenyltetrazolium chloride and 1,3,5 triphenyl formazan in aqueous-organic medium". *Acta Chim. Acad. Sci. Hung.* 86(3):205-210.
- [91] Pearse, A.G.E. *Histochemistry, Theoretical and Applied*. Little, Brown, and Co., Boston MA, 1961, pp. 536-568.
- [92] Maki, J. S., and C. C. Remsen. (1981). "Comparison of two direct-count methods for determining metabolizing bacteria in freshwater", *Appl. Environ. Microb.* 41(5):1132.
- [93] Benson, F. R. *The High Nitrogen Compounds*. Wiley Interscience, NY, 1984, 679 pp.
- [94] Baizer, M. M., and Lund, H. *Organic Electrochemistry, 2nd Edition*, Dekker, NY, 1983, 1149 pp.
- [95] Jambour, B. (1955). "Mechanism of reduction of tetrazolium salts", *Nature*, 174(4482):800
- [96] Jerchel, D. and Mohle, W. (1944). "Determination of the reduction potentials of terazolium compounds", *Ber. Dtsch. Chem. Ges.* 77:591-593 (cited in Raggio and De Raggio, 1951, reference # 67 of this bibliography).
- [97] Shofield, K. Grimmett, M. R., and Keene, B. R. T. *Heteroatomic Nitrogen Compounds: The Azoles*. Cambridge University Press, NY, 1976, pp. 241-249.
- [98] Neugebauer, F. A. (1968). "The constitution of the radical intermediate between formazan and tetrazolium salt", *Tetrahedron Letters*, 17:2129-2132.
- [99] Findlay, B. J., A. Span, and C. Ochsenbein-Gattlen (1983). "Influence of physiological state on indices of respiration rate in protozoa", *Comp. Biochem. Physiol.* 74A(2):211-219.
- [100] Collins, C. H., and Lyne, P. M. *Microbiological Methods*. University Park Press, MD, 1970, p. 149.
- [101] Dybowski, C., and Lichter, R. L. (Eds.). *NMR Spectroscopy Techniques*, Dekker, NY, 1987, pp. 1-170.
- [102] Southampton Electrochemistry Group. *Instrumental Methods in Electrochemistry*. Ellis Horwood Ltd./Wiley NY, 1985, 439 pp.
- [103] Lyman, W. J., Reehl, W. F., and Rosenblatt, D. H. *Handbook of Chemical Property Estimation Methods*. McGraw-Hill, NY, 1982, Sect. 17, pp. 1-24.

- [104] Watson, S. W., Novitsky, T. J., Quinby, H. L., and Valois, F. W. (1977). "Determination of bacterial number and biomass in the marine environment", *Applied Environ. Microb.* Vol 33, No. 4, 1977, pp. 940-946.
- [105] U. S. Environmental Protection Agency. *Test Methods for Escherichia coli and Enterococci in Water by the Membrane Filter Procedure.* EPA-600/4-85/076, pp. 1-25.
- [106] Maron, D. M., and Ames, B. N. (1983). "Revised methods for the *Salmonella* mutagenicity test", *Mutation Res.* 113:173-215.
- [107] Hayat, M. A. *Fixation for Electron Microscopy*, Academic Press, NY, 1981, pg. 392.
- [108] Rice, C. D., and B. A. Weeks (1988). "Influence of tributyltin on *in vitro* macrophage activation in the toadfish", *Aquatic Animal Health*, in press.
- [109] Maniatis, T., E. F. Fritsch, and J. Sambrook (1982). *Molecular Cloning -- A Laboratory Manual*, 1982 Cold Spring Harbor, NY, 545 pp.
- [110] Pouchert, C. J. *Aldrich Library of NMR Spectra II.* Aldrich Chemicals Inc. Wisconsin, 1983, Spectrum 502 D.
- [111] Zimmerman, S. B. (1982). "The three dimensional structure of DNA", *Ann. Rev. Biochem.* 51:395-427.
- [112] Aldrich, W. N. "The influence of organotin compounds on mitochondrial functions", in: *Organotin Compounds: New Chemistry and Applications.* 1976 ACS, Washington, D. C., pp. 186-195.
- [113] Wilson, D. F., Owen, C. S. and Erecinska, M. (1979). "Quantitative dependence of mitochondrial oxidative phosphorylation on oxygen concentration: a mathematical model", *Arch. Biochem. Biophys.*, 195(2):494-504.
- [114] Wilson, D. F., Erecinska, M., Drown, C. and Silver, I. A. (1979). "The oxygen dependence of cellular energy metabolism", *Arch. Biochem. Biophys.*, 195(2):485-493.
- [115] Nachlas, M. M., Margulies, S. I., and Seligman, A. M. (1960). "Sites of electron transfer to tetrazolium salts in the succinoxidase system", *J. Biol. Chem.* 235(9):2739-2743.
- [116] Higuti, T., Arakaki, R., Kotera, Y., Takigawa, M., Tani, I. and Shibuya, M. (1983). "Triphenyl tetrazolium and its derivatives are anisotropic inhibitors of energy transduction in oxidative phosphorylation in rat liver mitochondria", *Biochem. Biophys. Acta*, 725:1-9.
- [117] Neshow, S. and Bergman, H. (1979). "1,2-naphthoquinone: a mediator of nonenzymatic benzo(a)pyrene oxidation:", *Life Sciences* 25:2099-2104.

- [118] Lilienblum, W., B. S. Bock-Henning, and K. W. Bock (1985). "Protection against toxic redox cycles between benzo(a)pyrene-3,6-quinone and its quinol by 3-methyl cholanthrene-inducible formation of the quinol mono- and diglucuronide", *Molec. Pharmacol.* 27:451-458.
- [119] Ortiz de Montellano, P. R. (Ed.) *Cytochrome P-450. Structure, Mechanism, and Biochemistry.* Plenum Press, NY, 1986, pp. 275-300.
- [120] Chance, B. and G. R. Williams (1956). "Respiratory enzymes in oxidative phosphorylation, II. Difference spectra", *J. Biol. Chem.* 217:395-407.
- [121] Makita, T. and E. B. Sandborn (1971). *Histochemie* 26::305-310.
- [122] Hamilton, T. A., and D. O. Adams (1987). "Molecular mechanisms of signal transduction in macrophages", *Immunology Today*, 8:151-158.
- [123] Warriner, J. E., E. S. Mathews, and B. A. Weeks (1988). "Preliminary investigations of chemiluminescent response in normal and pollutant-exposed fish", *Marine Environ. Res.* 24:281-284.
- [124] Sieracki, M. E., and Webb, K. L. "Applications of Image Analyzed Epifluorescent Microscopy for Quantifying and Characterizing Planktonic Bacteria and Protists", in *Protozoa and Their Role in Marine Processes.* E. C. Reid and P. Burkhill (Eds.) Springer Verlag, NY, in press.

VITA

WILLIAM JAMES CATALLO III

Born in Holyoke, Massachusetts, 14 November 1959. Graduated from Seton Hall Preparatory School in 1977. Earned B.S. in Biology from Tulane University in 1981. Received M.S. in Marine Sciences from Louisiana State University (Baton Rouge) in 1984. Entered doctoral program at College of William and Mary, School of Marine Science in 1985.